Acoustic measurement of liquid density with applications for mass measurement of oil

Erlend Bjørndal

Dissertation for the degree philosophiae doctor (PhD)

at the University of Bergen, Norway

Date: 30.04.2007

Preface

The subject of this thesis is to investigate methods for measuring liquid density by acoustic means, and to investigate one or more promising methods experimentally. The liquids used in this work covers distilled water and various oil qualities (as pure phases). This work was performed at the Christian Michelsen Research AS, (CMR Instrumentation) with financial support from the Norwegian Research Council (NFR) through the 4 year Strategic Institute Program "Ultrasonic technology for improved exploitation of petroleum resources", in the period of 2003–2006.

I wish to express my gratitude to my supervisors, Associate Prof. Magne Vestrheim, Institute of Physics and Technology, University of Bergen (IPT, UoB), and Senior Scientist Dr. Kjell-Eivind Frøysa, CMR Instrumentation, for advice and discussions on a regular basis. A special thanks applies to Dr. Kjell-Eivind Frøysa for finding his time in a hectic environment to the numerous fruitful drop-in discussions in his office throughout these years. I would also like to thank Stig Heggstad, CMR Instrumentation, and Øyvind Elbert, formerly CMR Instrumentation, for contributing in the design of the measuring cells, and Kåre Slettebakken at the Mechanical Shop (IPT, UoB) for a most satisfactorily job manufacturing the measuring cells used in this work.

Many people have helped me during these years, but those that must particularly be mentioned are Svein-Atle Engeseth, Bergen University College, who contributed concerning the signal processing and the electronics system, and my fellow Ph.D. student Audun Pedersen, formerly CMR Instrumentation, for writing the oscilloscope acquisition program. A special thanks applies also to my colleagues at CMR Instrumentation, and my fellow Ph.D. students Audun Pedersen, Petter Norli, and Kjetil Lohne for making these years a nice experience.

Finally, I wish to acknowledge and thank my family, and in particular my wife Marit, and our children Espen, Sindre, Jørund, and Irmelin, for continued support throughout this program.

Part I General discussion

Chapter 1. Introduction

1.1. Motivation

Density (mass per unit volume) is a material property of utmost importance in many fields, such as in the process industry in general and also for fiscal use. Applications are within such diverse fields as flow measurement for converting volume flow to mass flow, basic research, fluid characterization, biomedical diagnostics (particularly measurement of bone density), process control in the industry, fluid monitoring in the petroleum industry and not the least in quality control in the food and beverage industry.

Density is measured for three main reasons [1]: 1) the conversion of volumetric flow measurement into mass flow, 2) the measurement of the quality of a fluid, and 3) the detection of different fluids.

The first point can be understood by considering the bulk measurement of oil, which may form large-scale mass flow measurement used in the fiscal mass transfer between seller and buyer. The second point concerns indicating the variations in the composition of a product (e.g. monitoring the mixing of different fluids), monitoring the fermentation process of beer, the measurement of product purity in a refining process, and characterization of crude oils. The third point can be considered as a part of the quality measurement, although it is a specialist part. Interface detection is used for indicating and isolating different fluids, where sometimes different products being pushed through the same pipeline.

Industrial density measurements of liquids are traditionally performed by non-acoustic measurement methods. However, the use of ultrasound for industrial applications is increasing, mainly due to its non-intrusiveness and its rapid response. However, drawbacks include the invasive measuring principle along with a dependence upon deposits and air bubbles.

If an acoustic density meter could be brought to industrial use, operational savings could result as the same technology was used throughout for the measurement of several parameters, such as sound speed and volumetric flow rate.

There has in the recent years been an increased interest for acoustic density measurements of liquids, as reflected in Table 1.1.

Table 1.1. Doctoral theses within acoustic density measurement of liquids.

Author	Year of dissertation	Country	Reference
J. Delsing	1988	Sweden	[2]
J. C. Adamowski	1993 (in Portuguese)	Brazil	[3]
A. Püttmer	1998	Germany	[4]
M. Hirnschrodt	2000 (in German)	Germany	[5]
J. van Deventer	2001	Sweden	[6]
N. Hoppe	2003 (in German)	Germany	[7]
E. Bjørndal	2007 *	Norway	–

* This work.

1.2. Thesis outline

This thesis is split in three parts, where the first part consists of four chapters containing a synthesis of a more introductory form (Chapters 1 – 4). The second part consists of two chapters regarding a description of the proposed measurement approach and some experimental results (Chapters 5 – 6). The third part consists of two papers submitted to an international journal.

The contents of the two first parts will now be described: Chapter 2 contains a summary of the acoustic plane-wave theory used in this work, along with a description of the most important non-ideal characteristics that may need to be corrected for, if accurate measurements are to be performed. Chapter 3 gives an introduction to different measuring principles for the measurement of liquid density, along with a brief introduction of how mass flow can be measured. Chapter 4 gives a survey of acoustical methods for measuring liquid density. In Chapter 5, the proposed measurement approach is explained. Chapter 6 gives some complementary measurement results beyond what is covered in the papers in the third part. Conclusions, perspectives and recommendations to further work are given in Chapter 7.

The reading of this thesis is recommended to be performed in the following sequence, in order to obtain the best succession.

1. Chapter 1 to 4
2. Papers I–II
3. Chapter 5 to 7

1.3. Objectives

In this work, the reason for studying the liquid density by acoustical means must be seen in connection with the use of acoustical transit-time volume flow meters. Such meters represent existing technology that is commercially available. When combined, a densitometer and a volume flow meter may give the mass flow, which is a parameter of considerable interest. However, acoustical transit-time volume flow meters will not be dealt with to any significant degree in this work.

The Norwegian Petroleum Directorate (NPD) specify a maximum allowed uncertainty of ± 0.30 kg/m^3 (using a 95 % confidence interval) at the component level, and a maximum loop uncertainty of ± 0.50 kg/m^3, when measuring the density of oils at fiscal transfer [8]. This represents an uncertainty almost an order of magnitude lower than previously claimed obtainable by acoustical means, as given in the literature (see also Chapter 4). The specified maximum uncertainty regarding fiscal transfer of oil is given as ± 0.30 % of standard volume (using a 95 % confidence interval).

Therefore any achievements that would seek to narrow this gap between requirements and the claimed obtainable uncertainty by acoustical means would be beneficial. The main objectives of this work are therefore to evaluate the different acoustical methods for density measurement of liquid, and to pursue the most promising method both theoretically and experimentally.

Two papers submitted to an international journal, and contributions at international conferences, along with a granted patent [9] are the results of this research work.

1.4. Publications and conferences

1.4.1. List of publications

1. E. Bjørndal and K-E. Frøysa, “Acoustic methods for obtaining the pressure reflection coefficient from a buffer rod based measurement cell”. Submitted to the IEEE Trans. Ultrason., Ferroelec., Freq. Contr. This paper is referred to as Paper I in this work.

2. E. Bjørndal, K-E. Frøysa, and S-A. Engeseth, "A novel approach to acoustic liquid density measurements using a buffer rod based measuring cell". Submitted to the IEEE Trans. Ultrason., Ferroelec., Freq. Contr. This paper is referred to as Paper II in this work.

1.4.2. Participation at conferences

1. E. Bjørndal, K-E. Frøysa, and M. Vestrheim, "Methods for acoustic density measurement of liquids". Conference paper presented at the 27th Scandinavian Symposium on Physical Acoustics, Ustaoset, Norway, January 25th – 28th, 2004, 29 pages. The Norwegian Physical Society, ISBN 82-8123-000-2.
2. E. Bjørndal, K-E. Frøysa, S-A. Engeseth, and M. Vestrheim, "Extension of the Papadakis buffer method for acoustic liquid density measurements". Presented at the 28th Scandinavian Symposium on Physical Acoustics, Ustaoset, Norway, January 23rd – 26th, 2005. The conference paper contains only an abstract. The Norwegian Physical Society, ISBN 82-8123-000-2.
3. E. Bjørndal, K-E. Frøysa, S-A. Engeseth, and M. Vestrheim, "A novel approach for ultrasonic liquid density measurements in comparison with the ABC-method". Presented at the 2005 meeting (Fysikermøtet) of The Norwegian Physical Society, Ulvik, Norway, August 11th – 14th, 2005. The conference paper contains only an abstract.
4. E. Bjørndal, and K-E. Frøysa, "Acoustic measurement of liquid density with applications for mass measurement of oil". Presented at the 30th Scandinavian Symposium on Physical Acoustics, Geilo, Norway, January 28th – 31th, 2007. The conference paper contains only an abstract. The Norwegian Physical Society, ISBN 82-8123-000-2.

I also had the pleasure of participating at the IEEE 2005 International Ultrasonics Symposium, which was held in Rotterdam, Holland.

Chapter 2. Theory

2.1. Introduction

This Chapter contains a brief introduction to the field of acoustic plane-wave propagation, where the concepts of reflection and transmission at interfaces at normal incidence, and of characteristic acoustic impedance, are introduced. The most important non-ideal characteristics relevant for this work are also introduced. The theory given here can be found in most standard text books in the field of acoustics, e.g. [10], and is included for the sake of completeness. The reason the plane-wave propagation is discussed, is because this theory is used throughout this work.

2.2. Plane-wave propagation

Probably the simplest of all theoretical approximations to the actual process of wave propagation is the plane-wave propagation, named so given that all of the acoustic variables are functions of only one spatial coordinate, the phase of any variable is a constant on any plane perpendicular to this coordinate. Such a wave is called a plane wave, and can to a certain degree be an approximation of the spherical wave characteristics found far from an acoustic source of sound. If the coordinate system is chosen so that this plane wave propagates along the x axis, the linear wave equation can be shown to reduce to

$$\frac{\partial^2 p}{\partial x^2} = \frac{1}{c^2}\frac{\partial^2 p}{\partial t^2}, \tag{2.1}$$

where $p=p(x,t)$. The variables used are:

- p: acoustic pressure
- x: distance
- t: time
- c: sound speed

The complex form of the harmonic solution for the acoustic pressure of a lossless plane wave is

$$p = P^{+}e^{j(\omega t - kx)} + P^{-}e^{j(\omega t + kx)}, \tag{2.2}$$

with k being the wave number of the media. By assigning

$$\begin{aligned} p_{+} &= P^{+}e^{j(\omega t - kx)} \\ p_{-} &= P^{-}e^{j(\omega t + kx)}, \end{aligned} \tag{2.3}$$

we find two waves propagating in opposite directions.

2.3. Reflection and transmission characteristics at normal incidence

Using the plane wave description, the reflection and the transmission characteristics at normal incidence will be given when the wave impinges on an interface separating two semi-infinite media, as given in Fig. 2.1, characterized by their sound speed c and their density ρ. There, three acoustic waves are seen. These are the incident pressure wave with amplitude A_{inc}, the reflected pressure wave with amplitude A_r, and the transmitted pressure wave with amplitude A_t in the adjacent medium. The expressions for these waves can be given as

$$\begin{aligned} p_{inc} &= A_{inc}e^{j(\omega t - k_1 x)} \\ p_r &= A_r e^{j(\omega t + k_1 x)} \\ p_t &= A_t e^{j(\omega t - k_2 x)}. \end{aligned} \tag{2.4}$$

Using index 1 in the original medium and index 2 in the adjacent medium, the pressure reflection coefficient R (abbreviated from now on as the reflection coefficient) can be given as

$$R = \frac{A_r}{A_{inc}}, \tag{2.5}$$

and gives the ratio of the reflected pressure amplitude to the incident pressure amplitude. Likewise, the pressure transmission coefficient (abbreviated as the transmission coefficient) can be given as

$$T = \frac{A_t}{A_{inc}}. \tag{2.6}$$

The relation between the transmission- and the reflection coefficient can be given as

$$T = 1 + R. \tag{2.7}$$

This model of the reflection and the transmission characteristics at an interface uses two boundary conditions: 1) the acoustic pressures on both sides of the boundary are equal, and 2) the particle velocities normal to the boundary are equal. Therefore, this model is referred to as a liquid-liquid model since any stiffening effects due to shear are neglected. This model will be used throughout this work, even if one or both of the media are solids, and therefore may be subjected to interference from shear waves (see Chapter 2.5.1).

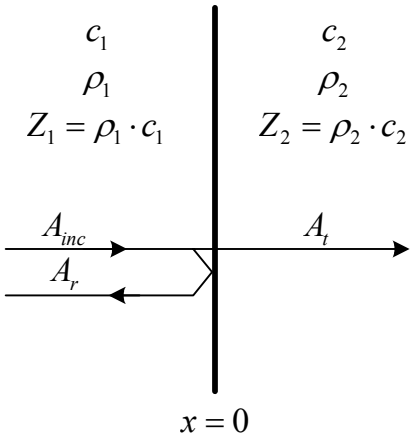

Figure 2.1. Plane-wave reflection and transmission at normal incidence.

2.4. Acoustic impedance

The specific characteristic impedance Z (abbreviated acoustic impedance for short) is given as the ratio of the acoustic pressure p in the media to the associated particle speed u as

$$Z = \frac{p}{u}. \tag{2.8}$$

For plane waves this ratio becomes

$$Z = \pm \rho c, \tag{2.9}$$

with c being the sound speed of a medium, and with the sign dependent upon the direction of the propagation. The acoustic impedance can be a complex or a real quantity dependent upon the viscoelastic properties of the media. For plane waves, reflection coefficient R can be related to the acoustic impedance of the propagation media according to

$$R = \frac{Z_2 - Z_1}{Z_2 + Z_1} = \frac{\rho_2 c_2 - \rho_1 c_1}{\rho_2 c_2 + \rho_1 c_1}. \tag{2.10}$$

from which the liquid density may be obtained according to

$$\rho_2 = \frac{\rho_1 c_1 (1+R)}{c_2 (1+R)}. \tag{2.11}$$

It is then understood that if the acoustic impedance of one of the media and the reflection coefficient are known, it is possible to obtain the acoustic impedance, and the density, of the other medium, assuming that sound speeds c_1 and c_2 are known. This forms the basis for the most common method in the acoustic field of characterizing media using a buffer separating the acoustic transducer and the medium to be characterized. In such a case, the acoustic impedance of the buffer needs to be known in order to obtain the characteristics of the medium under consideration.

2.5. Non-ideal characteristics

In order for the simple theory presented above to be applied to a description of acoustic phenomena in an accurate way, some non-ideal characteristics must be corrected for, or avoided, by some means. The most important of these are mode conversion and diffraction, and both of these will be briefly described.

2.5.1. Mode conversion

Mode conversion is the process of transformation of wave energy from longitudinal to shear, or vice versa, and appears when sound reaches an interface between two materials. The characteristics of mode conversion are known to be a function of the angle of incidence. In the present work, the effect of mode conversion on the measured liquid density is avoided by keeping the sought echo signals within timeframes free from interference from mode converted signals. Due to finite lateral dimension of an acoustic transducer when attached to a solid buffer material, the edges appear to transmit both longitudinal and shear waves, as indicated in Fig. 2.2. Part of the transmitted shear wave gets mode converted to a longitudinal wave and reflected at the buffer–liquid interface, and detected at the transducer, which normally is sensitive to longitudinal waves.

A further discussion of mode conversion is given by Weight [11], where he also introduced mode conversion factors as a function of the angle of radiation. Püttmer [4] used the results of Weight [11] together with a model for the diffraction correction in pulse-echo mode for predicting the received echo signals in connection with development of an acoustic liquid densitometer. In the present work, however, large dimensions were applied for the buffer, simplifying both the aspects of mode conversion and of diffraction correction. An experimental demonstration of mode converted signals are given in Paper II and in Chapter 5.4.

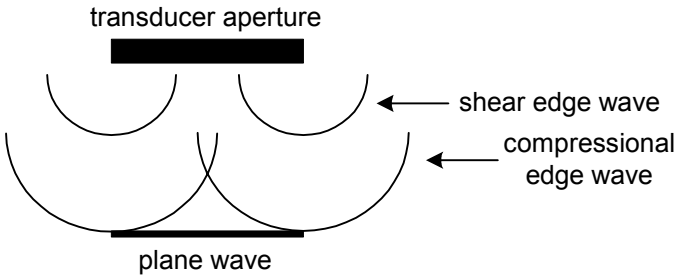

Figure 2.2. Mode conversion.

2.5.2. Diffraction

Diffraction is a particular type of wave interference, caused by the partial obstruction of a wave due to finite size of the source and the receiver. As measurements suffer from diffraction, corrections are called for which considers both the temporal characteristics and the amplitude characteristics of the pulses, if accurate measurements are sought. The details concerning how the diffraction correction is used in relation to the specific measurement method is discussed in Chapter 5.3.2.

2.6. Plane-wave theory applied on a measurement approach

In order to show how the theory of plane-wave propagation may be applied on an actual measurement approach, the proposed measurement approach as given in Chapter 5 is outlined using such theory. The results are given in Paper I.

Chapter 3. Principles of density- and mass flow measurements of liquids

3.1. Introduction to density measurements

Density ρ is defined as the mass per unit volume of a fluid or a solid, and depends in general on both temperature and pressure. The liquid density decreases as temperature increases, with water as an exception being at its most dense at a temperature of about 4 °C, whereas the effect of pressure on the density of liquids and solids is negligible at moderate pressures. The density ρ is also called the absolute density in order to distinguish it from relative density [12]. Liquid density for hydrocarbons is often reported in terms of relative density, or specific gravity (SG), defined as

$$\text{SG} = \frac{\text{density of liquid at temperature T}}{\text{density of water at temperature T}}. \tag{3.1}$$

The standard conditions adopted by the petroleum industry are 60 °F (15.5 °C) and a pressure of 1 atmosphere [12], therefore specific gravities of liquid hydrocarbons are normally reported at these conditions. The NPD states the standard conditions to be 15 °C and a pressure of 101.325 kPa [8]. Earlier, the *American Petroleum Institute* (API) defined the API gravity [12] as

$$\text{API gravity} = \frac{141.5}{\text{SG (at 60 °F)}} - 131.5, \tag{3.2}$$

from which we see that a hydrocarbon with lower specific gravity have a higher API gravity.

Perhaps the most important characteristic of a reservoir fluid is its density as a function of temperature and pressure [13]. It is important in both petroleum production and processing as well as its transportation and storage. The density is also used in calculations related to sizing of production equipment, required power to pumps and compressors and flow measuring devices. In connection with reservoir simulations, and the amount of production at various reservoir conditions, the density serves as a most important parameter.

In this work, however, absolute density measurements of various liquids will be given at a somewhat higher temperature of about 27.4 °C, due to practical considerations.

3.2. Principles of density measurements

Many principles for the measurement of liquid density are known, see for example [14]–[19], [4]. The most important of these will be briefly described. These are the

- Vibrating tube
- Weighing
- Buoyancy
- Hydrostatic pressure
- Gamma ray

Measuring instruments based on all of these sensor principles are available commercially and are used for density measurements in different process applications. However, their suitability in a given application may vary according to the specific use. In addition, the acoustic reflection mode principle using a reference material will be described, but instruments based on this sensor principle are to the author's knowledge not available commercially, although many acoustic density sensors have been devised, as will be discussed in Chapter 4.

3.2.1. Vibrating tube

The vibrating tube is often used for continuous density measurements in flowing systems in the process industry [4], [14], [18]–[19], and serves to a large degree as the industry standard. It usually consists of a U-shaped tube with fixed mounted ends, which is caused to oscillate by appropriate means. The square of the angular resonance frequency ω is inversely proportional to the tube's total mass, which consists of the mass of the tube m_0 and the mass of the liquid flowing in the tube given by its density ρ and the volume V of the tube, assuming that the diameter of the tube is small compared with its length, as given by

$$\omega^2 = \frac{c}{m_0 + \rho V}, \tag{3.3}$$

with c being a system constant. The oscillation period is normally measured instead of the frequency as a rather low audio frequency is used. As both the mass of the tube

and the tube's inner volume are known quantities, this method allows the density of unknown fluids to be determined in a single measurement, assuming a proper calibration of the instrument has been performed. Usually air and water are used as calibration fluids. A popular instrument often found in oil producing installations is the Solartron Type 7835 densitometer with a given accuracy of 0.15 kg/m^3 [20].

3.2.2. Weighing

Weighing (or pycnometry) [4], [14]–[16], [18]–[19], uses a known volume V filled with liquid to obtain the liquid density by weighing the mass m according to

$$\rho = \frac{m}{V}. \tag{3.4}$$

Laboratory methods for obtaining the liquid density are dominated by this principle. A relative uncertainty of less than $1 \cdot 10^{-6}$ may be obtained [14], and instruments based on this principle serves as the most accurate method. In addition to using pycnometers, this measuring principle can be applied to any vessel, or being part of a pipe system in which there is a flowing fluid. Then, typically a flexible pipe section is used whose weight acts on a balance. A U-shaped pipe section is normally used in which the ends of the pipe are elastically connected with the rest of the system and pivoted, although other designs are used as well.

3.2.3. Buoyancy

This method [4], [14], [16], [18]–[19], is based on the Archimedes' principle "When a body is immersed in a fluid, the fluid exerts an upward force on the body equal to the weight of the fluid that is displaced by the body". By either measuring the upward acting force of the body, or measuring the immersion depth, a measure of the liquid density can be obtained. Typical uncertainty is limited to about 1 %. This principle is not suited for flowing liquids, and therefore of limited interest for process measurements.

3.2.4. Hydrostatic methods

Two methods will be described that fall into this category. These are the pressure sensor method [4], [18], and the balanced-column method [4], [14], [18]. Each of these will be briefly described below.

Using pressure sensor

By measuring the hydrostatic pressure using a pressure sensor, the density can be determined from

$$\rho = \frac{p}{hg}, \tag{3.5}$$

with pressure p, height h between the pressure sensor and the liquid level, and acceleration of gravity g. If used in a closed vessel two pressure sensors placed at a height Δh from each other can be used. By also measuring the differential pressure Δp, the liquid density can be found.

Balanced-column method

If two vessels containing liquids of different densities ρ_1 and ρ_2 are connected by a U-tube standing upside down in which a pressure below atmospheric pressure is generated, the liquids rise by h_1 and h_2 above the respective liquid levels in the vessels. These methods have the great benefit of not being dependent upon deposits. However, these hydrostatic methods are not suitable for flowing media.

3.2.5. Gamma ray

As gamma rays are attenuated as they pass through a liquid, the amount of attenuation can be used as a measurement of the liquid density [4], [15], [18]–[19]. The Cs-137 and the Co-60 emitters are normally used. The law of attenuation of the radiation reads

$$I = I_0 e^{-\mu' d\rho}, \tag{3.6}$$

with measured intensity I, incident intensity I_0, the mass attenuation coefficient μ', and thickness of the attenuating substance d. For all the substances (except hydrogen) with a relative atomic number lower than 30, the mass attenuation coefficient can be considered constant, with values of 0.0767 cm^2/g for the Cs-137 emitter, and 0.0493 cm^2/g for the Co-60 emitter. The attenuation coefficient of hydrogen is about twice those of all other elements, so varying the water content and thereby the hydrogen content may give erroneous measurements.

Special considerations must be taken upon use of this principle due to its radioactive character. Also waste disposal considerations arise. Therefore, use of this principle are mainly found in borehole logging, and in level measuring in multiphase gravitational separators typically compound of water, oil and gas, where its advantage of being non-invasive, non-intrusive and robust are fully exploited. An uncertainty of about 1 % may be obtained.

3.2.6. Acoustic reflection mode principle using a reference material

As is well known (see Chapter 2.4), the liquid density can be found from the relation $Z = \rho c$, by measuring the sound speed c and the acoustic impedance Z. Measuring instruments based on this principle have, however, not been available on a commercial basis, probably due to limited accuracy. It should also be noted that the reflection coefficient senses the fluid adjacent to the wall, which may not be a good representation of the fluid's average density [21].

A temporal measurement is needed to obtain the sound speed, whereas amplitude measurements are needed for obtaining the acoustic impedance of the liquid. The measurements may be subjected to both random and systematic noise, which may be difficult to reduce to an acceptable level. As frequencies typically in the MHz-range are used, a somewhat conflicting situation exists for the digitizer as both a high temporal resolution and a high bit resolution are needed in order to obtain accurate results. A somewhat special property exists for this principle, as a combination of spot measurement (reflection coefficient) and integral measurement (sound speed along the path) are used. This may give rise to errors if the media possesses gradients in any form, particularly since the reflection coefficient then may not obtain a sufficiently good representation of the fluid's average acoustic impedance.

The acoustic sensor principle is given in Fig. 3.1, and can be explained in the following way: A transducer operating in the pulse-echo mode transmits an acoustic pulse into the reference material. The pulse gets partly reflected at the reference material–liquid interface, giving a measure of the reflection coefficient. A part of the incident pulse gets transmitted to the receiver transducer, in order to obtain the sound speed of the liquid. There are several aspects of this measuring principle that must be properly dealt with for this principle to be exploited in a measuring instrument. This will be further elaborated in Chapter 4.

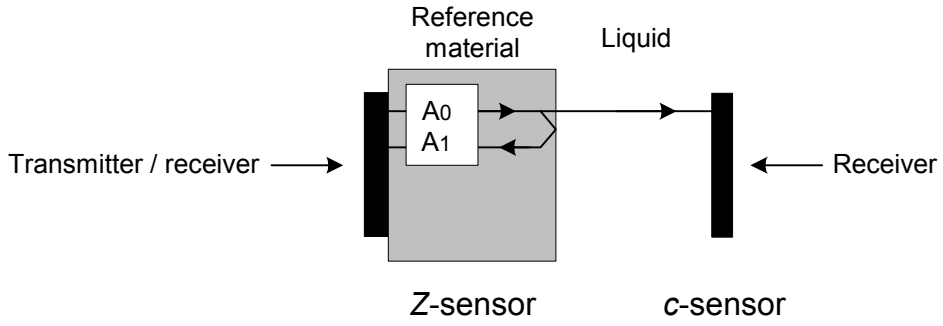

Figure 3.1. Acoustic reflection mode principle using a reference material.

3.3. Principles of mass flow measurements

3.3.1. Introduction

Two different methods lead to the measurement of mass flow rate q_m [22]. Either one can use a principle that has the mass flow rate as a direct measurement parameter, or it can be an indirect measurement parameter as exemplified by the combined measurements of density and volume flow rate rate q_v according to

$$q_v = \overline{v}(t) \cdot A, \tag{3.7}$$

where A is the cross-section area of the pipe and $\overline{v}$ is the mean flow velocity, and using that

$$q_m = q_v \cdot \rho. \tag{3.8}$$

Sensor principles using the mass flow rate as the direct measuring parameter include the thermal and the Coriolis meter, with the latter being extensively used in the process industry.

3.3.2. Coriolis meter

If a moving mass is subjected to an oscillation perpendicular to its direction of movement, Coriolis forces occur depending on the mass flow. The resulting phase shift in the oscillation geometry gives the mass flow rate. The oscillation frequency of the measuring tubes themselves is a direct measure of the fluid's density. Further description of the measuring principle is given in [22].

3.3.3. Ultrasonic transit-time volume flow meter

The measurement of volume flow can be performed by a variety of sensor principles such as differential pressure, variable area, positive displacement, turbine, fluid-dynamic, electromagnetic, and ultrasonic [22].

As this work utilize ultrasound for the measurement of liquid density, the use of ultrasound for the measurement of volumetric flow will be considered briefly. Four different ultrasonic techniques are known in the application of flow meters. These are the transit-time, the cross-correlation, the Doppler, and the swept beam technique [22]. However, only the transit-time method is suitable for measuring on single-phase flows where scattering is absent, or at least at a low level [23], and the required accuracy is high.

The principle of the ultrasonic transit-time flow meter is given in Fig. 3.2, and is based on that a sound wave traveling in the direction of the flow propagates faster than a sound wave traveling against the flow. The difference in the transit times

traveling in opposite directions can be shown to be directly proportional to the mean flow velocity of the fluid [24].

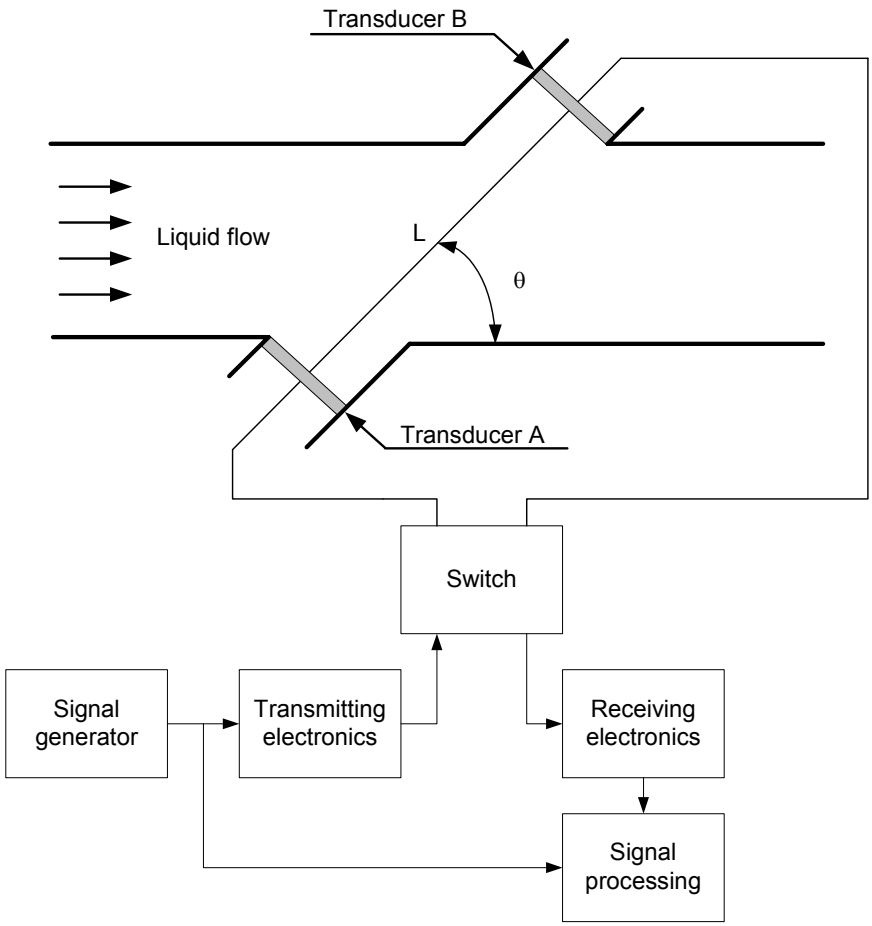

Figure 3.2. Principle sketch of a single path ultrasonic transit-time volume flow meter.

Chapter 4. Methods of acoustic liquid density measurements

4.1. Introduction

This Chapter deals with known methods for acoustic liquid density measurements, and forms the direct background material for the proposed measurement approach, as presented in Chapter 5. Even though many methods exist, none commercial densitometers based on acoustic principles are known to the author.

Several approaches for obtaining the liquid density by acoustical means have been proposed. Matson et al. [25] and Rychagov et al. [26] broadly divided these into three categories according to sound speed, acoustic impedance and waveguide propagation. In this work these categories will also be used, but additional categories will also be given.

4.2. Density from measured sound speed - or temperature

Obtaining the liquid density from measurement of the sound speed alone, have been suggested by several investigators. The resulting work include applications such as measurement on batteries electrolyte and the density of pure fluids. Swoboda et al. [27] and Vray et al. [28] used measurements of both sound speed and temperature in a sulfuric acid solution, and found that the evaluation of the density was possible in a relative density range exceeding 1.10–1.30 and in a temperature range exceeding 10 °C to 50 °C.

According to Rychagov et al. [26], the fluids must be sufficiently pure and well-defined so that the sound speed bears a reproducible relationship with density. Then, density and sound speed may be characterized as a function of temperature. This can be used to obtain a density versus sound speed relationship, which forms the basis for obtaining density from sound speed without actually measuring the temperature. In addition, proper temperature and pressure compensation must sometimes be applied.

However, Matson et al. [25] reported that measurements on diesel oil from several vendors had too much variability in the measured sound speeds, probably due to compositional changes, for this method to be useful. This method is therefore considered useful only for very pure fluids.

In a series of papers, Wang et al. [29]–[31] measured the sound speeds of different oils and found the sound speed to increase systematically with increasing density [31]. Based on regression analysis, empirical equations were established to calculate acoustic velocities in oils as a function of temperature and pressure if the densities are known. The sound speeds in oils can generally be predicted within a 3 to 4 % uncertainty over wide ranges of temperatures and pressures. The equations can also be inverted in order to give density as a function of measured sound speeds, with an uncertainty in density reflecting upon the uncertainty of the sound speed.

For some liquids, such as vegetable oils [32], and for alcohols [33], the sound speed was found to be linearly decreasing with increasing temperature. The same dependence was found for the density upon temperature. This means that if the density is known at one temperature, and knowing the temperature coefficient of the density, one can predict the density at a given temperature.

Takagi [34] presented in 1994 a new attempt to estimate density in halogenated benzenes from sound speed data using the liquid molar volume as derived by means of the Peng–Robinson equation of state with reasonable accuracy [35].

4.2.1. An exact thermodynamic approach

An exact method for obtaining volume changes under high pressures from acoustic sound speed measurements was developed by Davis and Gordon [36] in 1967. The calculation starts with the relation between the adiabatic compressibility κ_S and the sound speed c by

$$\kappa_S = 1/\rho c^2, \tag{4.1}$$

where

$$\kappa_S = -\frac{1}{V}\left(\frac{\partial V}{\partial P}\right)_S, \tag{4.2}$$

where V is the volume and P is the pressure. The thermodynamic relationship which link the adiabatic compressibility to the isothermal compressibility coefficient κ_T is

$$\kappa_T = \kappa_S + T\beta^2/\rho C_p, \tag{4.3}$$

in which β designates the isobaric coefficient of thermal expansion, and C_p the isobaric heat capacity at the absolute temperature T. By replacing the product $\rho\kappa_S$ by $1/c^2$, one obtains

$$\left(\partial\rho/\partial p\right)_T = 1/c^2 + T\beta^2/C_p. \tag{4.4}$$

By integrating with respect to pressure, one obtains a relationship that explicitly links the density to the sound speed.

$$\rho(P,T) = \rho(P_0,T) + \int_{P_0}^{P} c^{-2} dP + T\int_{P_0}^{P} \left(\beta^2 / C_p\right) dP. \tag{4.5}$$

The density is therefore seen to consist of three terms in which the main contribution is due to the direct measurement of the density at atmospheric pressure P_0. The first integral, which is the main additive contribution, can be evaluated directly by measuring the sound speed along the isotherms considered. To evaluate the second integral, two additional relations are used:

$$\left(\partial\beta / \partial P\right)_T = -\left(\partial\kappa_T / \partial T\right)_P \tag{4.6}$$

$$\left(\partial C_P / \partial P\right)_T = -\left(T / \rho\right)\left[\beta^2 + \left(\partial\beta / \partial T\right)_P\right]. \tag{4.7}$$

Extensive work have been performed by Daridon et al. [37]–[40] using this procedure for characterizing different oils from measurements of sound speed and compressibility at high pressures. A relative uncertainty of 0.1 % for the liquid density was claimed from such measurements [40].

4.3. Transmission methods

The transmission methods presented here considers use of two transducers; one as a transmitter and the other as a receiver.

4.3.1. Hale's approach

The sound transmission method as described by Hale [41] and also briefly discussed by McGregor [42], uses a two-transducer configuration as given in Fig. 4.1 in a pulsed mode where the received signal amplitude A_4 indicates the acoustic impedance of the liquid. The basic assumptions used are that the acoustic impedances of the transducers are equal, the assumption of equal liquid attenuation when moving from a reference liquid to the liquid to be measured, and the necessity of constant amplitude of the transmitted signal during all measurements. Therefore, severe errors are expected for liquids with high losses. A relative uncertainty of about 2 % was obtained using a solution of salt water [41].

Later, an extension of this approach was devised by Henning et al. [43] as given in Fig. 4.2, where the effect of attenuation was included. Then, the A_4 and the A_5 echo signals amplitudes are used in the calculation process. A relative uncertainty of 1.5 % was obtained for a wide range of liquids used.

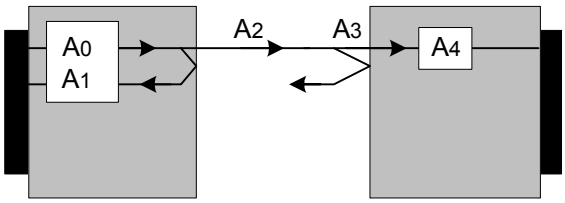

Figure 4.1. Schematic representation of the method used by Hale [41].

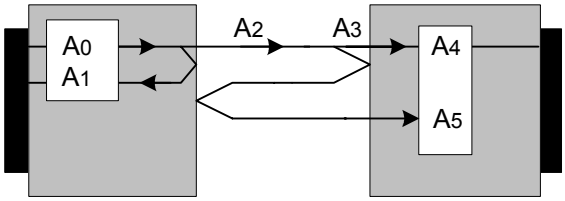

Figure 4.2. Schematic representation of the method used by Henning et al. [43].

4.3.2. Frequency sweep

Sukatskas et al. [44] devised in 1993 a transmission method for liquid density measurement whose schematic representation can also be given by Fig. 4.1, based on varying the frequency of the transmitted bursts, and linking the resulting bandwidth to the liquid acoustic impedance. However, varying environmental conditions were found to be troublesome. A relative uncertainty within 3.9 % was obtained using a wide range of liquids.

4.4. Acoustic impedance using a buffer-rod

Using a buffer-rod to obtain the acoustic impedance of the sample is the method that has drawn the most attention, as numerous papers have appeared based on this approach (see references in Table 1.1, and references therein). The principle of operation is given in Chapter 3.2.6. As the methods differ with regards to the number of transducers used, shape and composition of the buffer, and aspects regarding calibration of the methods, the methods will be subjected to a brief discussion. As all of these methods are based on the measurement of the reflection coefficient at the buffer–liquid interface, references to methods used for the measurement of reflection coefficient can be made, although the use of these methods in connection with density measurements not necessarily have appeared. In particular, Mak [45] and Paper I discusses methods for measurement of the reflection coefficient using a buffer-rod approach, and in Paper I, several new approaches of measuring the reflection coefficient using different echo signals are devised. Results using some of these new

approaches of obtaining the reflection coefficient, and thereby the density, are presented in Paper II and in Chapter 6.

For the buffer-rod approach to work, the acoustic impedance of the buffer needs to be known to a high degree of accuracy, and also the sound speed in the buffer and in the liquid needs to be known. The normal method for obtaining the acoustic impedance of the buffer is by calibrating the measurement cell using distilled water of which the sound speed and the density (and thereby the acoustic impedance) are accurately known versus temperature [46]–[47]. This approach, however, suffers from the need of recalibration in case of changes of the transmit waveform [48], due to the systematic corrections used.

4.4.1. Approximation due to loss in the liquid

This subject has been discussed by Mason et al. [49] and later by Moore and McSkimin [50], but is included for the sake of completeness.

Using a buffer-rod approach, the attenuation in the buffer is normally very low, so that the buffer's acoustic impedance can be obtained from its density and the measured sound speed. The situation is different for liquids possessing medium and high attenuation, as they are subject to a loss angle θ. By inserting the complex form of the reflection coefficient given as [49]

$$R_F = Re^{-j\theta}, \tag{4.8}$$

into

$$R_F = \frac{Z_2 - Z_1}{Z_2 + Z_1}, \tag{4.9}$$

where R is the magnitude of the reflection coefficient and θ the phase angle, the impedance of the liquid can be given as

$$Z_2 = R_2 + jX_2 = Z_1 \frac{\left(1 - R^2 - j2R\sin\theta\right)}{1 + R^2 - 2R\cos\theta}. \tag{4.10}$$

The real part of the liquid impedance then reads

$$R_2 = Z_1 \frac{\left(1 - R^2\right)}{1 + R^2 - 2R\cos\theta}, \tag{4.11}$$

which can be approximated as

$$R_2 \approx Z_1 \frac{1+R}{1-R}\left[1 - \frac{R\theta^2}{\left(1-R\right)^2}\right] = Z_1 \frac{1+R}{1-R} + O\left(\theta^2\right). \tag{4.12}$$

This way, it is found that for most buffer–liquid interfaces the magnitude of the reflection coefficient can be used to specify the resistive component of the liquid's

acoustic impedance. As the acoustic impedance of the liquids used typically are less than $0.1 \cdot (1 + j)$ that of the buffer, the loss angle was found not to exceed 5 ° [49].

4.4.2. Pulse-echo reflectometer

Several investigations using a simple pulse-echo reflectometer configuration measurement cell for density measurements of liquids have been performed. These include the work of McClements and Fairly [51]–[52], and by Kushibiki et al. [53] working in the VHF/UHF frequency range for bioultrasonic spectroscopy. The schematic of the method is given in Fig. 4.3.

Here, a buffer is used between the transducer and the liquid. The reflection coefficient can be determined by measuring the amplitude of the echo signal reflected from the end of the buffer when air is present and when liquid is present. The reflection coefficient is calculated by the ratio of two amplitude measurements. This mandates that the sensor components and the excitation signal do not change between the measurements. A drawback of this method is that non-repeatable behaviour of the transducer element or excitation signal can give error in the reflection coefficient (and thereby the acoustic impedance of the liquid). The liquid sound speed can be found from the echo signals arriving from the buffer–liquid interface and the liquid–reflector interface as indicated in Fig. 4.3.

McClements and Fairly [51] obtained a relative uncertainty of 0.5 % on the measured density for some aqueous NaCl solutions. Kushibiki et al. [53] obtained a relative uncertainty in density of 1 % for various oils.

Fox et al. [54] devised a method recently for measuring the specific gravity of industrial food batters using a buffer rod approach. In their work, a water buffer was used which was encapsulated in a Perspex outer housing which again was terminated in the form of a 45 ° conical tip such that it entered the batter cleanly without trapping any external air bubbles on the outer surface. The sound speed of the Perspex and of the batter was not measured during the operational phase, as a special “calibration” data set was applied. A relative uncertainty of the specific gravity within approximately 5 % was obtained.

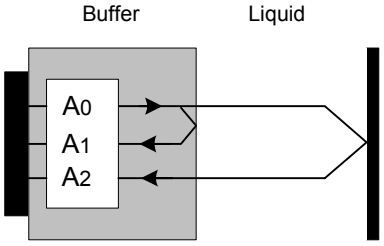

Figure 4.3. Schematic representation of the pulse-echo reflectometer as used by McClements and Fairly [51].

4.4.3. Greenwood's approach

Greenwood et al. [55]–[60] devised a method which consists of six transducers mounted at different angles to a wedge of which its base is inserted in the liquid to be measured. Five of the transducers are of longitudinal type, and one is a shear-wave type used for obtaining the liquid shear viscosity. The amplitude of the measured echo signals depends upon the angle of incidence, the acoustic impedance of the liquid, and upon the wedge parameters. By determining the reflection coefficient at two angles of incidence, the density and the sound speed of the fluid can be determined. Fig. 4.4 gives the schematic of the method. The obtained relative uncertainty in the density measurement was approximately 0.5 % for pure liquids and 1 to 2 % for typical slurries. This method suffers from the need of frequent calibration due to thermal drift and ageing of sensor components, as discussed above.

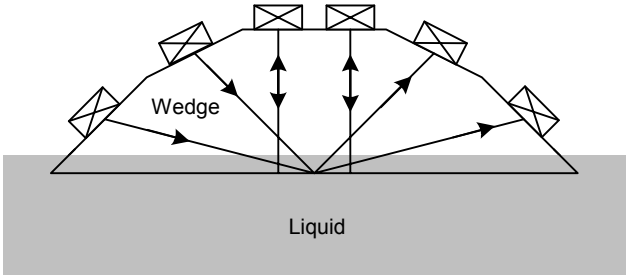

Figure 4.4. Schematic representation of Greenwood's approach using a wedge [57].

4.4.4. Wang's approach

Wang et al. [61] devised a method using a water buffer based on a broadband excitation pulse to obtain the frequency dependent reflection coefficient. From this the velocity-density product and the attenuation-density ratio can be obtained by use of a least-square regression procedure. If a separate sound speed measurement is performed, the resulting density can be obtained. This approach seems however to have been applied only on solids.

In order to overcome the weaknesses due to amplitude stability of the excitation signal and due to possible ageing of sensor components, several approaches have been devised where part of the transmitted signal is obtained from a reference acoustic path. Such approaches have paved the way for the most recently introduced methods for acoustical density measurements of liquids, as discussed in the remaining part of Chapter 4.4. One approach for performing in such a way includes the work of Lynnworth and Pedersen [62] and the patent of Jensen [63].

4.4.5. Stepped-diameter approach

In connection with an ultrasonic mass flowmeter, Lynnworth and Pedersen [62] suggested to use a stepped-diameter probe of which the difference in echo amplitudes at the wetted end and at the dry step is a function of the acoustic impedance of the liquid to be measured, as seen in Fig. 4.5. No accuracy of the density measurements was given in their work. The measurement of the liquid's sound speed was performed by independent means. Recently, van Deventer [64] performed a modeling study using the electrical circuit simulator program *PSpice* based on this approach. However, difficulties were encountered due to the way the buffer step-down was implemented.

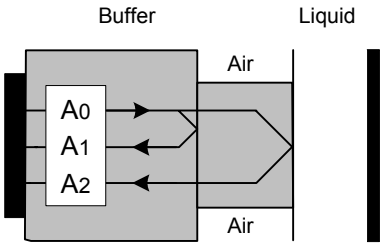

Figure 4.5. Schematic representation of the pulse-echo reflectometer of Lynnworth and Pedersen [62].

A somewhat similar probe was suggested by Jensen [63], where instead of the stepped-diameter approach of Lynnworth and Pederesen [62], a groove in the buffer was used to obtain the reference signal, as schematically given in Fig. 4.6.

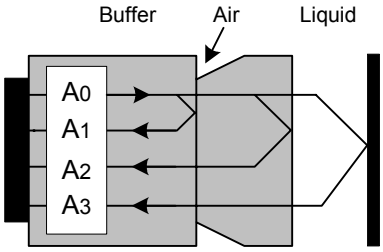

Figure 4.6. Schematic representation of the pulse-echo reflectometer of Jensen [63].

4.4.6. The ABC-method

The ABC-method was devised by Papadakis [65] in 1968 for the measurement of attenuation of solids and reflection coefficient at the buffer–sample interface. This method uses only one transducer in pulse-echo mode exploiting the three first echo signals arising from reflections at the buffer–sample interface. The reflection coefficient is found by forming amplitude ratios based on these echo signals. The method is also capable of measuring the sample attenuation by using the amplitude information from the first and the second echo signals, or from the second and the

third echo signals, respectively, along with the reflection coefficient. Assuming the sound speed in the sample is measured by considering the timing differences of the echo signals, the density, and thereby also the adiabatic compressibility can be obtained. In this respect this method has applications within fluid characterization, which might be of particular interest in many applications.

Some of the claimed inherent benefits of this method are 1) that the amplitude ratios are not affected by operating the transducer away from its resonance frequency since none of the echo signals considered arise from reflections at the buffer–transducer interface [65], and 2) that the measurement of the same amplitude ratios are not affected by the acoustical coupling layer between the transducer and the buffer.

This method has been quite extensively used, see e.g. references in Paper I for different characterization purposes, but to a limited extent for liquid density measurements. In 1974 Sachse [66] obtained the density of a fluid contained in a cylindrical cavity as given in Fig. 4.7, using this approach. Due to the method of acquisition and digitalization, a relative uncertainty of 25 % was claimed. Later, Kline [67] obtained a patent using the ABC-method with the liquid enclosing a reflector as given in Fig. 4.8. This was used for measuring the liquid density of aircraft fuels. Note that the reflector used by Kline must be terminated by the same liquid both on the front and on the back of the reflector. The name ABC stems from the individual signals involved with A=A_1, B=A_2, and C=A_3. Adamowski et al. [3], [68]–[72] have used this method for measurement of the reflection coefficient, but with a modification of the sensor arrangement. Their approach will be given in Chapter 4.4.11.

Based on Figs. 4.7 and 4.8, the reflection coefficient and the liquid attenuation α can be given as

$$R = -\left(1 - \frac{A_2^2}{A_1 A_3}\right)^{-0.5} \tag{4.13}$$

$$\alpha = \frac{1}{2l}\ln\left[\frac{A_1}{A_2}\left(R^2 - 1\right)\right] \tag{4.14}$$

$$\alpha = \frac{1}{2l}\ln\left[\frac{A_2}{A_3}R^2\right], \tag{4.15}$$

where the liquid attenuation is seen to be obtainable either from the first and the second echo signals, or from the second and the third echo signals, along with the reflection coefficient.

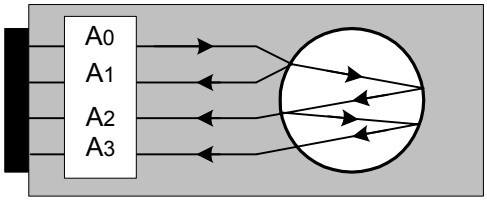

Figure 4.7. Schematic representation of the ABC-method as used by Sachse [66].

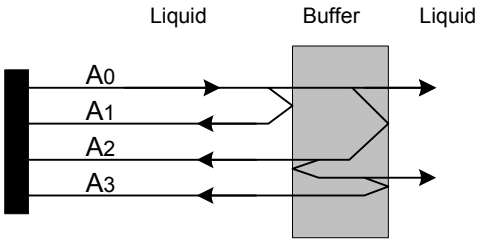

Figure 4.8. Schematic representation of the ABC-method as used by Kline [67].

4.4.7. Divider cell

In connection with development of an ultrasonic mass flow meter for liquids, Guilbert and Sanderson [73] devised a density meter using two transducers in a pulse-echo configuration as shown in Fig. 4.9. They used a divider plate, which for one of the transducers was terminated by the liquid on both sides, whereas for the other transducer, the divider plate was terminated in air (gas) on the back side. In this respect, the buffer (or divider) is not situated between the transducer and the liquid, but inserted in the liquid (upper part in Fig. 4.9), and between the liquid and the reference media (lower part in Fig. 4.9). By expressing the echo amplitudes as A_{xy}, where A_{xy} is the amplitude of the y^{th} reflection returning to the transducer x, the reflection coefficient at the liquid–divider interface can be given as

$$R = \frac{A_{12}A_{21}}{A_{11}A_{22}}. \tag{4.16}$$

Additionally, the attenuation of the divider plate can be obtained by each of the transducers separately. As two relative measurements are used no constraints with regard to matched characteristics for the gain and the aquisition signal paths are necessary. No separate uncertainty data for the density measurements were given.

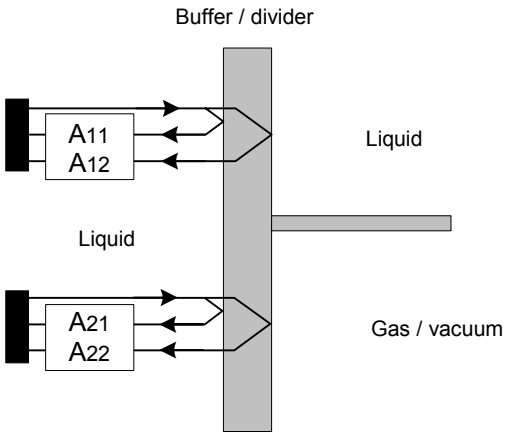

Figure 4.9. Schematic representation of Guilbert and Sanderson's approach using a divider cell [73].

4.4.8. Püttmer's approach

Another method for obtaining a reference acoustic path was devised by Püttmer et al. [4], [74]–[78]. The transmitted signal strength is obtained from the buffer on the rear side, which is terminated against air giving almost a total reflection. A separate receiver element is used on the far side of the liquid, for the measurement of sound speed. The main benefit of this method is considered to be that the reflection coefficient can be obtained without any wave propagation through the liquid layer. A relative uncertainty of the measured density of 0.2 % was claimed. The schematic of the method is given in Fig. 4.10.

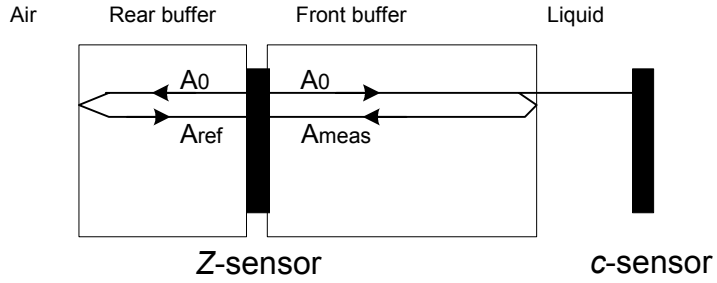

Figure 4.10. Schematic representation of Püttmer's approach [77].

This approach uses a low acoustic impedance type of ceramic transducer material in order to match the acoustic impedance of the buffers used, which typically are of a glass material. As the acoustical coupling of both sides of the transducer element cannot be guaranteed identical, a calibration approach is used, using typically distilled water to obtain the acoustic impedance of the buffer material as expressed as a function of the measured amplitudes A_{ref} and A_{meas}.

Salazar et al. [79] devised a method recently for measuring the acoustic impedance of industrial food batters using only the impedance sensor part of Püttmer's approach. The reason for using only the impedance sensor part was due to

the claimed very high attenuation of batter of about 500 dB/cm [79], although the frequency was not given. Therefore, it was proposed to measure acoustic impedance changes instead of density, and thereby avoiding having to transmit sound waves through the batter. It can also be shown that for a gas–liquid mixture the acoustic impedance shows a much greater relative change than the density does for a minor gas content [79]. The front buffer was formed as a 45 ° conical tip such that it enters the batter cleanly without trapping external air bubbles. The buffer rods were made of the plastic material Delrin.

4.4.9. Resonance anti-reflection

Hirnschrodt et al. [80]–[82] devised a method for obtaining a high sensitivity measurement of the reflection coefficient. This was done by inserting a reference liquid layer between the transmitter element and a half-wavelength buffer material in contact with the liquid to be measured, see Fig. 4.11. This buffer typically represents the wall separating different media, or a pipeline in which a fluid is flowing. The frequency is tuned so that the buffer is a half-wavelength in thickness, aiming at a direct acoustical interface between the reference liquid and the liquid to be measured, giving optimum sensitivity for the reflection coefficient. However, the claimed results indicate that further work is needed before the full potential of the method can be exploited. A claimed relative uncertainty of better than 1.5 % was given. The choice of buffer material is of great importance, and must be considered in view of the reference liquid and the liquid to be measured.

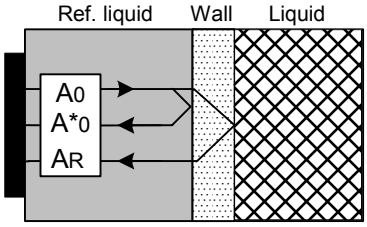

Figure 4.11. Schematic representation of Hirnschrodt et al.'s approach [82]. The measurement of the test liquid's sound speed is assumed to be performed by independent means.

4.4.10. Double front buffer

In order to obtain a reference acoustic path for the transmitted signal, the use of a front buffer consisting of two materials coupled together has been proposed. Generally, such an approach suffers from a reduced sensitivity as the sound wave meets multiple interfaces when propagating against a reflector [77]. Also, the quality and durability of the acoustical coupling between the buffer materials are of concern. Two applications of such an approach have been identified, and are presented below.

Delsing and van Deventer

Delsing [2], [83], van Deventer [6] and van Deventer and Delsing [84]–[85] used an approach, where the buffer consists of two materials glued together in order to obtain a reference signal of the transmitted signal strength. However, this approach implies that the attenuation in the buffer material in contact with the liquid is known in advance, as it is needed for the calculation of the liquid density. The schematic of the method is given in Fig. 4.12. A relative uncertainty within 2 % was obtained for a wide range of liquids. The determination of the liquid density is performed according to Eq. (4.17).

$$\rho_3 = \frac{Z_2}{c_3}\frac{\left[4A_1Z_1Z_2e^{-2\alpha_2 l_2} - A_2\left(Z_1^2 - Z_2^2\right)\right]}{\left[4A_1Z_1Z_2e^{-2\alpha_2 l_2} + A_2\left(Z_1^2 - Z_2^2\right)\right]} \tag{4.17}$$

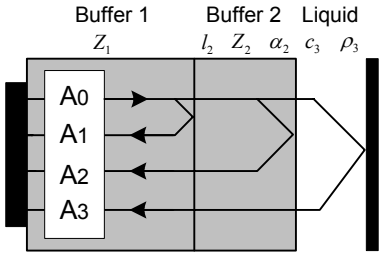

Figure 4.12. Schematic representation of the Delsing approach [84].

Fisher

Fisher et al. [86] was granted a European patent in 1995 in which a conical buffer element was used, consisting of two materials connected together, in order to obtain a reference echo of the transmitted signal strength. The buffer material in connection with the transducer element was given as Perspex, and the part of the buffer in contact with the liquid to be measured was given as a high-grade steel. A relative uncertainty of 1 % was obtained at laboratory conditions. The use of a high acoustic impedance buffer material in contact with the liquid to be measured seems somewhat strange, as it is known that in order to obtain a high sensitivity, one needs a buffer material of an acoustic impedance close to that of the liquid to be measured. The schematic of the method is given in Fig. 4.13.

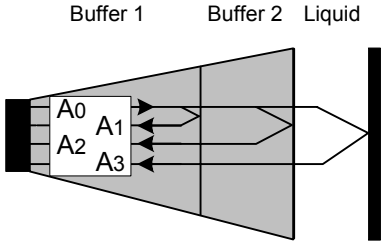

Figure 4.13. Schematic representation of Fisher et al.'s approach [86].

4.4.11. Split front buffer

Adamowski et al. [3], [68]–[69] and Higuti and Adamowski [70]–[72] used a split front buffer approach with a PVDF (or more recently a P(VDF-TrFE)) membrane transducer placed in between the buffers, as schematically illustrated in Fig. 4.14. The membrane transducer is used as a receiver, and has a larger diameter than the buffers. One then obtains a reference of the transmitted signal strength along with freedom from diffraction effects using this approach. The split buffer materials used are Perspex and borosilicate glass. The method used for obtaining the reflection coefficient is the ABC-method of Papadakis [65]. Higuti and Adamowski [70]–[72] recently proposed to process the amplitude signals using a frequency domain integration technique that seems to give improved accuracy relative to time domain amplitude measurements. This frequency domain processing can be explained by introducing the frequency domain equivalent of the ABC-method as

$$R = -\left(1 - \frac{\int_{-\infty}^{+\infty} \left|A_2(f)\right|^2 df}{\int_{-\infty}^{+\infty} \left|A_1(f)\right|\left|A_3(f)\right| df}\right)^{-0.5} . \tag{4.18}$$

A measured relative uncertainty of 0.2 % was claimed. This method suffers from the gluing of the receiver membrane transducer to the split buffers, and from a somewhat reduced operating temperature range due to the use of the membrane transducer element.

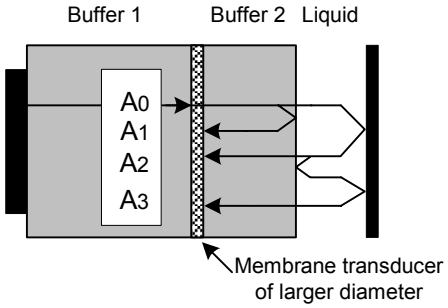

Figure 4.14. Schematic representation of the Adamowski approach [68].

4.5. Waveguide propagation

Lynnworth [87]–[88] developed a torsional wave sensor for the measurement of liquid density, which exploits the change in propagation time of a torsional ultrasonic wave in a metal transmission line as a function of the density of the surrounding media. The principle is given in Fig. 4.15, which shows a delay line and a waveguide of different cross sections connected together. The transducer generates an extensional stress pulse into the delay line from which it propagates to the waveguide (the sensor) and converts to a torsional wave propagating in the sensor. This principle has been reported used quite extensively by several groups during the last 25 years [89]–[100]. This approach has also been used for measuring on two-phase media. Different waves, such as torsional, flexural, or even a Rayleigh wave can be used [25].

According to Lynnworth [101] this approach suffers from viscosity effects that must be compensated for, and in order for the sensor to operate as a non-dispersive device, certain wavelength aspects must be fullfilled with regard to the dimensions used.

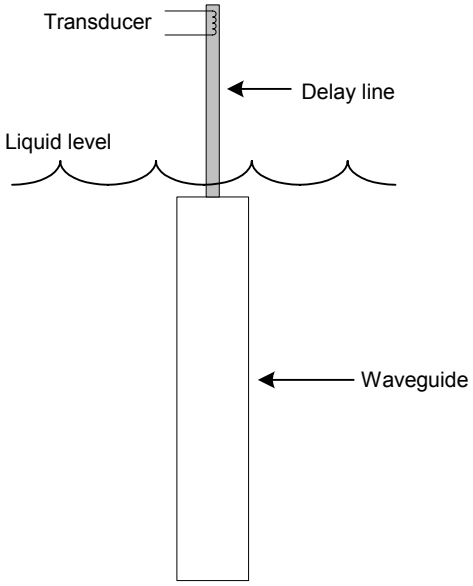

Figure 4.15. Schematic representation of the waveguide propagation approach.

4.6. Interferometry

4.6.1. Pope's approach

Pope et al. [102]–[103] used a non-invasive ultrasonic resonance interferometry technique to perform fluid density and concentration measurements. A brief description of the technique is as follows [103]: The specific gravity or solute concentration of a process fluid solution located in a selected structure is determined by obtaining a resonance response spectrum of the fluid / structure over a range of frequencies that are outside the response of the structure itself. A fast Fourier transform (FFT) of the resonance response spectrum is performed to form a set of FFT values. A peak value for the FFT values is determined, e.g. by curve fitting, to output a process parameter that is functionally related to the specific gravity and solute concentration of the process fluid solution. Calibration curves are required to correlate the peak FFT value over the range of expected specific gravities and solute concentrations in the selected structure. A reported relative uncertainty of better than 0.5 % was given for a solution of distilled water and salt. This is therefore a method for density measurements based on the measurement of the sound speed, and suffers the same limitations reported in Chapter 4.2.

4.6.2. Swept Frequency Acoustic Interferometry

Swept-Frequency Acoustic Interferometry (SFAI) is a non-intrusive liquid characterization technique developed specifically for detecting and identifying liquids inside sealed munitions. This method is described by Sinha [104] and by Sinha and Kaduchak [105]. It is primarily a frequency domain method where the density is determined based on parameters extracted from the characteristics of the standing wave pattern as observed by a receiver transducer. According to Sinha and Kaduchak [105], this method was developed with the goal to derive sound speed, attenuation and density with sufficient accuracy and resolution to be useful for practical applications; it was not meant for high-accuracy acoustic characterization. Typical relative uncertainty for a given set of measurements was for sound speed 0.5 %, whereas for attenuation and density the values were about 3 % and 5 %, respectively. This method therefore has applications within fluid characterization.

In private communication with Sinha [106], he indicates that it should be possible to obtain a relative uncertainty of measured density of better than 1 % using this method. The schematic representation of the used apparatus is given in Fig. 4.16.

This approach is commercially available [107] within the field of detecting contaminants in the water system.

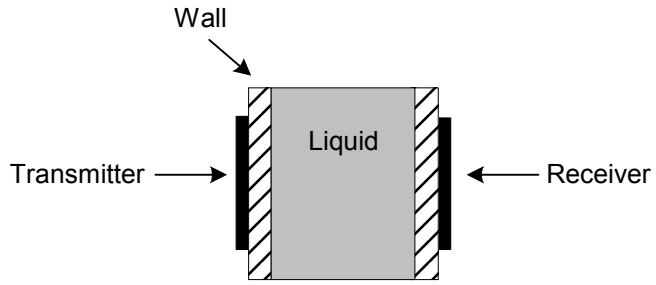

Figure 4.16. Schematic representation of the SFAI approach [105].

4.7. Various other approaches

4.7.1. Impedance loading of the pipe wall

Bamberger and Greenwood [108]–[110] proposed recently the concept of impedance loading, which simply means that an ultrasonic transducer clamped to a solid plate or wall in direct contact with the fluid to be measured, experiences different ring-down behavior depending upon the characteristics of the fluid. The schematic representation is given in Fig. 4.17. Depending upon the acoustic impedance of the fluid and of the transducer, with respect to the acoustic impedance of the solid plate, the ring-down characteristics of the solid plate when interrogating the plate with a short pulse will depend on the acoustic impedances. As the reflection process against the transducer depends upon the transducer internals and the coupling layer between the transducer and the plate, this method is not believed to be very accurate. Also, if the transducer needs to be remounted between measuring on different liquids, one faces the problem of calibration. Preliminary tests performed at various liquid sugar–water solutions indicated a relative uncertainty within 8.7 %, for various water–kaolin slurries a relative uncertainty of 2.5 % was obtained, and for various water–sodium solutions a relative uncertainty of 1.35 % was obtained.

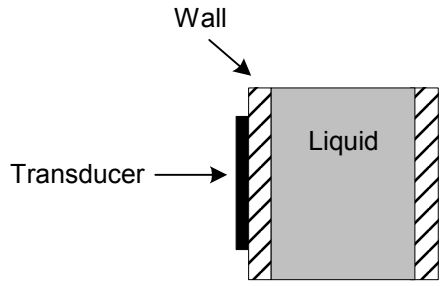

Figure 4.17. Schematic representation of the impedance loading method as used by Greenwood and Bamberger [110].

4.7.2. Levitation

Levitation means that a material in a fluid host media can be acoustically lifted or raised by using the radiation force to counterbalance the gravitational field [111]. This is a method primarily used on a drop of liquid for measuring the "compressadensity", a known function of the adiabatic compressability and the density of the liquid drop. A relative uncertainty of about 1 % was achieved [111], but the method is clearly not practical for use in an industrial environment as a density sensor.

4.7.3. Resonance loading

The electrical impedance of a transducer is affected by the radiation impedance of the transducer. Attempts have been made to see if the liquid density (or liquid acoustic impedance) could be extracted from the electrical impedance measurements. Shirley [112] tried to measure the acoustic impedance of marine sediments with this approach, but the varying environmental conditions were found to be of considerable significance. According to Lynnworth [113], this approach has been considered since 1955, but has not yet proven practical.

Also, a three-layered resonator has been used for the measurement of liquid density, where the liquid forms the middle layer [114]. The placement of the resonance frequencies change according to the sound speed and the density of the liquid as can be found from simulations of the sensor system. However, the relative uncertainty found was in the range of tens of per cent, and clearly indicated that this concept should be used in a more qualitative than quantitative way.

4.7.4. Backscattering

At least two different approaches regarding the use of backscattering applies to the measurement of density by acoustical means. In the medical research of osteoporosis, ultrasound has been used for obtaining the mechanical parameters of bone [115]–[117]. Correlations between the parameters sound speed, broadband ultrasound attenuation, and bone density are typically sought for. Clearly, this approach does not apply for liquids.

The other approach used involves the use of backscattered pressure from a wire immersed in a liquid, as the backscattered pressure depends on the liquid density [118]–[119]. To express this dependence, the classic resonant scattering theory is used. A relative measurement approach is used as measurements are performed using the same wire in both the liquid to be characterized and in a reference liquid. A relative uncertainty of 2 % was obtained.

4.8. Summary of acoustic methods for liquid density measurements

Based on the findings in this Chapter, the points that should be of particular attention for accurate liquid density measurements, can be stated as:

- The liquid density should preferably be measured as a primary parameter, without relaying on a given relation between different parameters, for instance a density–sound speed relationship, a density–temperature relationship, a velocity–density product, or an attenuation–density ratio.
- If possible, an approach where more parameters than just the density (and the sound speed) can be obtained would be beneficial for the sake of liquid characterization.
- A relative measurement approach should be used (e.g. based on measuring an amplitude ratio, and thereby the term “relative”) instead of an absolute approach (e.g. performing a single amplitude measurement which suffers from a larger influence from various systematic and random sources of noise), as the former approach can be performed with higher accuracy.
- For the buffer approaches: Use a reference path in which a part of the transmitted pulse in sensed. This has important benefits for the calibration process. Also, a single buffer separating the transducer and the liquid to be measured would be preferable due to improved sensitivity.
- Approaches involving additional interfaces between the acoustic transducer and the liquid to be measured (such as glue layers) should be avoided as this introduces additionally uncertainty.
- Liquid density should not be dependent upon the measurement of parameters that possess a high measurement uncertainty, i.e. attenuation or viscosity.

Part II Measurement approach

Chapter 5. Measurement approach

5.1. A new measurement approach

5.1.1. Line of recommendation

Based on the summary of Chapter 4.8, the ABC-method was found attractive due to its attributes, which are repeated here for convenience:

- More parameters than just the density (and the buffer- and the liquid sound speed) are measured. These are the reflection coefficient, the acoustic impedance, and attenuation. The adiabatic compressibility can also be found from the measured sound speed and the density, and this method therefore represents a potential to be used for fluid characterization purposes.
- Relative measurements are used, which presents higher accuracy than if absolute measurements were used.
- The buffer approach contains a reference path in which part of the transmitted pulse is sensed. A single buffer separating the transducer and the liquid is used, which is advantageous with respect to the sensitivity.
- The acoustical coupling between the transducer and the buffer does not contribute in the process of obtaining the reflection coefficient, as the buffer–transducer interface does not take part in the reflection process leading to the reflection coefficient. However, the sound field is influenced to a certain degree by the acoustical coupling, which therefore has consequences for the diffraction correction.
- The echo-amplitude ratios are in principle not affected by operating the transducer away from its resonance frequency [65].
- Both the sound speed and the reflection coefficient results from an integral measurement, meaning that the echo signals used in the calculation process do not come from spot measurements (i.e. only at the buffer–liquid interface), but results from propagation through the whole path length for a certain number of times.

The ABC-method does however present some disadvantages. These can be stated as:

- It is subjected to interference mainly from the buffer ring-down if a thin buffer is used, and mainly to mode conversion if a thick buffer is used.

This may corrupt the amplitudes necessary for the calculation of the reflection coefficient.

- As three echo signals are used for the calculation of the reflection coefficient, the second and the third echo signal may be subjected to severe attenuation. This may result in a substantial loss if a given combination of long path length, high measurement frequency, and a liquid with a high attenuation is used.
- A somewhat low sensitivity may be obtained, depending upon the buffer material used, as typically a high impedance material is used to enclose the liquid. This means that widely differing amplitude signals are expected between the echo signal resulting from the buffer–liquid interface and the echo signals traversing the liquid path. This has consequences for the effective bit resolution of the individual echo signals acquired.

In an attempt to reduce these disadvantages, a measuring cell containing two buffers enclosing the sample liquid in a symmetrical manner is proposed, using an acoustic transducer connected to each of the buffer rods, as shown in Fig. 5.1. The advantages of the proposed approach as compared to the ABC method are partly the topics of Paper I and Paper II.

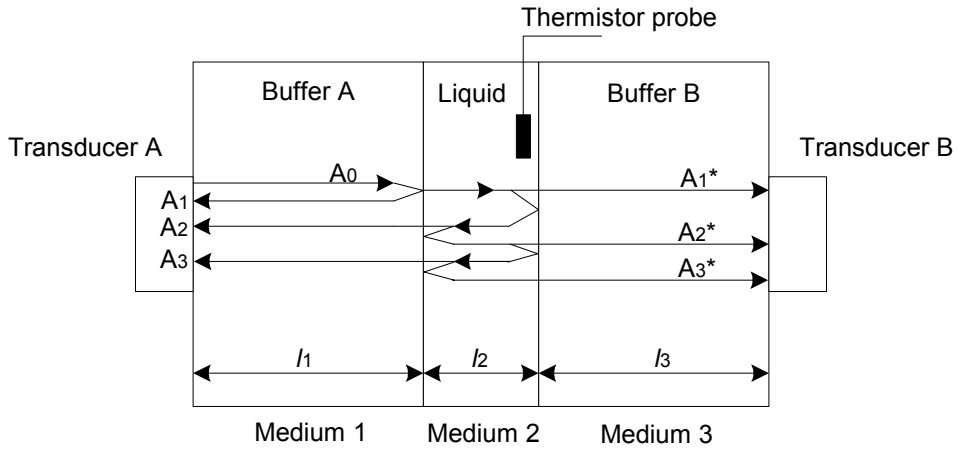

Figure 5.1. Schematic representation of the proposed class of methods, where some, or all, of the indicated echo signals, are exploited. Only the operational mode of using Transducer A for transmission is indicated.

5.1.2. Thin- versus thick buffer

The thickness of the buffer affects the characteristics of the measuring cell, as interference effects due to the buffer must be considered. These effects are mainly due to two different contributions, namely 1) the ring-down characteristics of the buffer, and 2) the effect of mode conversion at the buffer–liquid interface. This latter effect is further discussed in Paper II, and in Chapter 5.2.3.

However, in order to obtain the influence of the ring-down characteristics due to the buffer thickness on the echo signals, the electrical circuit simulator program *PSpice* was used according to Fig. 5.2, in which lossless plane wave propagation in all the media, including the transducer, was assumed. *PSpice* models of acoustic transducers and propagation media, including loss, are known [120]–[122], but were not considered necessary for the illustration purposes intended here. The simulation parameters are given in Table 5.1, for a burst mode using 5 periods at a frequency of 5 MHz. The *PSpice* code used is given in Appendix A.

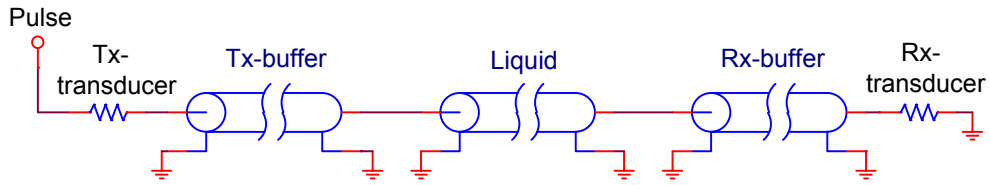

Figure 5.2. Lossless *PSpice* simulation model of the acoustic measuring cell.

Table 5.1. Simulation parameters.

	c [m/s]	Z [10^6 kg/m^{2}s]	l [10^{-3} m]
Transducer	–	2	∞
Buffer	6450	17	80 (thick buffer) and 8 (thin buffer)
Liquid	1500	1.5	5.7 (thick buffer) and 30 (thin buffer)

For the thick buffer approach, the echo signals are as in Fig. 5.3. There it is seen that the echo signals arising from the buffer–liquid interface used in the calculation for the ABC-method appear before the signal that has traversed twice back and forth in the buffer. This means that the buffer ring-down characteristics do not influence the sought echo signals, and maximum pure signals can be obtained, if the buffers used are thick enough.

For the thin buffer approach the situation is different, as the buffer ring-down must be settled to a level leaving a negligible contribution to the characteristics of the sought echo signals, see Fig. 5.4. As the buffer typically has low attenuation, the reflection characteristics at its interfaces govern the rate of the ring-down. This way, the acoustic impedance of the transducer as seen by the buffer is then a factor of great importance, along with the acoustic impedance of the liquid relative to that of the buffer material. Also, the correct identification of the echo signals may be troubled by the fact that the first echo signal in a group of buffer ring-down signals is not necessarily the highest amplitude echo signal in that group, but the first is the sought echo signal to be used in the calculation of the reflection coefficient. From plane-wave simulations, it has been found that the ratio of the acoustic impedance of the transducer to the liquid determines whether the first echo signal in a group is the highest amplitude signal or not.

In addition to these aspects, mode conversion may appear at the buffer–liquid interface and may introduce additional interference. Based on these considerations, the use of thick buffers seems beneficial to using thin buffers, and will be used for the further study.

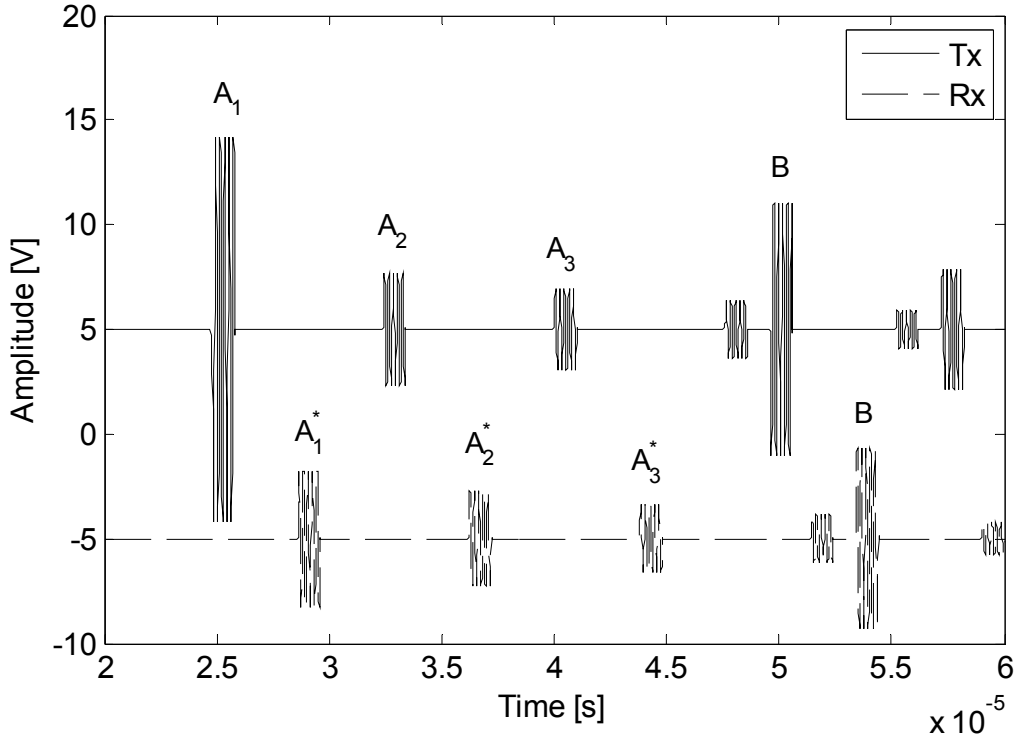

Figure 5.3. Simulation of echo signals using thick buffers. The buffer multiples are indicated by signals B. A buffer thickness of 80 mm was used, along with a liquid path length of 5.7 mm. The echo signals from each transducer are offset for clarity. Note that the transmit signal is not shown.

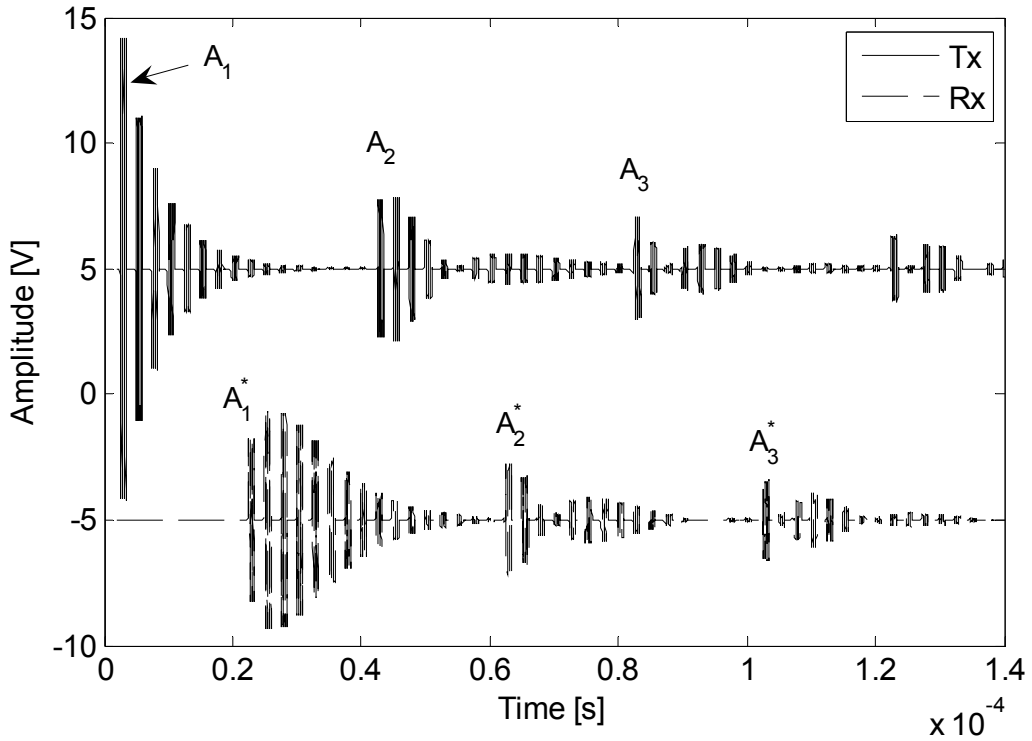

Figure 5.4. Simulation of echo signals using thin buffers. A buffer thickness of 8 mm was used, along with a liquid path length of 30 mm. The echo signals from each transducer are offset for clarity. Note that the transmit signal is not shown.

5.1.3. Aspects of using two transducers instead of one

By using two transducers as in Fig. 5.1, the reflection coefficient can be obtained by combining the echo signals in a variety of ways, as shown in Paper I. This holds even when assuming a maximum of three echo signals arising from the buffer–liquid interface, as for the ABC-method. Two different generic approaches were found. These are the relative amplitude approach, which bear some resemblance to the ABC-method, and the mixed amplitude approach. A detailed description of these approaches is given in Paper I.

By using two transducers some aspects will change relative to the ABC-method, which uses one transducer. These are:

- Influence from mode conversion at the buffer–liquid interface.
- Liquid path length (dimensional considerations).
- Measurement uncertainty.
- Effect of attenuation.
- Effect of bit resolution.

- Reduced acquisition record length as fewer echo signals may be used (the benefits of this is however dependent upon the specific acquisition system used).
- Amplitude quality indicator of the measured signals.
- Redundancy characteristics.
- Ratio of the transducer's sensitivity in receive mode.
- Ratio of the acquisition channel's sensitivity in receive mode.

These aspects will be discussed in Chapter 5.2 and in Papers I–II. Some experimental results concerning the amplitude quality indicator and the sensitivity factors are also given in Chapter 6.5.

5.2. Measurement cell

A detailed discussion regarding the dimensions of the proposed measurement cell is given in Paper II, where the details concerning differences between the proposed echo12_12 method (see Papers I–II, which uses only the two first echo signals on both transducers) and the ABC-method are given. The most important aspects that must be discussed are the effect due to mode conversion, the buffer material, the dimensional considerations, and the uncertainty characteristics.

5.2.1. Assembly

A detailed assembly drawing and a sectional drawing are given here in order to give a clear view of the mechanical design of the measuring cell, see Figs. 5.5–5.7. These drawings are not to scale compared with the used measuring cell, as the drawings are based on a buffer dimension of 50 mm in thickness and with a diameter of 140 mm, but the measurement results that are presented in this work are based on a modified measurement cell with a buffer dimension of 80 mm in thickness and with a diameter of 205 mm in order to properly account for the mode converted echo signal. Two different centre sections in the measuring cell were used enabling liquid path lengths of 5.7 and of 2.4 mm, see Chapter 5.2.3. A picture of the used measuring cell is given in Fig. 5.8.

The assembly is performed using rugged spacers keeping the liquid path length fixed. The measurement cell is tightened using a wrench to a torque of 28 Nm. Each part of the measurement cell is marked in order to obtain the same position of the components for each assembly. In these figures, a possibility to establish a liquid

flow is indicated (see Fig. 5.7), but this was not the case for the modified cell used in this work.

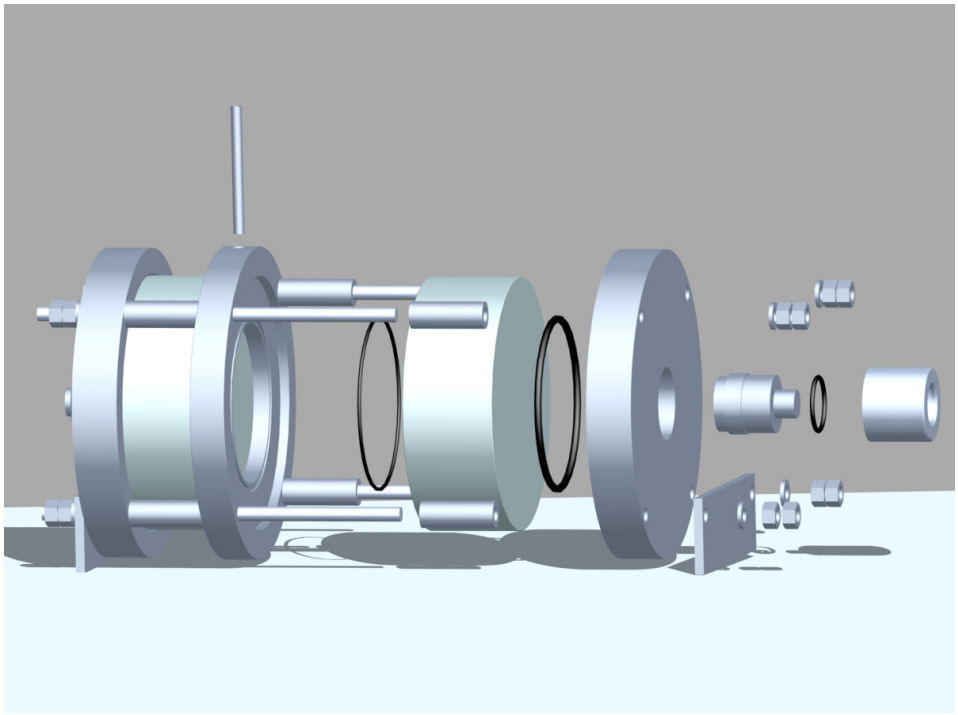

Figure 5.5. Exploded assembly drawing of proposed measuring cell.

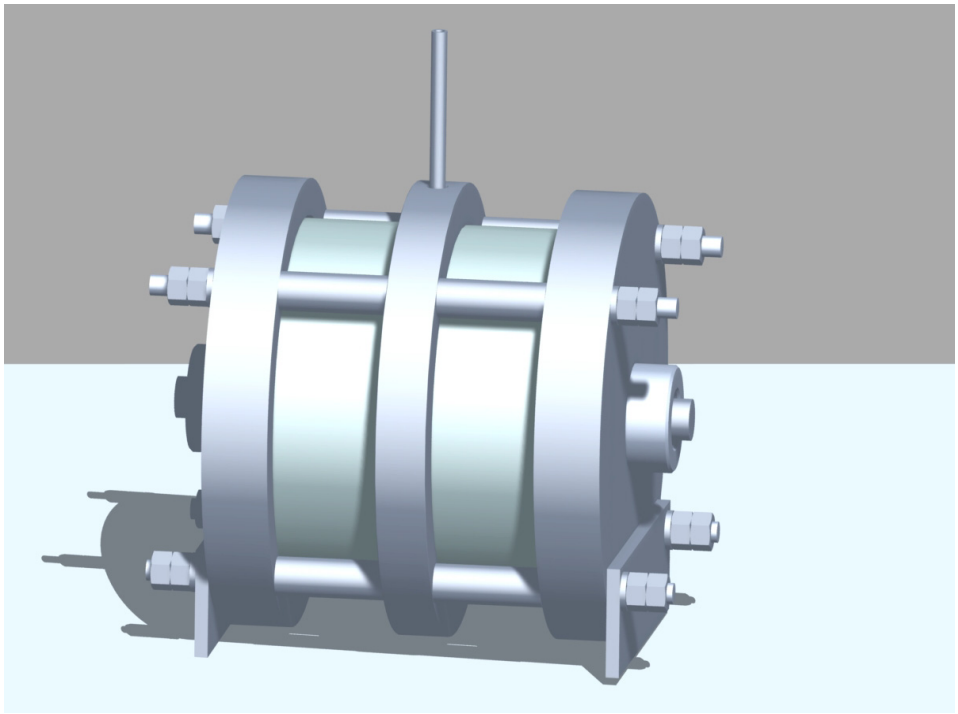

Figure 5.6. Assembly drawing of proposed measuring cell.

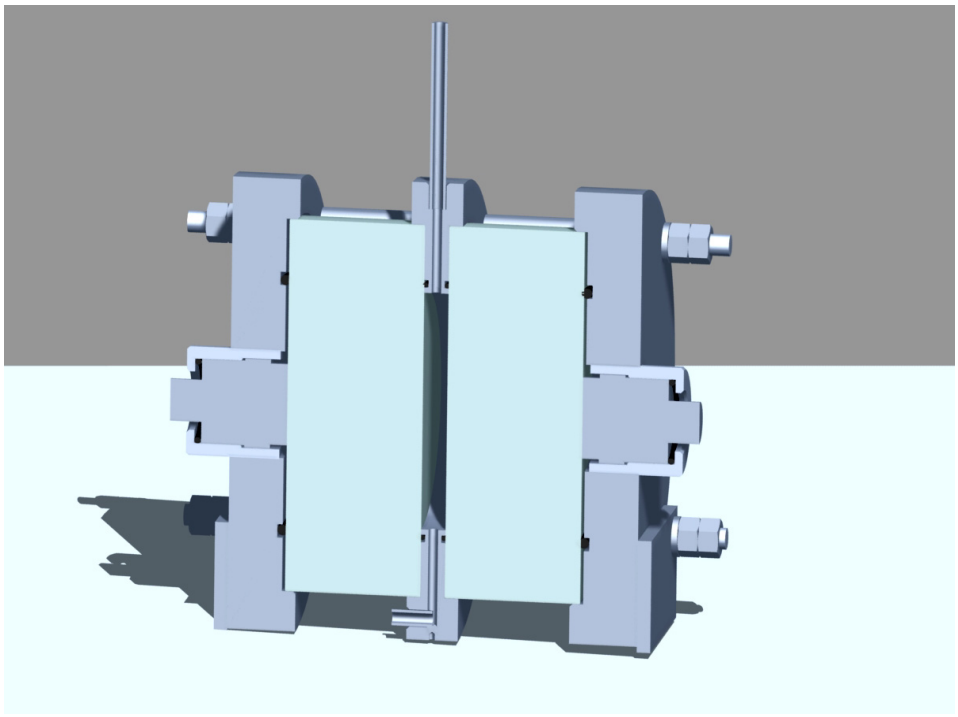

Figure 5.7. Sectional drawing of proposed measurement cell.

Figure 5.8. Picture of the used measurement cell. There is not a possibility of flowing a liquid through this measurement cell, in contrast to Fig. 5.7.

5.2.2. Buffer material

When a buffer material is to be chosen, several aspects must be considered. Durability, robustness, and sensitivity are considered the most important. If a material with low acoustic impedance such as Perspex is used (Z=3.2·10^6 kg/m^{2}s) [123], in which the acoustic impedance is of the same order as the liquids to be measured, a high sensitivity is obtained, as shown by Püttmer [76]. However, concerns regarding chemical damage and mechanical distortion due to absorption of water or other solvents may be raised. Therefore, a medium acoustic impedance material such as aluminum (quality 6082-T6) was selected due to its easy machining, although the durability would be compromised if it was exposed to water for an extended amount of time. This material has much the same acoustic parameters as the quartz glass and the glass ceramic material Zerodur, which have been found suitable for acoustic measurement of liquid density using a buffer-rod configuration measurement cell [124].

5.2.3. Dimensional considerations

In this section, the possible length of the liquid layer between the two buffers is addressed. The goal is that the echo signals A_1, A_2, and A_3 do not interfere with each other or with other signals like the mode converted signal or the multiple buffer signal. The possible combinations of echo signals durations and liquid layer lengths will be identified.

By considering disturbance effects arising in the propagation direction, the mode conversion seems to be the most important, assuming a negligible contribution due to scattering in the buffer. Then, interference between the mode converted echo signal and the echo signals arising from reflections at the buffer–liquid interface must be avoided, as discussed in Paper II. This is solved by placing the mode converted echo signal either after the sought echo signals, or by placing it in between the echo signals. By using the theoretical considerations in Paper II, these approaches led to the allowed liquid path length versus echo signal duration as given in Fig. 5.9 and in Fig. 5.10, for the ABC-method (and the other methods including the third echo signal on either transducer) and for the echo12_12 method (and the other methods including not more than the second echo signal on either transducer), respectively. The lines increasing versus echo signal duration means *larger* than, and the lines decreasing versus echo signal duration means *less* than. When combined, these lines make restricted areas where the allowed ranges of liquid path lengths are given, as shaded regions. In these figures, a range of liquid sound speeds of 1100 to 1550 m/s was assumed. This means that a wide range of liquids is covered, including water and quite a lot of different oils. The simulation parameters of the buffer materials are given in Paper II as 6450 m/s and 3085 m/s, for the compressional, and for the shear sound speed, respectively. The thickness of the aluminum buffers was 80 mm.

Two allowed (low-noise) areas are identified in each figure. For the ABC-method shown in Fig. 5.9, the lower area (1) is restricted by the requirement of non-

overlapping liquid echoes and that the A_3 echo signal appears before the mode converted signal. The upper area (2) is restricted by the requirement of the appearance of the A_3 echo signal before the buffer multiple signal, and that the mode converted signal appears before the A_3 signal.

For the echo12_12 method, the situation is as given in Fig. 5.10, the large lower area (1) is restricted by the requirement of non-overlapping liquid echoes and that the A_2 echo signal appears before the mode converted signal. The upper area (2) is restricted by the requirement of the appearance of the A_2 echo signal before the buffer multiple signal, and that the mode converted signal appears before the A_2 signal.

From these figures, it can be understood that the echo12_12 method can be used with a larger liquid path length and with an increased signal duration than the ABC-method. It should also be noted that a greatly increased flexibility both with respect to the liquid path length and to the signal duration occur if the effect of the mode converted signal can be neglected. This will be further discussed in Chapter 6.6.2.

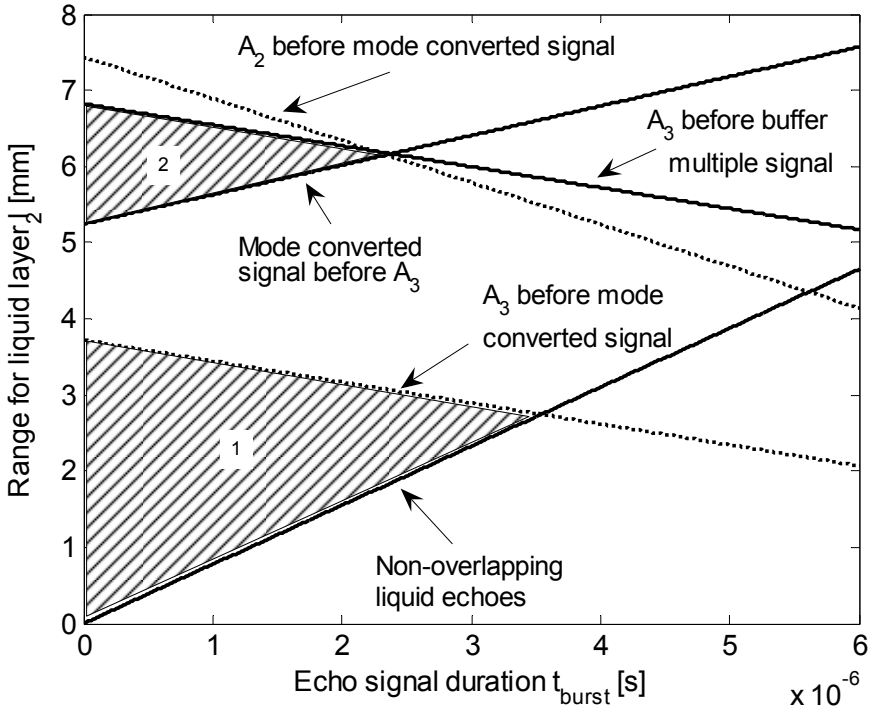

Figure 5.9. Liquid path length versus echo signal duration assuming a range of liquid sound speed of 1100 to 1550 m/s, for the ABC-method. Limitations due to mode conversions are shown with dotted lines. The shaded areas are the regions where interference between the signals is avoided.

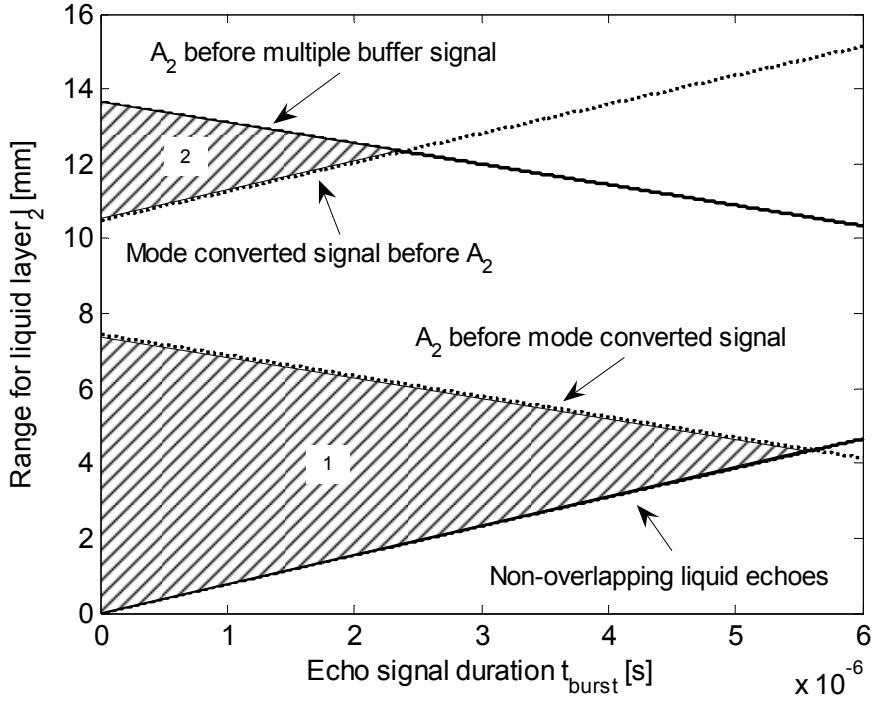

Figure 5.10. Liquid path length versus echo signal duration assuming a range of liquid sound speeds of 1100–1550 m/s, for the echo12_12 method. Limitations due to mode conversions are shown with dotted lines. The shaded areas are the regions where interference between the signals is avoided.

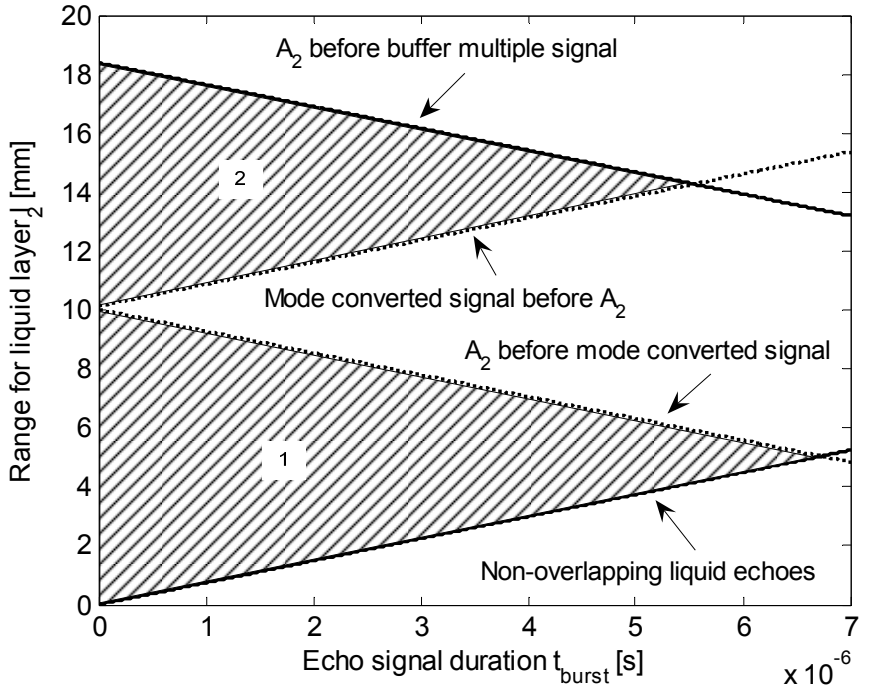

Figure 5.11. Liquid path length versus echo signal duration assuming a range of distilled water sound speeds of 1482.4–1496.7 m/s, corresponding to a temperature range of 20 to 25 °C for the echo12_12 method. Limitations due to mode conversions are shown with dotted lines. The shaded areas are the regions where interference between the signals is avoided.

However, if a reduced range of sound speeds could be assumed, an increased range of liquid path length could be obtained. As an example of this, consider distilled water in a temperature range of 20 to 25 °C, resulting in a range of sound speeds of 1482.4–1496.7 m/s [46]. The results for the echo12_12 method is given in Fig. 5.11, where it is seen that both the upper and the lower areas are significantly increased compared to Fig. 5.10, in which a much larger range of sound speeds was assumed.

5.2.4. Aspects of non-ideal instrumentation on dimensional considerations

A certain amount of crosstalk was observed on the oscilloscope traces. This may stem from the combined effect from the cables, the unshielded custom made electronics, and from the minimum claimed channel-to-channel isolation of 40 dB of the oscilloscope (assuming channels at the same V/div sensitivity).

Such crosstalk may corrupt the amplitude measurements of the sought echo signals. Two different cases must be considered:

- The echo signals originating from the buffer–liquid interface must not interfere between the transmit (Tx) channel and the receive (Rx) channel.
- The Tx-buffer multiple signal must not interfere with the A_2^* signal for the echo12_12 method.

In order to show how such interference may appear, the relevant equations will be stated. For the first case, the relevant equation can be given as

$$l_2 > c_2 \cdot t_{burst}, \tag{5.1}$$

where c_2 is the liquid sound speed, l_2 is the liquid path length, and t_{burst} is the combined duration of the transmit burst and the transducer ring-down. For the second case, the liquid path length must satisfy

$$l_2 < \frac{c_2}{3}\left[\frac{2l_1}{c_1} - t_{burst}\right], \tag{5.2}$$

where c_1 is the sound speed of the buffer material.

A typical example of such crosstalk is given in Fig. 5.12, where a level of crosstalk from the Tx-channel to the Rx-channel of –40 dB was measured. In the reverse direction, the measured level was –48 dB. The reason for this difference in level of crosstalk is not clear.

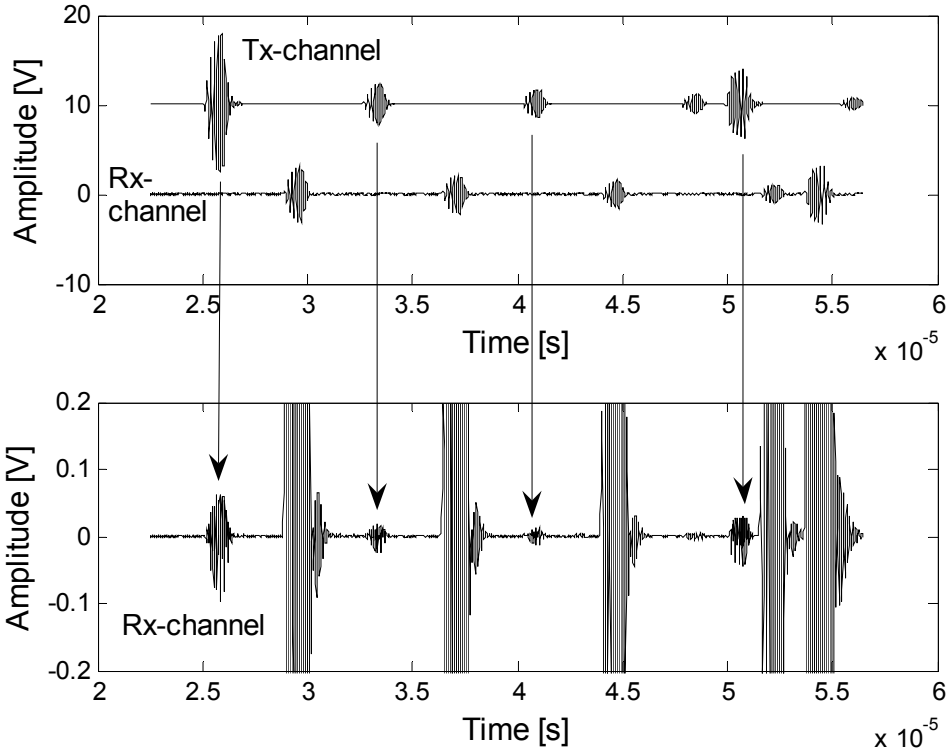

Figure 5.12. Example of measured crosstalk from the Tx-channel to the Rx-channel using water in the 5.7 mm measuring cell. The frequency used was 6 MHz in a 5 period burst mode. In the lower part of the figure, a zoom-in on the Rx-channel is shown.

In order to avoid the interferences described in this Section, the allowed liquid path length versus echo signal duration changes from those given in the preceding section. For the echo12_12 method, Fig. 5.10 of the preceding section gets modified as in Fig. 5.13. The lower area (1) of Fig. 5.10 is reduced, while the upper area (2) is completely lost. For the ABC-method, the situation is somewhat less dramatic. Fig. 5.9 gets modified as in Fig. 5.14, and only the lower area (1) is reduced. In these figures, only the changes from the preceding section are included.

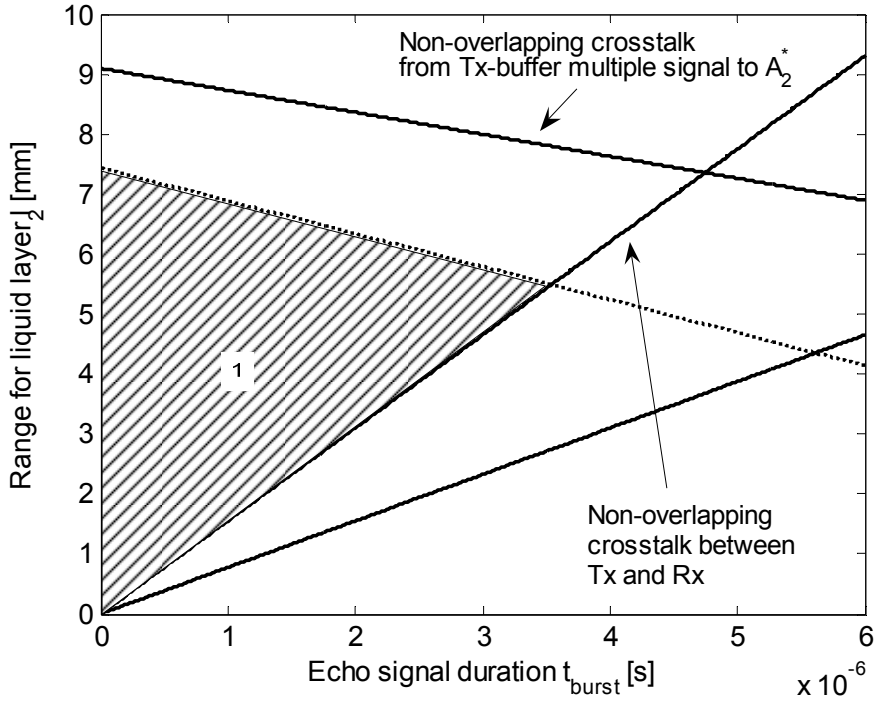

Figure 5.13. Liquid path length versus echo signal duration assuming a range of liquid sound speeds of 1100–1550 m/s, for the echo12_12 method, when limitations due to crosstalk are introduced. Limitation due to mode conversion is shown with dotted line.

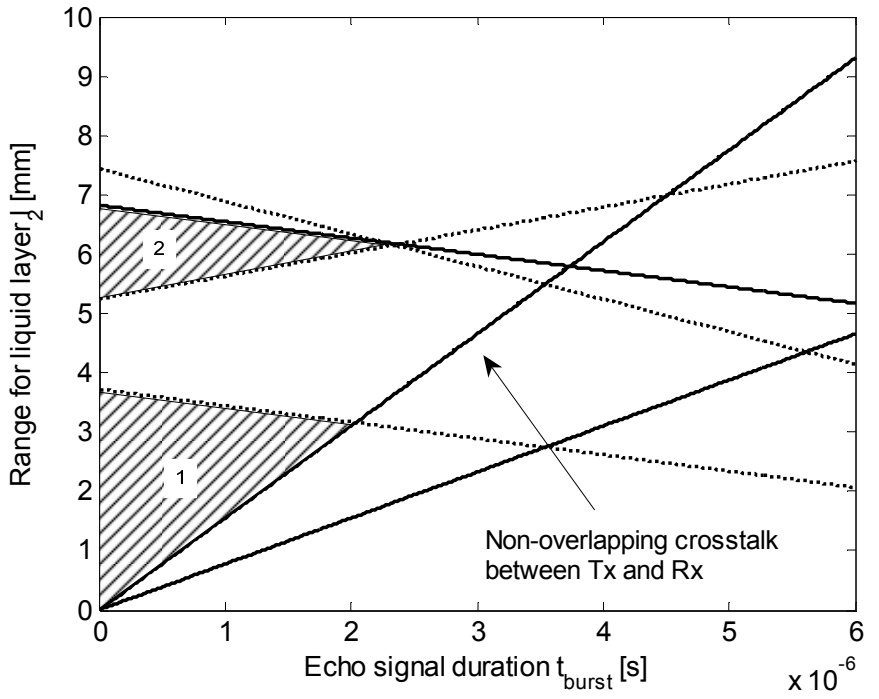

Figure 5.14. Liquid path length versus echo signal duration assuming a range of liquid sound speeds of 1100–1550 m/s, for the ABC-method, when limitations due to crosstalk are introduced. Limitations due to mode conversions are shown with dotted lines.

5.2.5. Uncertainty

It is the expanded relative uncertainty of the liquid density that is dealt with in this Section. This is in contrast with the total uncertainty, which depends upon the choice of instrumentation set-up. Here, the effect of bit resolution when all the echo signals (a maximum of three for each transducer) are acquired simultaneously. This may give a good indication of the various methods characteristics.

As shown in Papers I–II, the expanded relative uncertainty as obtained by using the proposed echo12_12 method instead of the ABC-method is reduced to a significant degree, depending upon the liquid attenuation, as also shown in Fig. 5.15. At low values of liquid attenuation, the uncertainty of the ABC-method is about double the value of the echo12_12 method, but this ratio quickly increases for increasing liquid attenuation. Also, the echo12_12 method is seen to follow the lowest uncertainty and case-dependent echo123_123 method using six echo signals split equally on both transducers, as further discussed in Paper I. This behavior would, however, change if the acoustic impedance of the buffer material approached that of the liquid, as shown in Papers I–II.

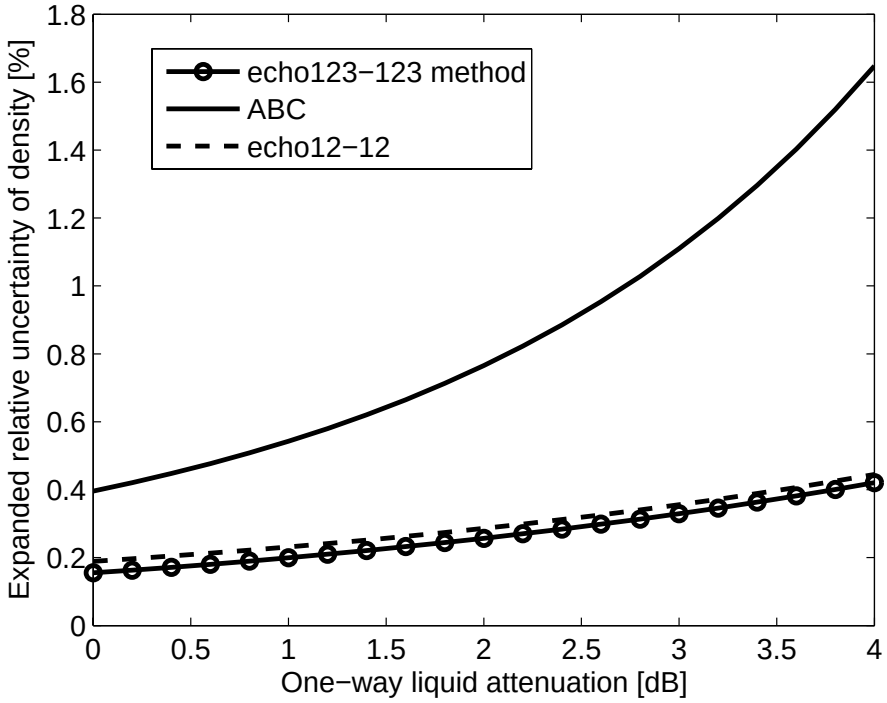

Figure 5.15. Calculated expanded relative uncertainty of the density for the echo12_12 method and the ABC-method compared with the lowest uncertainty echo123_123 method. All of these methods are of the relative amplitude approach. The parameters of the aluminum buffer and the liquid used are given in Table 5.1. The relative uncertainty of the sound speeds was 0.01 %. The uncertainty of the density for the buffer material was neglected. A bit resolution of 12 bits was assumed.

5.2.6. Amplitude quality indicator, sensitivity aspects, and redundancy characteristics

Typically, ultrasound measurement systems have few indicators of the quality of the measurements performed. Often, a transit-time or a sound speed measurement is performed, from which the measured values may indicate whether "sound" values, or not, are obtained. The control voltage of a variable gain amplifier (VGA) can be monitored, if such a device is used. This could indicate whether problems occurred regarding the electronics gain or with the attenuation characteristics of the media. If the acoustic signals are monitored by using an oscilloscope, some visual indications of the signal-to-noise-ratio (SNR) can be given, or the amplitude ratio of a given echo signal to a given coherent noise contribution may also be obtained. Berrebi [125] discusses how self-diagnostics can be used for error reduction for ultrasonic transit-time flow meters.

In the temporal domain, time information is sufficient to obtain a transit time or a sound speed. Such parameters are usually less dependent upon the SNR than parameters dependent upon the measurement of amplitudes, such as reflection coefficient and attenuation. In this work, methods have been devised concerning the quality of the measurements performed both with regard to the measurement of amplitudes, but also with respect to the characterization of the measurement system by utilizing acoustic measurement signals. Additionally, the improved redundancy characteristics of the proposed approach relative to the ABC-method will be discussed.

Amplitude quality indicator

As the amplitudes of the acoustic echo signals directly affects the measured reflection coefficient, a test of whether the correct portions of the echo signals are exploited or not has been devised. This approach is based on the amplitude measurement of three consecutive echo signals as sensed by the receive transducer (or using an amplitude ratio from both transducers).

This is performed by forming the relationships for an amplitude quality indicator AQI as

$$AQI = \frac{A_1^*}{A_2^*}\frac{A_3^*}{A_2^*} = \frac{A_2}{A_3}\frac{A_2^*}{A_1^*} = \frac{A_2}{A_3}\frac{A_3^*}{A_2^*} \equiv 1, \tag{5.3}$$

which may be found by inserting for Eqs. (16)–(20) of Paper I. Any deviation from this amplitude quality indicator relationship may point to non-ideal behavior of the acquisition system, such as too low voltage resolution, too low temporal resolution, saturation effects in the preamplifier, or to non-ideal behavior of the waves traversing the liquid. This may be due to waveform distortion effects such as dispersion and attenuation. Additionally, systematic contributions due to diffraction and noise sources may contribute. Examples of measured amplitude quality indicator values are given in Chapter 6.5.

Sensitivity aspects in receive mode

By using measured amplitude information, two sensitivity ratios can be obtained. This demands, however, that the measurement cell is used in a bidirectional manner where first transducer A is used in pulse-echo mode with transducer B as a receiver, and then the operation is switched, with transducer B operating in pulse-echo mode and transducer A acts as a receiver. The details are given in Paper I.

The sensitivity ratios that are obtainable are:

- The ratio of the transducers sensitivity both being operated in receive mode.
- The ratio of the electronic channels sensitivity both being operated in receive mode.

The equations describing these ratios can be given by (see Paper I)

$$\left(\frac{R_A}{R_B}\right)^2 = \frac{A_1 B_1^*}{A_1^* B_1}, \tag{5.4}$$

and

$$\left(\frac{R_T}{R_R}\right)^2 = \frac{A_2^2 B_1}{A_1 A_2^* B_1^*}, \tag{5.5}$$

respectively. The R_A and the R_B factors describe the transducers sensitivity in receive mode, for the transmit transducer, and for the receive transducer, respectively, according to

$$R_{A,B} = \frac{\text{plane wave volt. ampl. from transducer A or B}}{\text{plane wave incoming press. ampl. at transducer A or B}}. \tag{5.6}$$

The R_T and the R_R factors describe the electronic channels sensitivity in receive mode, for the transmit channel, and for the receive channel, respectively, according to

$$R_{T,R} = \frac{\text{plane wave volt. ampl. after preamplifier of channel A or B}}{\text{plane wave volt. ampl. from transducer A or B}}. \tag{5.7}$$

Several aspects can be deduced from these sensitivity ratios. These include

- A check of the transducers sensitivity ratio versus time, including the quality of the acoustic coupling between the transducer and the buffer. Any changes versus time may point to a gradually deteriorating transducer, or to changes in the acoustic coupling between the transducer and the buffer.

- A check of the electronic channels sensitivity ratio in receive mode, which may indicate changes in the channels electrical loading conditions.

Such a beneficial behavior is to the author's knowledge not commonly seen in ultrasound measuring systems, and will be further discussed in Chapter 6.5.

Redundancy characteristics

In this work, redundancy is increased relative to the ABC-method due to

- Use of two transducers: Each transducer is able to measure the sound speeds of the liquid and the buffer material independently, even though only one transducer is used for transmission purposes. Then, averaging of measured sound speeds as obtained by both transducers may be performed.
- Bidirectional use of the measuring cell: The cell is operated in both directions in a sequential manner. This way, all the sensor components involved are given the same weight on the measurements. Therefore, an extended averaging process can be used, in which every measured parameter involved in the density measurement has been exposed to a bidirectional averaging process.

5.3. Acoustic considerations

In order to operate the proposed measuring cell for liquid density measurements, certain characteristics of the sensor components must be known, and some corrections must be applied. As large buffers are chosen, certain simplifications arise, particularly in connection with the aspects of mode conversion and diffraction correction, as also discussed in Paper II.

5.3.1. Transducer

As seen in Fig. 5.9, the allowed duration of the echo signals exceed 2 μs if liquid path lengths of 2.4 mm or 5.7 mm are to be used, even assuming a large range of liquid sound speeds (1100 m/s to 1550 m/s). In order to obtain such a short echo signal duration, a commercial broadband transducer was sought. An immersion type large diameter case style Panametrics transducer was chosen [126] due to its specified waveform duration versus –6 dB bandwidth characteristics. Transducers with centre frequencies of 2.25 MHz (type V304-SU) and of 5.0 MHz (type V307-SU) were used

in this work. The 5.0 MHz transducers compliance sheets are given in Appendix B. In order for the 2.25 MHz transducer to be operated with a waveform duration within given limits, a few periods were used in the transmitted burst. The element diameter of the transducers used is 1".

5.3.2. Diffraction correction

In order to correct for the effects of diffraction, a proper correction factor D_C must be applied. The exact integral expression of diffraction using a plane, uniform, circular piston source and receiver, as given by Williams [127], is used for the calculations, according to Eq. (5.8)

$$D_C = 1 - \frac{4}{\pi} \int_0^{\pi/2} e^{ikz\left[1-\sqrt{1+\frac{4a^2}{z^2}\cos^2\theta}\right]} \sin^2\theta d\theta, \tag{5.8}$$

where k is the wavenumber, a is the radius of the plane piston, and z is the axial distance. This expression applies for calculating the diffraction correction in an isotropic, homogeneous medium exposed to a continuous acoustic radiation between two circular uniform transducers, with an axially concentric alignment and of the same size. A large number of publications have appeared on the subject of diffraction correction. A recently performed review regarding the history of diffraction correction is given in [128].

In using the proposed measuring cell, the various echo signals propagate through different media, such as acoustic coupling layer, buffer rods, and liquid path, and therefore the propagation media do not appear to be isotropic and homogeneous as the model assumes. However, since the propagation distances in the buffer rods are much larger than in the other media, the Papadakis method [129] was applied. This method is more fully described in [128]–[130], with the main aspects of this method being:

- The total propagation length is obtained by adding the propagation length of each media normalized by the Fresnel length of each media, where the Fresnel length is given as a^2/λ, in which λ is the wavelength, so that the diffraction correction is performed according to Eq. (5.8). The Fresnel length gives the last axial pressure maximum, and serves as the boundary between the nearfield and the farfield.
- The product kz is obtained using the wave number k of the buffer rod, as the difference of the propagation distance of the signal that has propagated back and forth in the buffer and the echo signals emanating from reflections including the liquid path length, are of the order of a few per cent.

The axial distance normalized to the last axial pressure maximum in the piston model, S, can be given as

$$S = \frac{z}{a^2/\lambda} = \frac{z \cdot c}{a^2 \cdot f}. \tag{5.9}$$

By inserting z from Eq. (5.9) into Eq. (5.8), one obtains

$$D_C = 1 - \frac{4}{\pi} \int_0^{\pi/2} e^{i\frac{S(ka)^2}{2\pi}\left[1-\sqrt{1+\frac{16\pi^2}{S^2(ka)^2}\cos^2\theta}\right]} \sin^2\theta d\theta. \tag{5.10}$$

The normalized axial distances for the various echo signals used can be expressed as

$$S_{A1} = \frac{2l_1 \cdot c_1}{a^2 \cdot f} \tag{5.11}$$

$$S_{A2} = S_{A1} + \frac{2l_2 \cdot c_2}{a^2 \cdot f} \tag{5.12}$$

$$S_{A3} = S_{A1} + \frac{4l_2 \cdot c_2}{a^2 \cdot f} \tag{5.13}$$

$$S_{A4} = 2S_{A1}. \tag{5.14}$$

These S-values are inserted in Eq. (5.10) for calculating the diffraction correction for the signals acquired by the transmit transducer. For the receive transducer, the corresponding equations read

$$S^*_{A1} = \frac{2l_1 \cdot c_1}{a^2 \cdot f} + \frac{l_2 \cdot c_2}{a^2 \cdot f} \tag{5.15}$$

$$S^*_{A2} = S^*_{A1} + \frac{2l_2 \cdot c_2}{a^2 \cdot f} \tag{5.16}$$

$$S^*_{A3} = S^*_{A1} + \frac{4l_2 \cdot c_2}{a^2 \cdot f} \tag{5.17}$$

$$S^*_{A4} = S^*_{A1} + \frac{2l_1 \cdot c_1}{a^2 \cdot f}. \tag{5.18}$$

The A_4 subscript indicates the buffer multiple echo signal, which is used together with echo signal A_1 for obtaining the sound speed in the buffer connected to the transmit transducer. For the buffer multiple echo signal, diffraction correction is only used in order to obtain a corrected sound speed, as the amplitude information from this signal is not exploited.

In order to show the influence of diffraction, a simulation example will be given which is considered realistic with regards to the dimensions of the measuring cell used. The same model for the diffraction correction as discussed above will be used. The input parameters are as in Table 5.1 for the thick buffer approach using the lossless *PSpice* simulation model of the acoustic measuring cell, as given in Fig. 5.2, using the following excitation parameters: f = 1–6 MHz, burst length = 5 periods. The normalized propagation distance, the *ka*-number in the buffers, the time advance and

the amplitude correction factor are given in Table 5.2 for the A_1 echo signal versus frequency, in order to more closely relate the obtained corrections to the used frequency range.

The simulated relative diffraction corrections for the sound speeds of the liquid and the buffer are given in Fig. 5.16. There, it is seen that the effect of the diffraction correction of the liquid sound speed contributes significantly less than that of the buffer sound speed. This is due to the short path length of the liquid layer relative to the buffer. The correction of the density based on the echo12_12 method and the ABC-method, due to diffraction is given in Figs. 5.17–5.18, where the contributions due to the liquid and the buffer sound speed, amplitudes, and the total contribution, are given. It is found that the amplitude correction is rather independent upon the frequency. This is due to the normalizing action of the relative amplitude approach. Therefore, the diffraction correction due to the sound speeds (in particular due to the buffer sound speed) dominates over the correction due to amplitude. Relative to 6 MHz, the correction due to sound speeds is seen to exceed 0.1 % for frequencies lower than about 3 MHz. The echo12_12 method is also seen to give a somewhat less correction for the density than the ABC-method.

Recently, it was shown by Lerch et al. [131] how the ABC-method could be used for estimating attenuation without having to resort to the use of diffraction corrections. This was obtained by using the transducer in water aiming against a reflector material to be characterized. The water path length was adjusted such that the diffraction effects were the same, and thereby cancelled, for each interface reflection involved. This approach, however, was not convenient in this work, due to the use of solid buffers.

Table 5.2. Diffraction correction parameters for the echo signal A_1 versus frequency.

Frequency [MHz]	S	ka in buffer	Time advance [s]	Amplitude correction
1	6.605	12.177	$1.761 \cdot 10^{-7}$	1.428
2	3.302	24.353	$5.575 \cdot 10^{-8}$	1.162
3	2.202	36.530	$2.288 \cdot 10^{-8}$	1.126
4	1.651	48.707	$1.411 \cdot 10^{-8}$	1.142
5	1.321	60.884	$1.124 \cdot 10^{-8}$	1.122
6	1.101	73.060	$7.946 \cdot 10^{-9}$	1.097

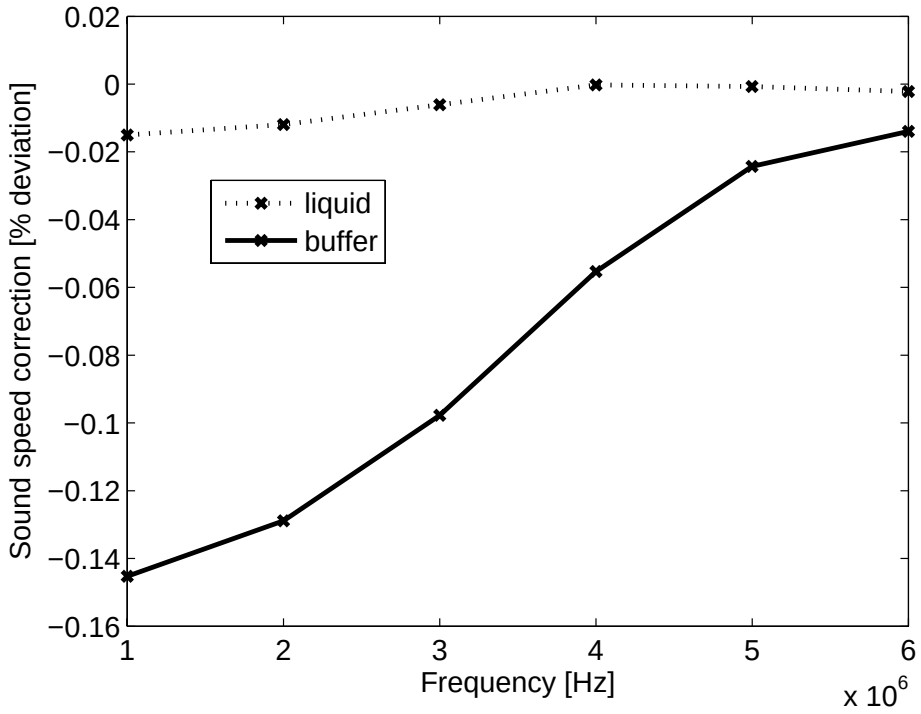

Figure 5.16. Simulated relative correction of the liquid- and the buffer sound speed versus frequency, due to diffraction.

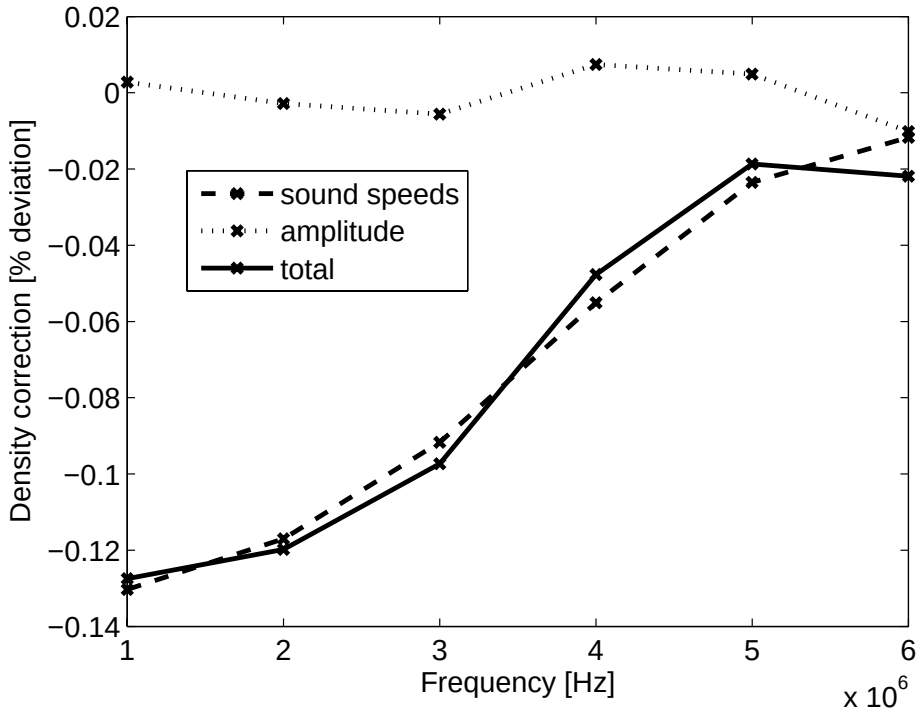

Figure 5.17. Simulated relative diffraction correction of the density for the echo12_12 method versus frequency, using a time domain processing approach.

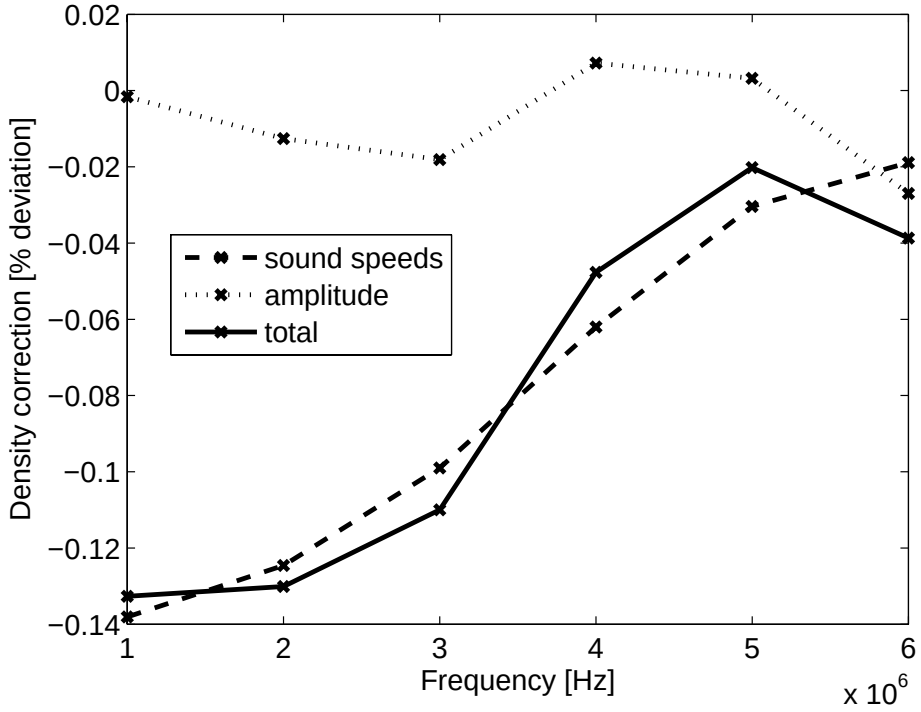

Figure 5.18. Simulated relative diffraction correction of the density for the ABC-method versus frequency, using a time domain processing approach.

5.4. Instrumentation set-up

The instrumentation used in this work is based on standard laboratory equipment, or off the shelf equipment, and consists of

- Agilent 33220A function generator.
- Panametrics V304-SU (2.25 MHz) and V307-SU (5 MHz) 1” immersion transducers.
- Agilent 54642A 500 MHz digital oscilloscope.

Additionally, some low noise amplifiers were designed and built, and also a switch arrangement was made that let the transmit transducer be terminated against the function generator, or disabled the connection between the function generator and the transmit transducer. The detailed electronic schematics and the components used are given in Appendix C. A more detailed description of this measuring system is given in Paper II. The measuring system is given schematically in Fig. 5.19. The measuring cell was placed in a thermostat regulated water bath keeping the temperature at a given level.

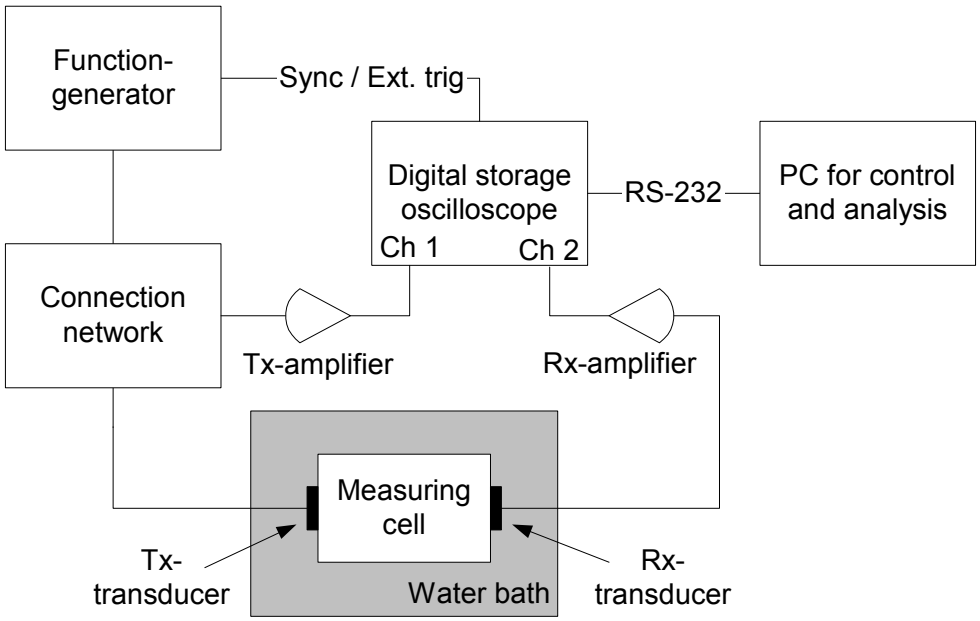

Figure 5.19. Schematic of the instrumentation set-up used.

The simplest possible form of the connection network consists of a direct connection between the function generator, the Tx-transducer and the Tx-amplifier, as shown in Fig. 5.20, where the 50 Ω output resistance of the function generator is indicated.

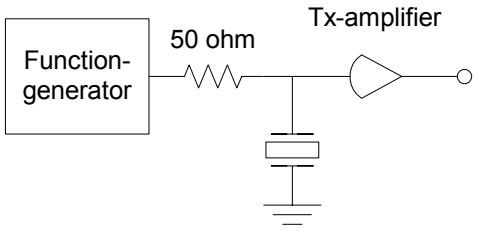

Figure 5.20. Direct connection between the function generator and the Tx-transducer.

However, the noise level experienced at the Tx-transducer using this direct connection network was seen to be quite high. The noise level was found not to be influenced by the excitation level directly, but by the range of the excitation level as correlated to some internal relay setting in the function generator. In order to improve the SNR, a switch arrangement was designed according to Fig. 5.21. The switching network consists of an arrangement of two switches connected in series with opposite action, with the Tx-transducer connection in-between. The operational mode of the switch arrangement is as follows: The Tx-switch is initially active, making a connection between the signal source and the Tx-transducer. After the source has fed the Tx-transducer with the predetermined number of periods the Tx-switch is opened and the Rx-switch is closed in order to let the echo signals be acquired. Then the Rx-

switch opens and the Tx-switch closes in order for the repeated cycle. The operation of the switches performs in a break-before-make mode.

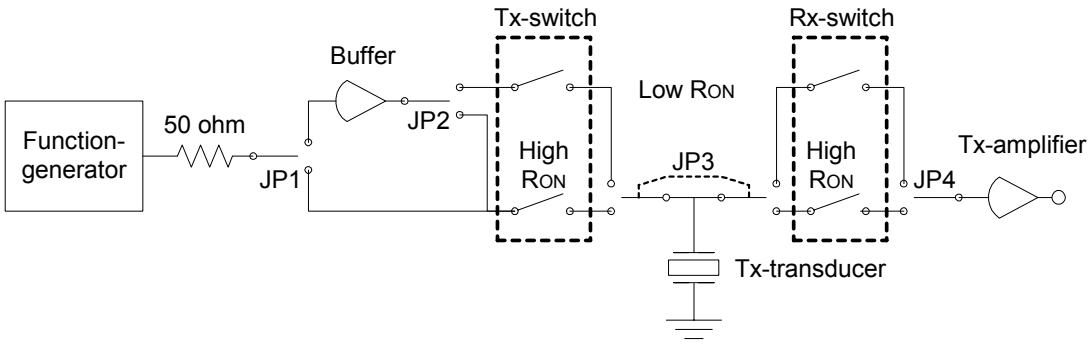

Figure 5.21. Schematic of the switching arrangement.

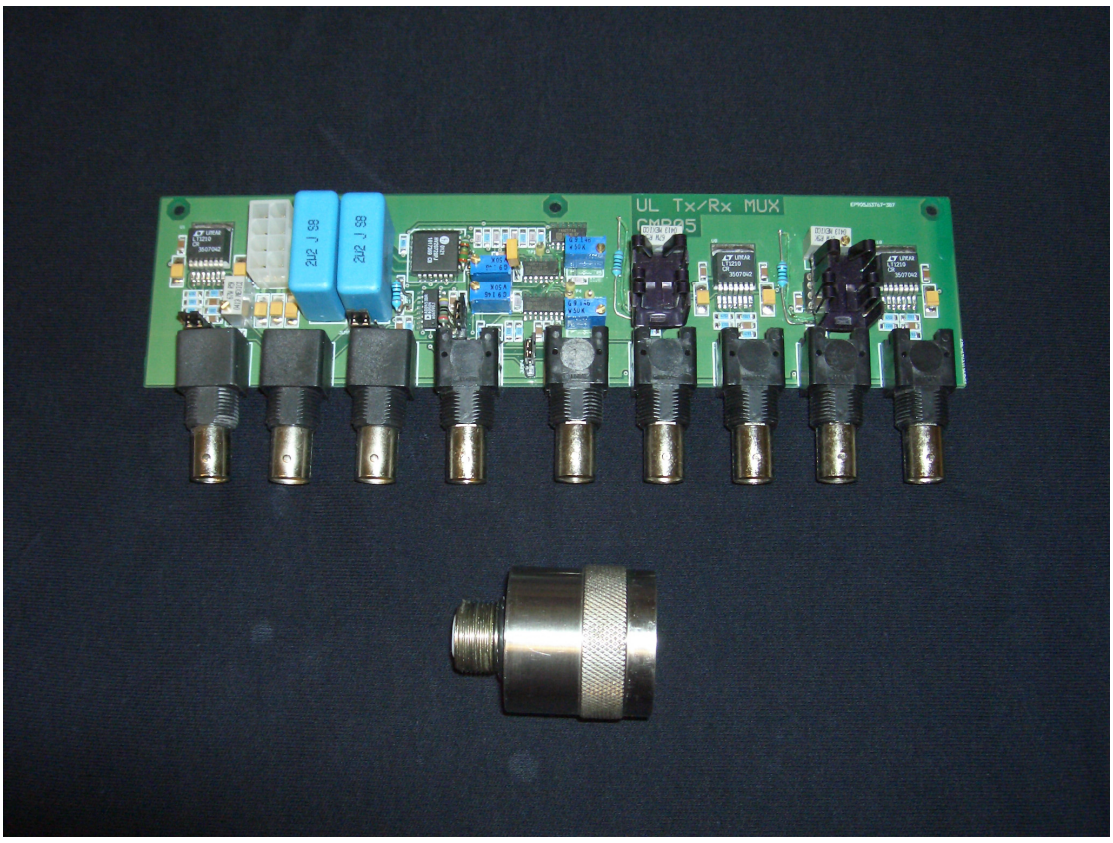

Figure 5.22. Picture of the electronics together with a transducer.

Two versions of the switching network are implemented; 1) a low on-resistance of 2 Ω (Analog Devices ADG453, two switches in parallel for each action) for excitation levels less than 30 $V_{p\text{-}p}$, 2) a switch with a much higher on-resistance of 22 Ω (Supertex HV20720) alleviating excitation levels in excess of 200 $V_{p\text{-}p}$, if used in direct mode without the function generator as the source. This switch however has quite long turn-on and turn-off times of 5 μs, which apply for a resistive termination

of 82 Ω across the transducer, as a compromise between sensitivity and DC-stabilization time after operation of the switches. A picture of the electronics used together with a transducer is given in Fig. 5.22. The operation of the Analog Devices ADG453 switch is given in Fig. 5.23, and the operation of the Supertex HV20720 switch is given in Fig. 5.24. Some jumpers (JP) are used in order to set the correct switching action. In addition a buffer amplifier with high current drive capacity (Linear Technology LT1210) was used to reduce the function generator's 50 Ω output resistance to a low value. Also, at the receiver end a low-noise preamplifier (Linear Technology LT1226) accommodated the signal levels, and a LT1210 buffer was used to drive some short length 50 Ω coaxial cables connecting to the oscilloscope inputs which were used in 1 MΩ input impedance mode.

In this configuration the following aspects must be fulfilled; 1) the preamplifier must be operated in the linear range of operation, and 2) due to the given offset range factor for the oscilloscope, the maximum echo signal must have a peak-to-peak voltage exceeding 200 $mV_{p\text{-}p}$/division, in order not to introduce severe overload on the Tx oscilloscope channel. This restraint does not apply for the Rx oscilloscope channel.

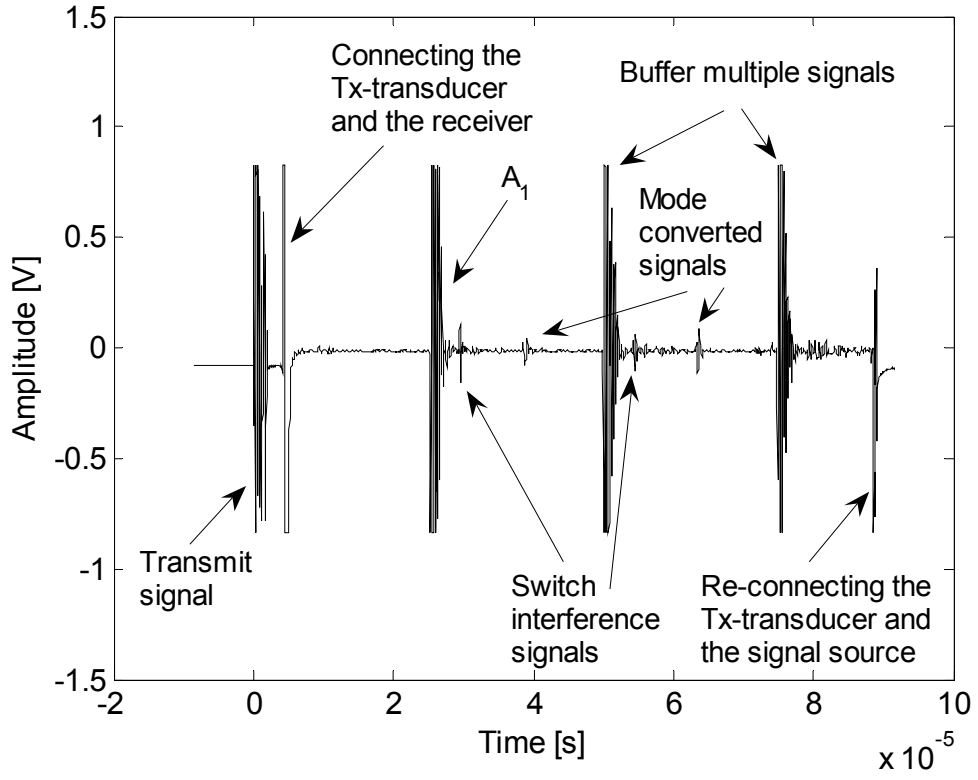

Figure 5.23. Action of the Analog Devices ADG453 switch on the transmit channel on an empty measurement cell. The interference of the switching action is evident.

Due to the low on-resistance of the ADG453 switch, the switching action generates due to charge injection small interference signals propagating back and forth in the measurement cell, which may interact with the desired signals. Both of

the switching actions may cause such interference; the disconnection of the Tx-transducer and the signal source, and the connection of the Tx-transducer and the receiver. The former cannot, however, be seen in Fig. 5.23, as it is hidden in the transmit waveform in this particular case. Due to the increased interference characteristics of this switch, it was used only in a preliminary phase.

The Supertex HV20720 switch was found not to be troubled with switching action induced interference. This must be attributed due to its higher on-resistance. No specification of its charge injection could be found in the datasheet. A limitation due to its long turn-on and turn-off times of 5 μs is the minimum thickness (or rather minimum propagation time) of the buffer. Using 80 mm of aluminium is close to the minimum in this application, as can be seen if zooming in front of the echo signal A_1 in Fig. 5.24 was performed. Results based on using the Supertex HV20720 switch are given throughout this work, unless otherwise stated.

After most of this work was performed, a switch was launched which seems as an ideal candidate for this application. This is the Analog Devices ADG1233/ADG1234 switch, with an on-resistance of 120 Ω with ultralow capacitance and charge injection. Such a switch would be able to perform in applications where both low glitch and fast settling are required.

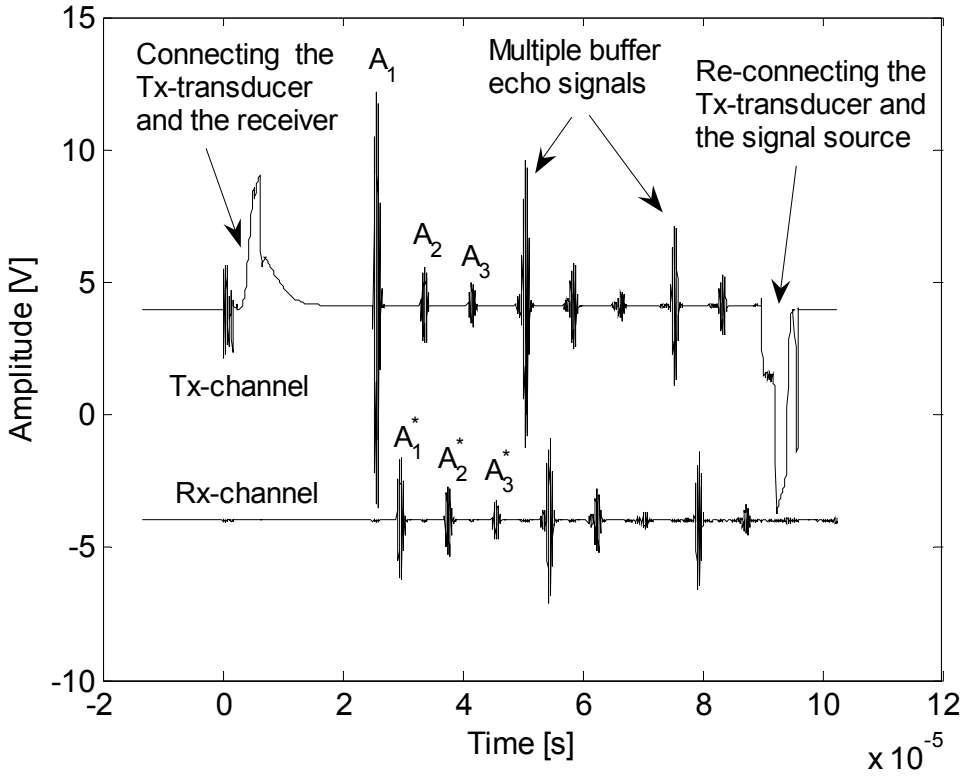

Figure 5.24. Action of the Supertex HV20720 switch on the transmit channel. The long on- and off times of the switch are evident. The liquid used was the Cannon N35 oil. The waveforms were offset for clarity.

As mentioned above, quite a high noise voltage was found when the function generator was used in direct connection with the Tx-transducer and with the Tx-amplifier, according to Fig. 5.20. This noise level can be seen in Fig. 5.25, where no averaging was applied. By using the switch network, the noise on the Tx-channel was reduced by a factor of 3–4. The noise at the Rx-channel was not found to change. It is believed that inserting an impedance matching transformer between the function generator and the Tx-transducer would reduce the observed noise voltage level.

When an averaging factor of 10 times was applied, the noise reduction factor for both cases (whether or not the switch) was about 7 for the Tx-channel and about 14 for the Rx-channel. A strict dependence according to $\sqrt{N}$ cannot be assumed, where N is the number of measurements performed, as the oscilloscope achieves a higher bit resolution when activating the average function. This deviation may be due to the oscilloscope actually performing 12 bits conversion even at such a low number of averaging.

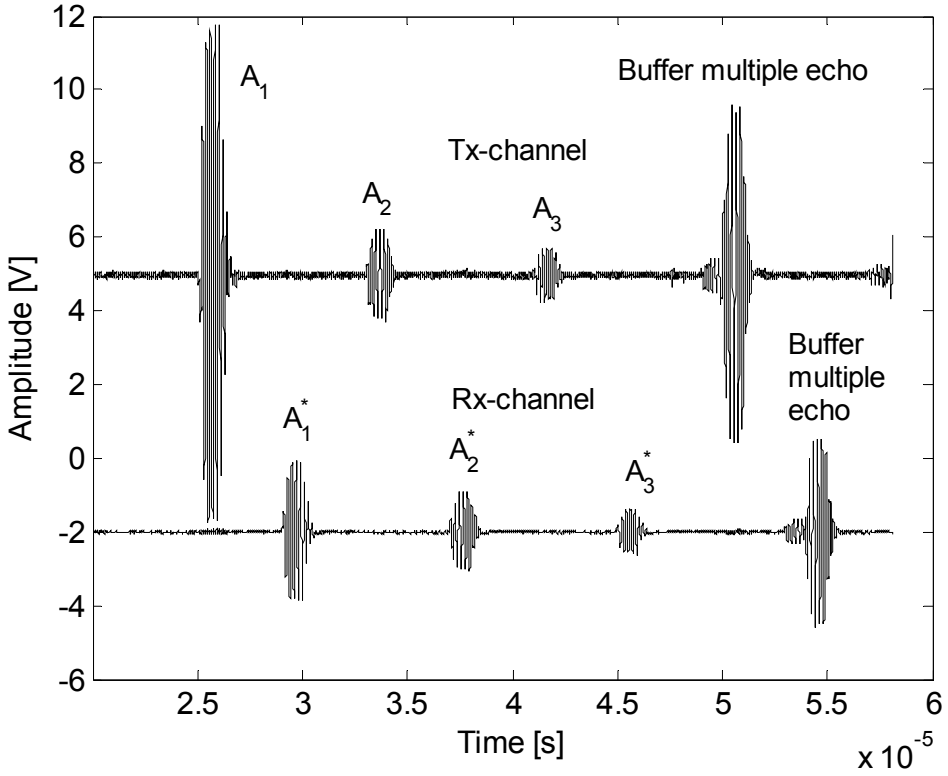

Figure 5.25. Noise on the transmit- and the receive channel when not using the switching network. No averaging on the oscilloscope was used. The liquid used was the N35 oil, where interference is seen to occur for the buffer multiple echo signal. The waveforms were offset for clarity.

5.5. Signal processing

In order to obtain useful information from the acquired echo signals as shown in the above figures, these signals must be processed. From the temporal and the amplitude characteristics of the measured echo signals, information about the liquid's and the buffer's sound speed can be obtained, in addition to the reflection coefficient at the buffer–liquid interface, and the liquid's attenuation. In this Section, different aspects of the signal processing are discussed. A more theoretical discussion on the subject of signal processing is given in Paper II, where also simulation results are included.

5.5.1. Least squares sense cubic spline approximation

As the oscilloscope can only output 2000 measurement points when used in average mode, a least squares sense cubic spline approximation was used to improve both the temporal- and the vertical resolution. A processed, cubic spline temporal resolution of 1 ns was typically used. This cubic spline approximation avoids at the same time the situation of nearby samples having the same voltage value, which could trouble the procedure used for obtaining the sound speeds. As the oscilloscope outputs 12 bits of vertical resolution in average mode, it should be understood that the least squares sense cubic spline approximation performs an approximation based on the 12 bits of input data, and would be improved if an increased vertical resolution of the input data was available.

5.5.2. Sound speed

The measured sound speeds of the buffers and of the liquid are obtained from the temporal characteristics using a matched waveform procedure. This simply means that the echo signals are compared in a manner that lets the same period in the various echo signals be identified. It should also be noted that the A_1 signal gets inverted, due to the acoustic conditions at the buffer–liquid interface. Then, the liquid sound speed can be obtained if the propagation path length is known, according to

$$c_2 = \frac{2l_2}{t_{A2} - t_{A1}} = \frac{2l_2}{t_{A3} - t_{A2}} = \frac{4l_2}{t_{A3} - t_{A1}}. \tag{5.19}$$

Equation (5.19) is given for the signals on the transmit transducer, but the equal situation exists for the signals on the receive transducer. In this work, the matched waveform procedure uses a time delay set independently for each of the eight echo signals used (four for each transducer). Also, a common voltage threshold is used. Then, the individual echo signals may be correctly identified.

Various representations of the liquid sound speed are calculated based on using the different echo signals. This serves two purposes: 1) Control of the matched waveform parameters as the same sound speed shall be obtained independent of

which echo signals are used in the calculation process, 2) Averaging of the measured sound speed may be performed by using more representations. This last point applies however only to the liquid sound speed. In this work, only the two first echo signals on each transducer are used for obtaining the liquid sound speed, whereas the measurement of sound speeds using the third echo signal on each transducer in combination with earlier arrived signals, are used for control purposes to assure that the correct periods of the third echo signals are identified. The measured sound speeds are also corrected due to the effect of diffraction, as discussed in Paper II and in Chapter 5.3.2.

If such an identification procedure is to function in the process industry, it must be automated. That can be done, but this has not been addressed here. An alternative approach would be to use cross-correlation for obtaining the various sound speeds.

5.5.3. Amplitude measurements

The amplitude values leading to the reflection coefficient are measured both in the time domain and in the frequency domain. In the time domain the echo signals peak-to-peak values are used throughout the burst. This way, any DC-offsets in the acquired traces do not matter in the further calculation process. In the frequency domain, such DC-offsets matter, as it may affect the low frequency content of the various signals differently.

Higuiti and Adamowski [70]–[72] performed the integration according to the l^1-norm given as

$$G_1 = \int_{f_1}^{f_2} \left| Z(f) \right| df. \tag{5.20}$$

In this work, the l^2-norm was used according to

$$G_2 = \sqrt{\int_{f_1}^{f_2} \left| Z(f) \right|^2 df}, \tag{5.21}$$

as the processed density was found in Paper II to be less dependent upon the choice of the upper frequency integration limit by using the l^2-norm compared to using the l^1-norm.

The reflection coefficient can for the echo12_12 method be given in the time domain as

$$R = \pm \left(1 - \frac{A_2 A_1^*}{A_1 A_2^*} \right)^{-0.5}. \tag{5.22}$$

For the same method in the frequency domain, using the l^2-norm, the reflection coefficient reads

$$R = \pm\left(1 - x\right)^{-0.5}, \tag{5.23}$$

where x is an auxiliary variable given as

$$x = \sqrt{\frac{\int_{f_1}^{f_2}\left[A_2(f)\right]^2 df \int_{f_1}^{f_2}\left[A_1^*(f)\right]^2 df}{\int_{f_1}^{f_2}\left[A_1(f)\right]^2 df \int_{f_1}^{f_2}\left[A_2^*(f)\right]^2 df}}. \tag{5.24}$$

Higuiti and Adamowski [70]–[72] performed the frequency integration limits according to the –50 dB bandwidth. In this work, the frequency limits used are typically 0–10 MHz. In order to speed up the integration process, a triangular integration method was applied using typically a frequency resolution of about 30 kHz.

5.5.4. Frequency domain processing

The main components in the frequency domain signal processing are shown in Fig. 5.26. The theoretical formulation is given in Paper II. A brief explanation of the processing steps follows: 1) DC-offset correction is performed on the time traces by measuring the average voltage value in a short time window just prior to the appearance of the first echo signal on each trace, and subsequently subtracting the offset value from every sample in the trace. Unless this is performed, a low frequency tail will appear in the frequency spectrums in a non-coherent manner for the individual echo signals, thereby introducing errors. 2) A temporal diffraction correction is applied for the sound speeds during the initial time domain processing. Therefore, only the amplitude diffraction needs to be corrected for at the frequency domain processing stage. 3) A Hanning window function is used to reduce spectral leakage in a coherent manner on each echo signal, meaning that the placement of the window occur at the same relative position in all the echo signals. The width of the window function is limited in one end by the start of the acquired trace, and in the other end by the requirement of being symmetrically placed around the relevant voltage extreme value. If a width of the window function narrower than one period of the burst is used, the characteristic of the spectrums would change from band pass to low pass. 4) A triangular integration method is used in obtaining the frequency spectrums.

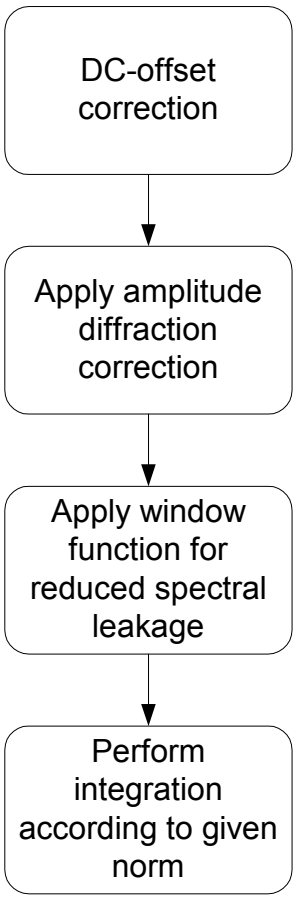

Figure 5.26. The main components of the frequency domain signal processing.

As an example of the time- and frequency domain characteristics, Fig. 5.27 shows the relevant signals using distilled water in the 5.7 mm measuring cell. The frequency spectrums shown do not show deviations when normalized, as was expected since distilled water for all practical purposes is free from dispersion [53]. When measuring on the Cannon N100 oil using a frequency of 6 MHz, at which an attenuation of about 800 dB/m was obtained (see Chapter 6.4), the situation is different, as can be seen in Fig. 5.28. The echo signals that have traversed the liquid are shown to be significantly attenuated. By using the signals on the Tx-channel, a shift in the centre frequency of about 0.1 MHz for each round-trip in the N100 oil was obtained, or of about 88 kHz/cm, at a frequency of 6 MHz. This is, however, attributed to be an effect due to attenuation, and not due to dispersion. Such a filtering effect gives rise to waveform distortion, as discussed in Chapter 6, and in Paper II.

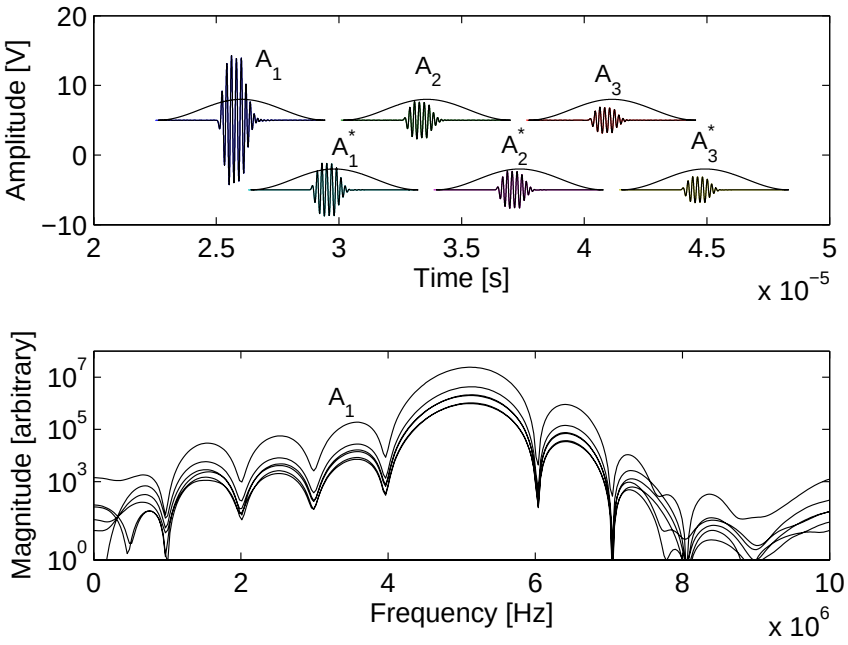

Figure 5.27. Time domain signals and a wide window function along with the magnitude representation of the frequency spectrums using distilled water in the 5.7 mm measuring cell at a frequency of 5 MHz and a burst mode using 5 periods.

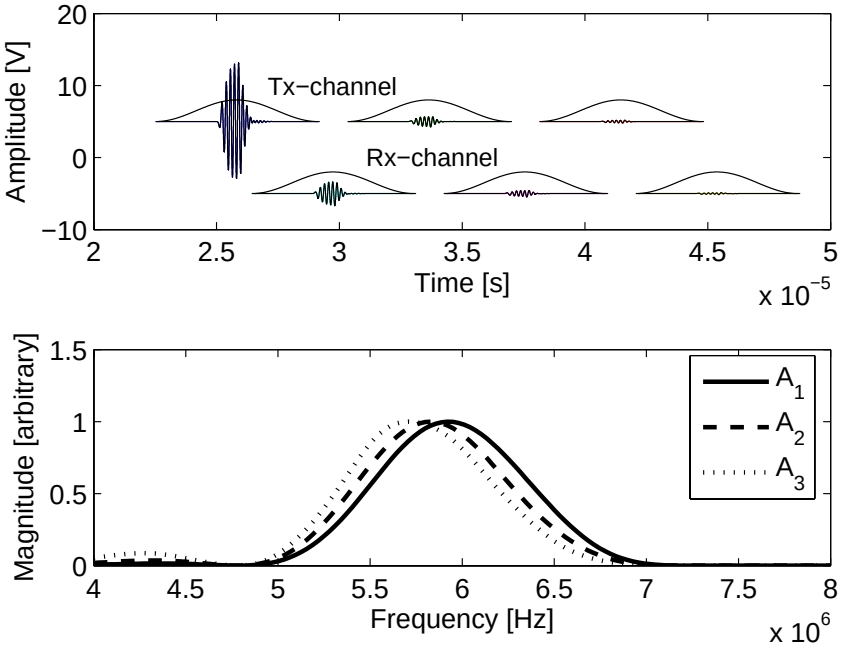

Figure 5.28. Time domain signals and a wide window function along with the magnitude representation of the frequency spectrums using the N100 oil in the 5.7 mm measuring cell at a frequency of 6 MHz and burst mode using 5 periods. The gain scaling factors used for the frequency spectrums were $1.244 \cdot 10^7$, $9.923 \cdot 10^4$, and $7.197 \cdot 10^3$, for the A_1 signal, the A_2 signal, and the A_3 signal, respectively.

5.5.5. Considerations of the SNR and bit resolution

Using the oscilloscope for the acquisition process, there are two aspects of main concern regarding SNR and bit resolution. These are the temporal resolution, which is important in obtaining both the sound speed and the signals amplitudes, and the bit resolution, affecting mainly the signals amplitudes. The operation of the increased bit resolution of the oscilloscope when used in average mode is discussed in [132].

In this work a sampling rate of 500 MSa/s was used, which is significantly higher than the highest frequency content of the echo signals. An oversampling ratio (*OSR*) can be given according to

$$OSR = \frac{f_s}{2f_0}, \tag{5.25}$$

where f_s is the sampling rate, and f_0 is the input signal bandwidth. The use of oversampling reduces the in band quantization noise by the square root of the *OSR* [133]–[134], or alternatively, for each doubling of the *OSR*, the SNR within the DC to the $f_s/2$ bandwidth increases by 3 dB [135]. By using the oscilloscope built-in low pass filter having a 25 MHz cut-off frequency, an increase in the SNR of about 13 dB was obtained. However, this increase in SNR does nothing with respect to increasing the bit resolution.

It should also be noted that an increase in the bit resolution might be obtained by additionally low pass filtering the acquired traces before (or after) the use of the least squares sense cubic spline approximation. This could be performed in software, but was, however, not performed in this work.

5.5.6. Aspects of averaging

In obtaining the liquid density from Eq. (2.11), several averaging approaches are used. These are briefly discussed in the following:

Acquisition

During the acquisition phase, repetitive measurements are acquired for a given number of times and finally presented to the PC in an averaged form by the oscilloscope. By this approach, two aspects are obtained: 1) The averaged traces are accurate to 12 bits resolution, assuming a high enough number of averaging is performed (256 or higher), and 2) the random noise is significantly reduced.

Integer number of periods

For the measurement of the reflection coefficient to be performed in a comparable fashion between the time domain and the frequency domain approaches, an integer

number of periods in the bursts was used at the processing stage. This is a necessary condition for the time domain approach as it uses peak-to-peak values, as otherwise the DC-offsets would contribute, but for the frequency domain approach a single half-period in each echo signal could be used for the calculation of the reflection coefficient.

Bulk aspects of the pulses

In order to improve the statistics of the temporal and the amplitude characteristics, several periods in the bursts were typically used. This way, the averaged phase velocity was obtained, which may be found using the propagation time of a fixed point in the signals, along with the propagation distance.

Bidirectional use

As both transducers were used in the acquisition of the echo signals, an approach was assigned to ensure an equivalent importance of each transducer in the transmitting and in the receive operation. This was accomplished by using both transducers as transmitters in a sequential manner, where the measured sound speeds and the reflection coefficients as obtained using transmission from either side were averaged. Hence, an increased use of averaging and redundancy was introduced. It should, however, be noted that an alternative formulation regarding such form of averaging is possible, see Eq. (36) in Paper I.

As the electronics system used in this work does not permit such a bidirectional operation automatically, it was solved by manually change the connections of the transducer coaxial cables to the electronics system after measurements in one direction had been performed. The duration of such a recess was typically about one minute before the second half of the measurement series could continue.

5.6. Calibration approach

In order for the chosen approach to be able to measure liquid density in an absolute manner, calibration must be performed. For the buffer approach, this is performed by introducing a liquid with known characteristics versus temperature, such as distilled water. The sound speed and the density of distilled water versus temperature as used in this work are given in Appendix D. Then, the water serves two purposes; 1) from the known sound speed versus temperature, the path length can be obtained along with the thermal expansion coefficient for the measuring cell, and 2) sound speed combined with known density versus temperature gives the acoustic impedance,

which in turn is used to obtain the acoustic impedance of the buffer material. Such an approach is dependent upon the specific waveform of the signals used, as the choice of using a short pulse or a longer pulse may give different acoustic impedance [48]. This has also been observed in this work, see Paper II. One simple explanation of why the pulse length matters when obtaining the acoustic impedance, is that diffraction is different for different pulse lengths. The diffraction correction used in this work, does, however, not account for different pulse lengths.

In this work, a different approach of calibration was devised, in which the liquid sound speed was used only to obtain the liquid path length. In order to obtain the acoustic impedance of the buffer material, a combination of measurements of density and sound speed was used, where the density measurement was performed at different temperatures at a national calibration laboratory using a weighing method, and the buffer sound speed was obtained from the measured echo signals, corrected for diffraction. The main advantages of this new approach are believed to be the low uncertainty of the buffer density, combined with the assumption that sound speed is less dependent upon the wave form of the echo signals than amplitude parameters needed for obtaining the reflection coefficient. In Figs. 5.29–5.30, the schematics of both calibration approaches are given.

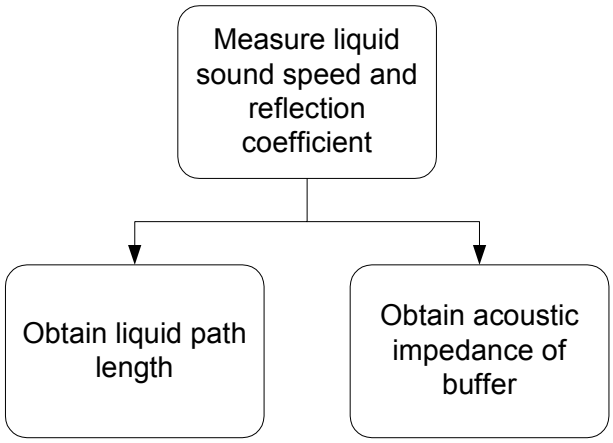

Figure 5.29. Schematic of the normal calibration approach.

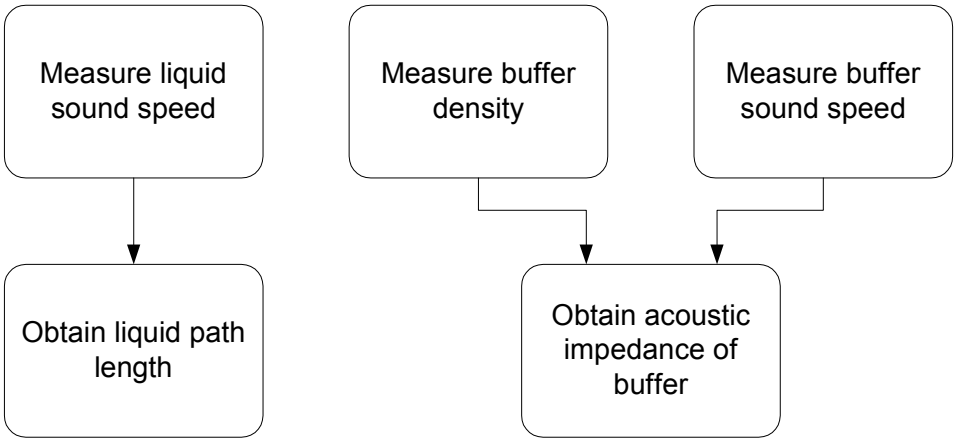

Figure 5.30. Schematic of the proposed calibration approach.

Most often, acoustic density measurements are compared with reference measurements performed with a calibrated pycnometer [85], [71], giving a great flexibility in which liquid to measure. Such pycnometers do, however, typically have a relative uncertainty of ± 0.1 %. In order to avoid the uncertainty of the pycnometer, it was found desirable to use liquids with a calibrated density across a certain temperature range.

Two such vendors have been identified. H&D Fitzgerald Ltd., UK, [136] delivers certified reference materials for liquid density sold in sealed 10 ml glass ampoules for the market of calibration of density meters. Most of their standards have an uncertainty of ± 0.01 kg/m^3 over the stated temperature range. These ampoules are rather expensive.

Cannon Instrument Company [137] supplies certified reference standards (oils) from which some general purpose viscosity standards were used in this work. For these viscosity standards, the density, the shear viscosity, and the kinematic viscosity values were printed on the label for a wide temperature range. The density uncertainty of these standards is ± 0.1 kg/m^3. The detailed information of the viscosity standards used is given in Appendix E.

All temperature measurement devices used in this work are calibrated with respect to the *International Temperature Scale* of 1990 (ITS-90).

5.7. Summary

This Chapter acts together with Papers I–II as a description of the proposed measurement approach. By using this approach, the following beneficial characteristics were obtained relative to the ABC-method:

- Reduced uncertainty.
- Reduced systematic error due to diffraction.
- Less prone to mode conversion.
- Possibility for using a larger liquid path length and an increased pulse duration.
- Obtains an amplitude quality indication of the measured echo signals.
- Improved redundancy characteristics of measured parameters.
- The receive sensitivity ratio of the acoustic transducers can be obtained.
- The receive sensitivity ratio of the acquisition system can be obtained.

However, the proposed measurement approach needs an additional transducer, and access to both sides of a measurement cell, in contradiction to the ABC-method, which may be operated using only one transducer.

Chapter 6. Experimental results

6.1. Introduction

Beyond the experimentally obtained results given in Paper II, some measured results are presented here to further discuss the operation of the proposed measurement cell and to show how some of the non-ideal factors may influence its operation if not corrected for.

As the relative amplitude approach seems as the most important approach regarding the measurement of liquid density, detailed measurement results are given for both the echo12_12 method and for the ABC-method, using liquids with a wide range of shear viscosities. Additional measurement results are also presented regarding attenuation, the amplitude quality indicator, and for both of the sensitivity factors discussed in Chapter 5.2.6.

6.2. Relative amplitude approach for density measurements

For the relative amplitude approach, the amplitude ratios between two or more echo signals on each transducer are used for obtaining the reflection coefficient. For this approach it is understood that the effect of the acoustic coupling or sensitivity aspects of the transducers or the electronics do not apply, due to the relative operation (using measured amplitude ratios), see Paper I.

Measurements using only a few of the methods as given in Paper I will here be presented. These are the ABC-method of Papadakis [65], and the newly proposed echo12_12 method, using the first two echo signals from both transducers, as given in Paper I. Both of these methods were subjected to the averaging process given in Chapter 5.5.6.

As a base for the obtained results presented in Paper II for the relative amplitude approach, the detailed measurement results will be given for both the measurement cells used in this work. This includes the measurement of liquid density, using the relative amplitude approach and the mixed amplitude approach, as given in

Chapter 6.2 and in Chapter 6.3, respectively. Measurement results regarding the liquid attenuation are given in Chapter 6.4. In Chapter 6.5, results regarding the amplitude quality indicator and the sensitivity factors are given, and in Chapter 6.6 are various factors, which have influence on the measured parameters, discussed.

The results given are all performed using the switching arrangement described in Chapter 5.4. The liquids used are distilled water and the various Cannon oils (N4, N7.5, N35, and the N100) further described in Papers II, Appendix D, and in Appendix E.

All of the measurements to be presented were performed at a temperature of 27.44 °C. The temperature stability was within ± 0.04 °C. The uncertainty of the viscosity standards density was given as ± 0.1 kg/m^3, together with a relative uncertainty for the viscosity of 0.29 %. No information about the viscosity standards sound speed or attenuation characteristics was given, or found in the literature.

6.2.1. Obtained results using the 5.7 mm measuring cell

The reference densities and shear viscosities for the liquids used are given in Table 6.1. These data are obtained using the polynomials given in Appendix D and in Appendix E, except where noted.

Table 6.1. Reference densities and shear viscosities for the liquids used when performing measurements using the 5.7 mm measuring cell.

Liquid	Temperature [°C]	Reference density [kg/m^3]	Shear viscosity [mPa s]
Distilled water	27.44	996.40	0.8513 @ 27 °C *
N4	27.40	781.20	4.24
N7.5	27.42	796.02	8.74
N35	27.48	862.73	49.62
N100	27.46	877.32	172.83

* Reference: The reference value for the distilled water's density is from [47] and for the shear viscosity at a temperature of 27 °C it is given by [138].

The measured densities for the different liquids and for the frequencies used are given in Tables 6.2–6.5, along with the relative density difference according to

$$\text{Relative difference} = 100\% \frac{\left(\text{measured density} - \text{reference density}\right)}{\text{reference density}}. \quad (6.1)$$

The measurements using the most viscous oil (the N100 oil) were found to have quite increased deviations from the density reference value compared with the other liquids. This is believed to be due to the significant waveform distortion, as evidenced in Fig. 6.1 for a frequency of 6 MHz.

Table 6.2. Measured results for the echo12_12 method using a time domain signal processing.

Liquid	4 MHz		5 MHz		6 MHz	
	Measured density [kg/m^3]	Relative difference [%]	Measured density [kg/m^3]	Relative difference [%]	Measured density [kg/m^3]	Relative difference [%]
Distilled water	992.779	-0.363	996.093	-0.031	996.141	-0.026
N4	778.037	-0.405	778.877	-0.297	780.135	-0.136
N7.5	793.674	-0.295	794.200	-0.229	795.894	-0.016
N35	859.851	-0.334	862.815	0.010	859.318	-0.395
N100	866.268	-1.260	871.352	-0.680	868.679	-0.985

Table 6.3. Measured results for the ABC-method using a time domain signal processing.

Liquid	4 MHz		5 MHz		6 MHz	
	Measured density [kg/m^3]	Relative difference [%]	Measured density [kg/m^3]	Relative difference [%]	Measured density [kg/m^3]	Relative difference [%]
Distilled water	994.036	-0.237	996.713	0.031	996.124	-0.028
N4	778.778	-0.310	779.882	-0.169	780.906	-0.038
N7.5	795.161	-0.108	796.997	0.123	800.272	0.534
N35	862.541	-0.022	864.504	0.206	860.268	-0.285
N100	867.609	-1.107	878.110	0.090	852.037	-2.882

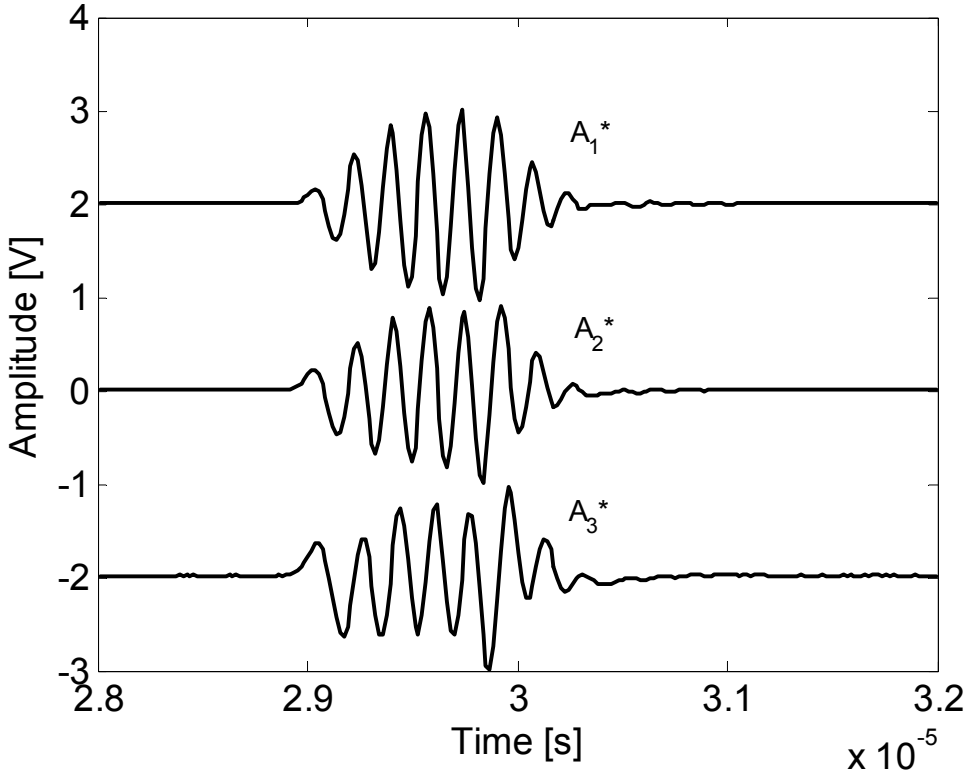

Figure 6.1. An example of waveform distortion for the N100 oil for 6 MHz, using the 5.7 mm measurement cell. The receiver transducer's echo signals are plotted with the amplitudes normalized and offset for clarity, and time aligned for better illustration. The gain scaling factors used are 0.612, 2.095, and 6.979, respectively.

Table 6.4. Measured results for the echo12_12 method using a frequency domain signal processing.

Liquid	4 MHz		5 MHz		6 MHz	
	Measured density [kg/m^3]	Relative difference [%]	Measured density [kg/m^3]	Relative difference [%]	Measured density [kg/m^3]	Relative difference [%]
Distilled water	993.083	-0.333	995.120	-0.128	995.340	-0.106
N4	777.239	-0.507	778.014	-0.408	778.815	-0.305
N7.5	792.835	-0.400	793.385	-0.331	794.252	-0.222
N35	858.257	-0.518	860.739	-0.231	856.484	-0.724
N100	861.139	-1.844	865.874	-1.305	857.128	-2.302

Table 6.5. Measured results for the ABC-method using a frequency domain signal processing.

Liquid	4 MHz		5 MHz		6 MHz	
	Measured density [kg/m^3]	Relative difference [%]	Measured density [kg/m^3]	Relative difference [%]	Measured density [kg/m^3]	Relative difference [%]
Distilled water	993.308	-0.310	996.614	0.021	996.243	-0.016
N4	777.061	-0.530	779.065	-0.273	779.807	-0.178
N7.5	794.465	-0.195	795.017	-0.126	797.792	0.223
N35	860.607	-0.246	861.482	-0.145	856.328	-0.742
N100	857.383	-2.272	860.867	-1.875	837.819	-4.502

In order to present the obtained measurement results in a condensed form, Table 6.6 was prepared, in which all of the liquids used are included, except the N100 oil, as it gave significant increased deviations compared with the other liquids. In this table, each frequency has two columns. The first gives the mean (or systematic) deviations in per cent from the density reference values, whereas the second column gives half the span in per cent between the maximum and the minimum deviation from the reference values. This way, the second column can easier be compared with predicted uncertainties. These column headlines can be better described by the equations

$$\text{Mean deviation} = \frac{1}{4}\sum_{1}^{4}\left(100\frac{\rho_i - \rho_{ref,i}}{\rho_{ref,i}}\right), \tag{6.2}$$

$$\text{Span} = \max\left(100\frac{\rho_i - \rho_{ref,i}}{\rho_{ref,i}}\right) - \min\left(100\frac{\rho_i - \rho_{ref,i}}{\rho_{ref,i}}\right), \tag{6.3}$$

where ρ_i is the mean measured density for liquid i, and $\rho_{ref,i}$ is the reference liquid density as given in Table 6.1.

In Table 6.6 quite clear indications of systematic deviations from density reference values exists. The reason for this is believed to be due to systematic effects such as signal processing and diffraction. It is also noted that the ABC-method has a lower systematic deviation compared with the echo12_12 method. A possible explanation for this behavior may be due to diffraction correction as the ABC-method uses only one transducer, whereas the echo12_12 method uses two transducers. As the transducers cannot be expected to be identical (and thereby have identical sound fields), the added error upon the use of identical diffraction correction on different transducers is believed to be responsible for such a behavior. To reduce the effect of such a systematic error, a zero-point correction could be applied by subtracting the obtained systematic deviation based on measurements on several liquids from the actual measured density for a given liquid.

Table 6.6. Summary of density measurement results using the 5.7 mm measuring cell. The N100 oil was excluded due to the mentioned pulse distortion characteristics.

Method	4 MHz		5 MHz		6 MHz	
	Mean dev. [%]	0.5 · Span [%]	Mean dev. [%]	0.5 · Span [%]	Mean dev. [%]	0.5 · Span [%]
echo12_12 time domain	-0.349	0.055	-0.137	0.154	-0.143	0.190
echo12_12 freq. domain	-0.440	0.093	-0.275	0.140	-0.339	0.309
ABC time domain	-0.169	0.144	0.048	0.187	0.046	0.410
ABC freq. domain	-0.320	0.167	-0.131	0.148	-0.178	0.483

From the second column in Table 6.6 half the span in per cent between the maximum and the minimum deviation from the reference values are given. These numbers are based on all the liquids, except the N100 oil. In general, the measured span was found to increase with frequency, with an exception for the ABC-method using a frequency domain signal processing at a frequency of 5 MHz. Such a behavior was expected as a fixed sampling rate was used.

The standard deviation δ of the density was measured with results given in Tables 6.7–6.8 for the 5.7 mm cell, based on 10 measurements for each liquid. The average standard deviation was obtained according to

$$\delta = \left(\delta_A^2 + \delta_B^2\right)^{0.5}, \tag{6.4}$$

where subscript A means standard deviation as obtained by transmission from Transducer A, and vice versa for subscript B.

Table 6.7. Measured average standard deviation for the echo12_12 method using the 5.7 mm cell.

Liquid	4 MHz		5 MHz		6 MHz	
	Time	Frequency	Time	Frequency	Time	Frequency
Distilled water	0.289	0.219	0.380	0.266	0.466	0.206
N4	0.518	0.317	0.395	0.232	0.405	0.304
N7.5	0.570	0.346	0.447	0.259	0.396	0.295
N35	0.353	0.175	0.474	0.252	0.656	0.446
N100	0.748	0.417	0.579	0.415	1.272	0.678

Table 6.8. Measured average standard deviation for the ABC-method using the 5.7 mm cell.

Liquid	4 MHz		5 MHz		6 MHz	
	Time	Frequency	Time	Frequency	Time	Frequency
Distilled water	0.670	0.492	0.742	0.441	0.914	0.438
N4	0.905	0.350	0.844	0.613	0.931	0.704
N7.5	1.088	0.748	0.691	0.395	0.928	0.510
N35	0.781	0.300	1.269	0.539	1.652	1.095
N100	1.954	1.078	1.908	1.424	3.572	2.857

The results of Tables 6.7–6.8 are given in Fig. 6.2, in the form of the ratio between the standard deviation of the ABC-method to the standard deviation of the echo12_12 method, together with the simulated ratio of the method's relative uncertainty, using the theoretical approach given in Papers I–II.

The parameters used in the simulation were: Buffer impedance = $17 \cdot 10^6$ kg/m^{2}s, liquid impedance = $1.5 \cdot 10^6$ kg/m^{2}s, buffer sound speed = 6450 m/s, liquid sound speed = 1500 m/s, relative uncertainty of sound speeds = 0.01 %, and a negligible uncertainty in the buffer density was assumed. The vertical resolution used was 12 bits. For the distilled water, the N4 oil and for the N7.5 oil, the average ratio of the corresponding standard deviations over the three frequencies were used in Fig. 6.2, due to the low attenuation of these liquids. For the N35 and for the N100 oil, the separate experimental results are given corresponding to the actual frequencies used (the 4–6 MHz frequency range). Fig. 6.2 indicates a clear correspondence between the measured and the simulated uncertainty characteristics of the different methods versus attenuation, adding confidence both to the quality of the measurements and to the theoretical uncertainty approach of Papers I–II. The solid curve in Fig. 6.2 is based on the results given in Fig. 5.15. The results for the 2.4 mm cell did not deviate significantly from the results obtained using the 5.7 mm measuring cell.

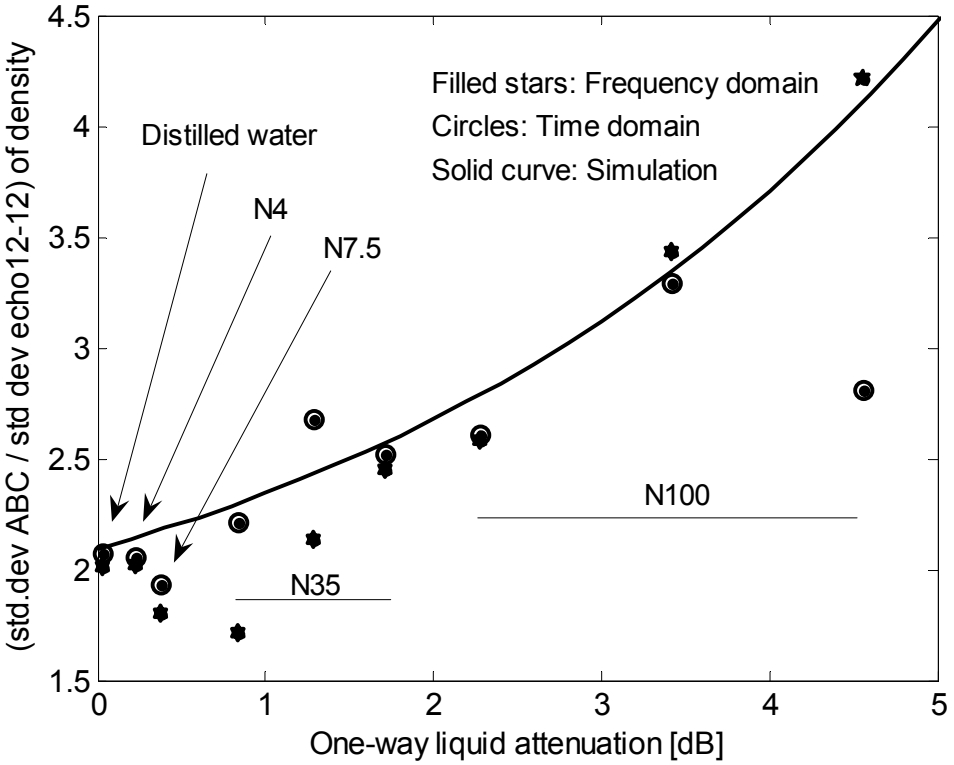

Figure 6.2. Measured ratio of the ABC-method's standard deviation to the echo12_12 method's standard deviation for the 5.7 mm measuring cell. The solid line gives the simulated ratio of the ABC-method's relative uncertainty to the relative uncertainty of the echo12_12 method.

6.2.2. Obtained results using the 2.4 mm measuring cell

The reference densities for the liquids used are given in Table 6.9, and the measured densities for the different liquids and for the frequencies used are given in Tables 6.10–6.13.

Table 6.9. Reference densities for the measurements performed using the 2.4 mm measuring cell.

Liquid	Temperature [°C]	Reference density [kg/m^3]	Shear viscosity [mPa s]
Distilled water	27.45	996.40	0.8513 @ 27 °C *
N4	27.44	781.17	4.23
N7.5	27.45	796.00	8.73
N35	27.42	862.75	49.78
N100	27.44	877.35	173.04

* Reference: The reference value for the distilled water's density is from [47] and for the shear viscosity at a temperature of 27 °C it is given by [138].

Table 6.10. Measured results for the echo12_12 method using a time domain signal processing.

Liquid	4 MHz		5 MHz		6 MHz	
	Measured density [kg/m^3]	Relative difference [%]	Measured density [kg/m^3]	Relative difference [%]	Measured density [kg/m^3]	Relative difference [%]
Distilled water	994.269	-0.214	993.410	-0.300	998.369	0.198
N4	775.130	-0.773	780.617	-0.071	784.505	0.427
N7.5	792.186	-0.479	794.624	-0.173	796.344	0.043
N35	858.051	-0.545	861.213	-0.178	859.096	-0.424
N100	877.380	0.003	876.685	-0.076	872.473	-0.556

Based on the measured results from Tables 6.10–6.13, it was found that the N100 oil does not show an increased deviation from the density reference value compared with the other liquids. A probable reason for this is discussed in Chapter 6.4.3.

In Table 6.14, the obtained measurement results are given in a condensed form, in which all of the liquids used are included. In general, the systematic deviation from reference values is larger for the echo12_12 method than for the ABC-method, as for the 5.7 mm measuring cell. However, the measured span was largest at 6 MHz and lowest at 5 MHz, with the values for the time domain signal processing at 4 MHz being at the same level as for 6 MHz, and the level at 4 MHz using a frequency domain signal processing being double the level as found at 5 MHz. The reason for this behavior is not clear.

Table 6.11. Measured results for the ABC-method using a time domain signal processing.

Liquid	4 MHz		5 MHz		6 MHz	
	Measured density [kg/m^3]	Relative difference [%]	Measured density [kg/m^3]	Relative difference [%]	Measured density [kg/m^3]	Relative difference [%]
Distilled water	996.283	-0.012	993.035	-0.338	998.975	0.258
N4	776.034	-0.657	781.913	0.095	789.180	1.025
N7.5	796.605	0.076	794.839	-0.146	794.472	-0.192
N35	861.517	-0.143	861.369	-0.160	859.874	-0.333
N100	883.365	0.686	878.051	0.080	879.149	0.205

Table 6.12. Measured results for the echo12_12 method using a frequency domain signal processing.

Liquid	4 MHz		5 MHz		6 MHz	
	Measured density [kg/m^3]	Relative difference [%]	Measured density [kg/m^3]	Relative difference [%]	Measured density [kg/m^3]	Relative difference [%]
Distilled water	992.856	-0.356	993.764	-0.265	994.136	-0.227
N4	776.094	-0.650	779.609	-0.200	783.535	0.303
N7.5	792.676	-0.418	793.840	-0.271	792.577	-0.430
N35	858.269	-0.519	859.566	-0.369	857.175	-0.646
N100	872.161	-0.591	874.102	-0.370	870.109	-0.825

Table 6.13. Measured results for the ABC-method using a frequency domain signal processing.

Liquid	4 MHz		5 MHz		6 MHz	
	Measured density [kg/m^3]	Relative difference [%]	Measured density [kg/m^3]	Relative difference [%]	Measured density [kg/m^3]	Relative difference [%]
Distilled water	994.768	-0.164	994.524	-0.188	995.518	-0.089
N4	776.443	-0.605	780.776	-0.050	787.797	0.848
N7.5	794.612	-0.174	794.797	-0.151	792.648	-0.421
N35	859.320	-0.398	860.244	-0.290	859.004	-0.434
N100	875.347	-0.228	875.955	-0.159	874.146	-0.365

Table 6.14. Summary of density measurement results using the 2.4 mm measuring cell.

Method	4 MHz		5 MHz		6 MHz	
	Mean dev. [%]	0.5 · Span [%]	Mean dev. [%]	0.5 · Span [%]	Mean dev. [%]	0.5 · Span [%]
echo12_12 time domain	-0.401	0.389	-0.160	0.115	-0.062	0.492
echo12_12 freq. domain	-0.507	0.147	-0.295	0.085	-0.365	0.564
ABC time domain	-0.010	0.672	-0.094	0.217	0.193	0.680
ABC freq. domain	-0.314	0.221	-0.168	0.120	-0.092	0.642

6.2.3. Discussion

For both measuring cells, it was in general found that the ABC-method possesses a less systematic deviation than the echo12_12 method. This is probably due to diffraction correction, as discussed in Paper II. The effect of such a systematic deviation may be reduced by a suitable zero-point correction.

The echo12_12 method was found to have a reduced span compared with the ABC-method. This is in accordance with the uncertainty characteristics for both methods, as given in Paper II. The measurement span was found to be within ± 0.15 % for both measuring cells at 5 MHz for both time and frequency domain processing for the echo12_12 method, using liquids within a wide range of shear viscosities.

6.3. Mixed amplitude approach for density measurements

Until now, only methods for the measurement of the reflection coefficient that make use of the relative amplitude approach have been discussed. That is, at least two echo signals from each transducer are used in order to avoid the dependence upon the transducer- and the electronic channel sensitivities. However, if a dependency upon these sensitivities can be accepted, alternative formulations for the reflection coefficient are possible. These alternative formulations are named the mixed amplitude approach. The name can be explained by considering Eq. (50) in Paper I, which is repeated here as

$$\left(\frac{A_1}{A_2}\right)\left(\frac{A_2}{A_3}\right)^{1+b}\left(\frac{A_1^*}{A_2^*}\right)^{d}\left(\frac{A_3^*}{A_2^*}\right)^{\frac{1}{2}(5+3b+c+2d)}\left(\frac{A_3}{A_3^*}\right)^{1+b+c}=\left(\frac{R_A R_T}{R_B R_R}\right)^{1+b+c}\frac{R_{12}^2}{R_{12}^2-1}, \quad (6.5)$$

and considering the last term on the left side, which consists of signals from both transducers. The mixed amplitude approach is more fully described in Paper I.

When measuring on liquids possessing high attenuation, the echo signals that have traversed the longest distance gets progressively more damped, compared to signals which have traversed a shorter distance. Such attenuation may give rise to waveform distortion of the echo signals as it has a frequency dependent characteristic. It would in such circumstances be beneficial to be able to use echo signals that possess the least possible distortion.

The relative amplitude approach can only to a limited degree be compensated for such non-ideal behavior, as the same number (and at least two) of the echo signals from each transducer is used. The mixed amplitude approach, however, has certain characteristics very useful when exposed to such distortion effects, as this approach may use a different number of echo signals from the transducers. These

characteristics will be discussed below. When using both transducers for transmitting in a sequential manner, it can be shown that the transducer's sensitivity ratio in receive mode may be omitted, so that only the ratio of the acquisition channels sensitivity in receive mode is left (see Paper I), along with the relevant echo signals for the particular reflection coefficient measuring method. Although the echo signals may be exposed to waveform distortion to a certain degree, due to the effect of attenuation, the acquisition channels sensitivity ratio may be obtained from previous measurements on low loss liquids, being less exposed to waveform distortion effects, or from measurements on the electronics directly.

Here, some results using castor oil in the 5.7 mm measuring cell are presented. This oil gave severe waveform distortion, as can be seen in Fig. 6.3. This distortion is probably due to its high attenuation value (see below). Such a waveform distortion was sought as it was necessary in order to distinguish the reflection coefficients (and thereby the densities) as obtained by the many echo signal combinations, as otherwise they were found to give closely spaced results. On the right side in Fig. 6.3 is shown how many times the acoustic wave has propagated one way through the liquid. The density reference value used for the castor oil is approximately 953 kg/m^3 [139] for a temperature of about 27 °C. The attenuation at 6 MHz was measured to approximately 1100 dB/m (see Chapter 6.4), in close accordance with reference values [140]–[141].

Results using the mixed amplitude approach are given for the echo12_1, echo1_12, echo13_1, and the echo1_13 method that were initially presented in Paper I. The motivations for using the various methods may be different. The echo1_12 and the echo1_13 method are believed to be useful for applications where a large difference in amplitudes exists between the A_1 and the A_2 echo signals, resulting in a low number of effective bits for the latter signal, and where a much lesser amplitude difference between the signals on the receive side exists. The echo12_1 method seems beneficial when waveform distortion causes the relative amplitude approach to give significant errors, as less distorted signals are used. An example of this latter method using pulses exposed to significant waveform distortion will now be given.

Measured density for castor oil using the 5 MHz transducers in a burst mode using 5 periods are given in Fig. 6.4 in the 4–6 MHz frequency range for the mixed amplitude approach, in comparison with the echo12_12 method and the ABC-method of the relative amplitude approach using a frequency domain signal processing approach. The echo12_12 method is seen to give results close to that of the echo12_1 and the echo1_12 method (although somewhat lower value). The echo13_1 and the echo1_13 method are seen to give significantly larger deviation from the reference value than the echo12_1 and the echo1_12 method, probably due to the increased waveform distortion of the pulses. The ABC-method is seen to give the largest deviation of all the methods shown.

By using a measured representation of the receive channel gain ratio R_T/R_R using water and various Cannon oils which do not suffer from significant waveform distortion, corrected density values using the mixed amplitude approach are given in Fig. 6.5. The measured R_T/R_R ratio using castor oil and the other liquids are given in

Table 6.15 for the different frequencies used. In Fig. 6.5 it is seen that the corrected mixed amplitude approach give significantly less deviation from the reference value than using the measured R_T/R_R obtained using castor oil.

Table 6.15. Measured R_T/R_R ratio using castor oil and average R_T/R_R from earlier measurements on water and various low loss Cannon oils.

Frequency [MHz]	Measured R_T/R_R using castor oil		Average values of R_T/R_R using water and Cannon oils	
	Time	Frequency	Time	Frequency
4	0.880	0.874	0.875	0.872
5	0.850	0.849	0.853	0.854
6	0.851	0.844	0.863	0.867

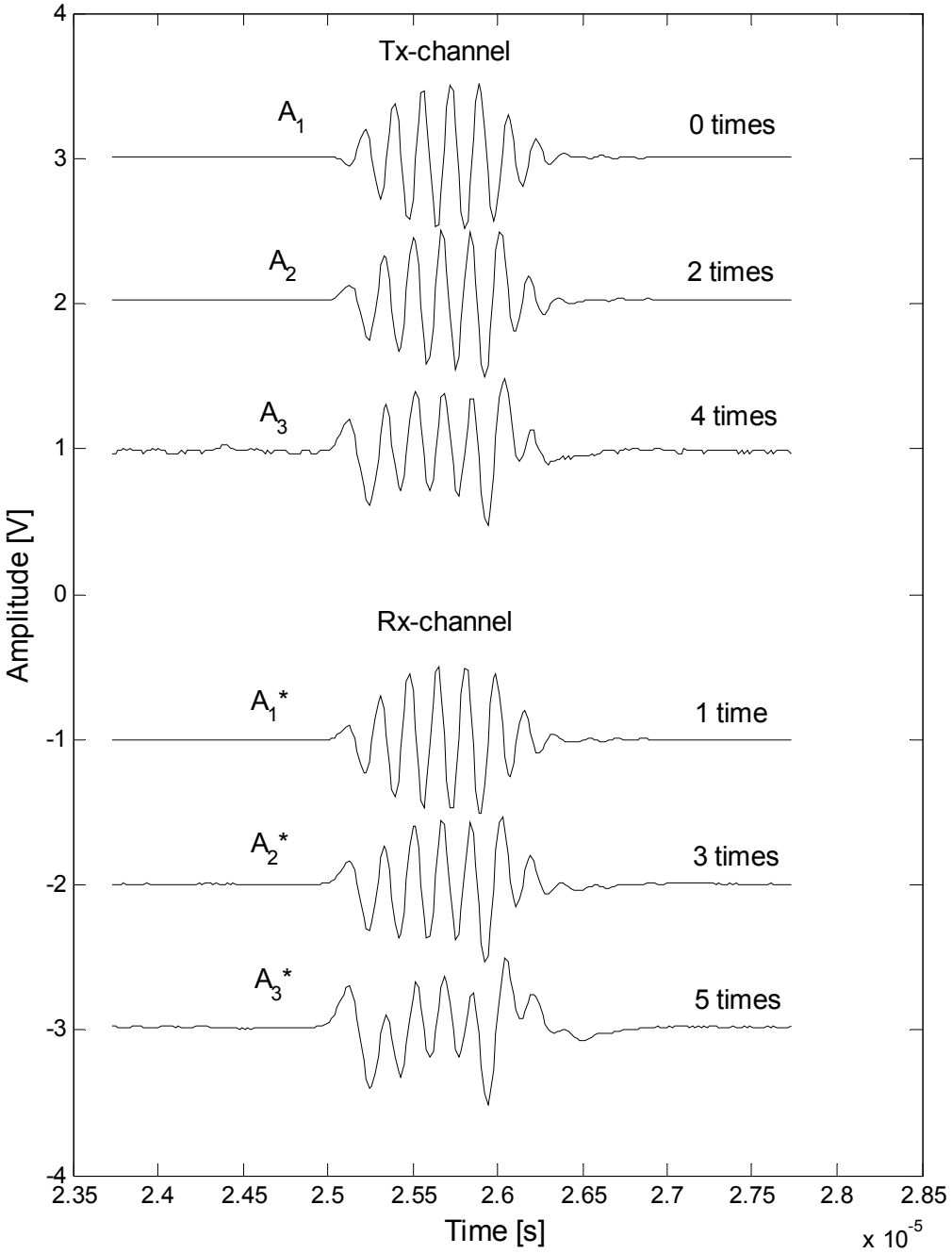

Figure 6.3. Waveform distortion using castor oil in the 5.7 mm measuring cell in burst mode using 5 periods at 6 MHz. On the right side of the figure is shown how many times the acoustic wave has propagated one way through the liquid. The amplitudes are normalized and offset for clarity, and time aligned for better illustration. The gain scaling factors used for the echo signals were 14.79, 0.976, and 0.209 for the Tx-channel, and 2.705, 0.525, and 0.128 for the Rx-channel, respectively.

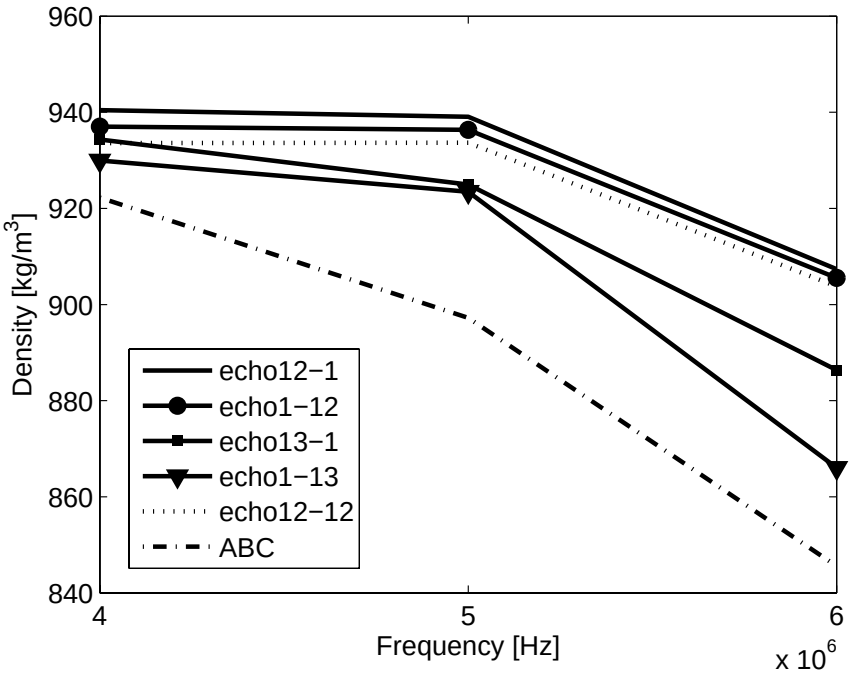

Figure 6.4. Processed density of castor oil using a frequency domain signal processing. Results are shown for the relative amplitude approach (dashed line and dashed-dotted line) and for the mixed amplitude approach (various solid lines). The density reference value is approximately 953 kg/m^3.

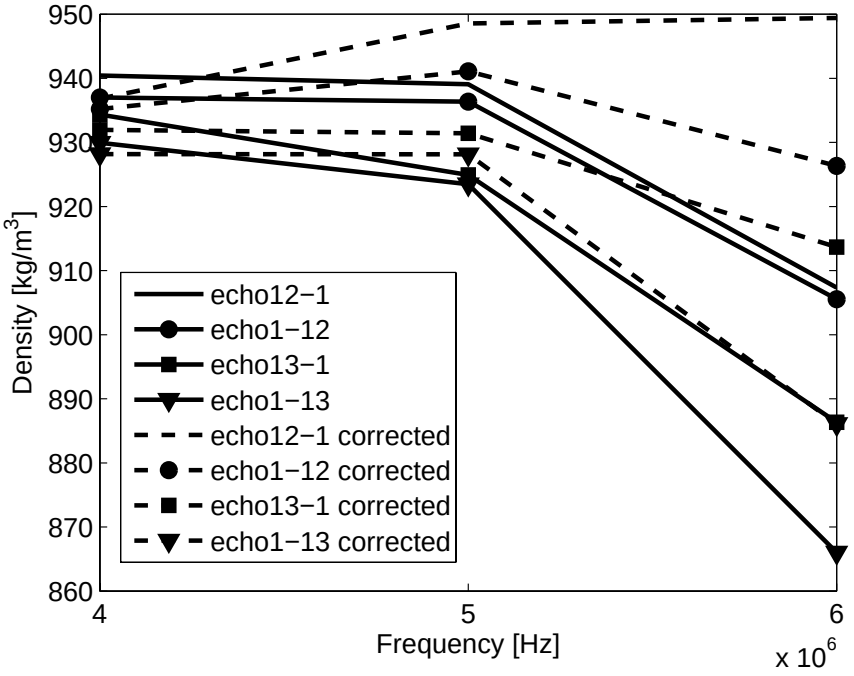

Figure 6.5. Processed density of castor oil using a frequency domain signal processing. Results are shown for the mixed amplitude approach using the R_T/R_R ratio from measurements on castor oil (various solid lines), and from previous measurements on low loss liquids (corrected, various dashed lines). The density reference value is approximately 953 kg/m^3.

6.4. Attenuation measurements

The knowledge of additional liquid parameters beyond density and sound speed would be beneficial for the sake of characterization purposes. Such characterization may be important (or even necessary) in an environment such as the process industry. As an example one may imagine that some small particles are unintentionally introduced to a liquid flow. The corresponding change in sound speed and density may be rather small, but the change in attenuation will probably be significant due to a large change in scattering due to the particles compared to a pure fluid. In such a case, the additional measurement parameter (liquid attenuation) may give early indications on a change in the characteristics of a liquid.

A variety of combinations for the measurement for the liquid attenuation can be put forth, dependent upon which amplitude ratio is used and on which transducer is used. Some of the possible combinations are given below, and stems from Eqs. (15)–(20) of Paper I.

$$\alpha_2 = \frac{1}{2l_2}\ln\left[\frac{A_1}{A_2}\left(R^2-1\right)\right] \tag{6.6}$$

$$\alpha_2 = \frac{1}{2l_2}\ln\left(\frac{A_2}{A_3}R^2\right) \tag{6.7}$$

$$\alpha_2 = \frac{1}{2l_2}\ln\left(\frac{A_1^*}{A_2^*}R^2\right) \tag{6.8}$$

$$\alpha_2 = \frac{1}{2l_2}\ln\left(\frac{A_2^*}{A_3^*}R^2\right) \tag{6.9}$$

These equations apply when using the first and the second signals, or the second and the third signals on the transmit transducer, or the receive transducer, respectively. Measurement results will be presented based on these four alternative formulations for the liquid attenuation. The measured average attenuation (Mean α, as given in Table 6.17) using these four formulations along with the corresponding span (maximum value minus minimum value) is given below for both measuring cells using different signal processing schemes. The equations used for obtaining the Mean α and the corresponding Span are given below.

$$\text{Mean } \alpha = \frac{1}{4}\sum_{i=1}^{4}\alpha_{2i}, \tag{6.10}$$

$$\text{Span} = \max\left(\alpha_{2i}\right) - \min\left(\alpha_{2i}\right), \tag{6.11}$$

where α_{2i} is the individual measured attenuation for combination i. The averaging process was operated on the dB/m scale.

Attenuation measurements were performed using distilled water and the various Cannon viscosity standards, but in addition, castor oil was used in the 5.7 mm

measuring cell in order to provoke the combination of a high liquid attenuation with the maximum path length of the used equipment. The reference attenuation values for distilled water and for the castor oil are given in Table 6.16.

Table 6.16. Reference attenuation values for distilled water and castor oil.

	Attenuation α [dB/m]			
	4 MHz	5 MHz	6 MHz	Reference
Distilled water @ 27 °C	3.0	4.7	6.7	*
Castor oil @ 25 °C	640	934	1271	[141]
Castor oil @ 30 °C	528	773	1054	[141]

* The reference values for the distilled water's shear viscosity, density, and sound speed at 27 °C are from [138], [47] and [46], respectively. The reference attenuation values for distilled water are based on using classical theory [142].

6.4.1. Obtained results using the 5.7 mm measuring cell

The liquid's attenuation as measured using the 5.7 mm measuring cell are presented in Tables 6.17–6.20 for the echo12_12 method and the ABC-method using both time- and frequency domain signal processing. As stated before, all of the presented measurements were performed at a temperature of 27.44 ± 0.04 °C.

Table 6.17. Measured attenuation for the echo12_12 method using a time domain signal processing.

Liquid	4 MHz		5 MHz		6 MHz	
	Mean α [dB/m]	Span [dB/m]	Mean α [dB/m]	Span [dB/m]	Mean α [dB/m]	Span [dB/m]
Distilled water	5.2	1.5	7.8	0.6	10.0	0.3
N4	24.6	1.7	37.5	1.1	50.4	1.5
N7.5	44.5	2.9	66.9	3.0	90.4	5.2
N35	145.0	3.2	223.9	1.8	304.8	2.5
N100	399.0	4.8	600.0	11.8	797.4	17.8
Castor oil	577.2	1.9	840.4	9.3	1110.7	15.3

Table 6.18. Measured attenuation for the echo12_12 method using a frequency domain signal processing.

Liquid	4 MHz		5 MHz		6 MHz	
	Mean α [dB/m]	Span [dB/m]	Mean α [dB/m]	Span [dB/m]	Mean α [dB/m]	Span [dB/m]
Distilled water	5.7	0.3	8.5	1.4	10.2	0.9
N4	26.3	0.4	38.3	1.2	50.2	1.1
N7.5	46.8	1.8	67.6	1.8	89.4	3.9
N35	150.2	4.1	224.4	1.2	298.6	0.3
N100	401.6	10.4	593.4	17.3	768.9	43.1
Castor oil	571.2	27.2	815.4	49.7	1016.9	159.0

The measured attenuation for distilled water as seen in Tables 6.17–6.20 is 2 to 4 dB/m higher than its reference values for all the frequencies. The measured attenuation for castor oil is seen in Fig. 6.6 to fit within the reference values given for temperatures of 25 °C and 30 °C, except at 6 MHz, using the frequency domain processing. From this, it seems that one can have a reasonably confidence in the performed measurements, in which the liquids used span a very wide range of attenuation.

Table 6.19. Measured attenuation for the ABC-method using a time domain signal processing.

Liquid	4 MHz		5 MHz		6 MHz	
	Mean α [dB/m]	Span [dB/m]	Mean α [dB/m]	Span [dB/m]	Mean α [dB/m]	Span [dB/m]
Distilled water	5.1	1.5	7.7	0.6	10.0	0.4
N4	24.6	1.8	37.5	1.2	50.5	0.9
N7.5	44.6	2.9	67.0	3.1	90.6	5.0
N35	145.1	3.3	223.9	1.7	304.8	2.4
N100	399.0	4.8	600.0	12.2	797.4	17.8
Castor oil	577.2	2.7	840.6	10.5	1110.9	15.3

Table 6.20. Measured attenuation for the ABC-method using a frequency domain signal processing.

Liquid	4 MHz		5 MHz		6 MHz	
	Mean α [dB/m]	Span [dB/m]	Mean α [dB/m]	Span [dB/m]	Mean α [dB/m]	Span [dB/m]
Distilled water	5.7	0.3	8.4	1.4	10.2	0.9
N4	26.3	0.4	38.3	1.2	50.3	1.1
N7.5	46.9	1.8	67.7	1.8	89.6	3.9
N35	150.2	4.1	224.4	1.2	298.6	0.3
N100	401.6	10.4	593.4	17.3	768.8	43.1
Castor oil	571.5	27.2	816.1	49.7	1017.4	159.0

The differences between the echo12_12 method and the ABC-method was found to be negligible for a given signal processing. For attenuation values less than approximately 400 dB/m, the frequency domain signal processing seems to give higher attenuation values than the time domain processing, whereas the opposite seems to occur for higher attenuations. It should also be noted that the span (or deviation) between the different readings, is of the order of a few dB/m for a value of attenuation up to at least 300 dB/m. For the higher range of attenuation the frequency domain signal processing was found to give significantly higher deviation than the time domain processing.

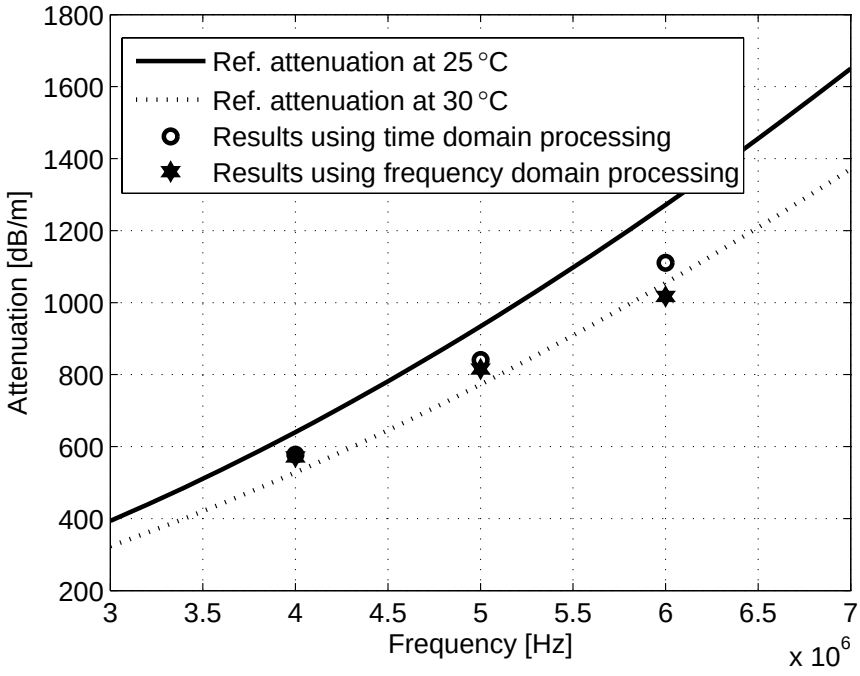

Figure 6.6. Measured attenuation for castor oil and reference attenuation versus frequency. The reference values are given for temperatures of 25 °C and of 30 °C [141].

6.4.2. Obtained results using the 2.4 mm measuring cell

The liquid's attenuation as measured by the 2.4 mm measuring cell are presented in Tables 6.21–6.24 for the echo12_12 method and the ABC-method using both time- and frequency domain signal processing.

Table 6.21. Measured attenuation for the echo12_12 method using a time domain signal processing.

Liquid	4 MHz		5 MHz		6 MHz	
	Mean α [dB/m]	Span [dB/m]	Mean α [dB/m]	Span [dB/m]	Mean α [dB/m]	Span [dB/m]
Distilled water	9.1	6.6	10.9	4.4	14.3	4.1
N4	27.4	4.4	41.5	3.4	54.8	12.7
N7.5	46.1	11.4	67.3	0.8	89.5	4.8
N35	148.2	9.1	226.9	2.9	307.8	1.9
N100	406.6	23.3	607.7	3.3	813.4	15.9

Table 6.22. Measured attenuation for the echo12_12 method using a frequency domain signal processing.

Liquid	4 MHz		5 MHz		6 MHz	
	Mean α [dB/m]	Span [dB/m]	Mean α [dB/m]	Span [dB/m]	Mean α [dB/m]	Span [dB/m]
Distilled water	9.5	4.1	12.5	4.1	16.1	3.5
N4	29.8	4.0	43.1	3.1	56.7	12.0
N7.5	49.1	5.0	69.7	2.5	90.2	2.5
N35	155.1	3.4	228.8	1.9	304.6	4.4
N100	415.4	9.6	609.6	4.4	801.0	14.6

Table 6.23. Measured attenuation for the ABC-method using a time domain signal processing.

Liquid	4 MHz		5 MHz		6 MHz	
	Mean α [dB/m]	Span [dB/m]	Mean α [dB/m]	Span [dB/m]	Mean α [dB/m]	Span [dB/m]
Distilled water	8.9	6.6	10.9	4.4	14.2	4.1
N4	27.5	4.3	41.6	3.6	55.2	12.3
N7.5	46.5	11.5	67.3	0.8	89.4	5.5
N35	148.3	9.1	226.9	2.9	307.8	3.1
N100	406.5	23.7	607.7	4.0	813.4	15.9

Table 6.24. Measured attenuation for the ABC-method using a frequency domain signal processing.

Liquid	4 MHz		5 MHz		6 MHz	
	Mean α [dB/m]	Span [dB/m]	Mean α [dB/m]	Span [dB/m]	Mean α [dB/m]	Span [dB/m]
Distilled water	9.3	4.2	12.4	4.1	15.9	3.5
N4	29.8	4.0	43.2	3.0	57.1	12.0
N7.5	49.3	5.0	69.8	2.5	90.2	2.4
N35	155.1	3.4	228.8	1.8	304.6	4.5
N100	415.3	9.6	609.5	4.4	801.0	14.6

The measured attenuation using the 2.4 mm measuring cell gives attenuation values approximately 4 dB/m higher than for the 5.7 mm measuring cell. This applies throughout the liquids used (castor oil was not used in this measuring cell), except for the N100 oil, which gave between 10 and 23 dB/m higher attenuation than the 5.7 mm measuring cell. This deviation between the cells for the N100 oil is believed to be due to the waveform distortion observed when using the 5.7 mm cell, whereas such a distortion was not evident in the 2.4 mm cell. It was also noted that the span for the N100 oil was significantly reduced compared with the results using the 5.7 mm measuring cell, otherwise much the same observations as for the 5.7 mm measuring cell applies here as well.

6.4.3. Discussion

The attenuation of different liquids was measured covering a wide range of attenuation. For the 2.4 mm measuring cell a systematic increase of the liquid attenuation of approximately 4 dB/m was found, compared to the 5.7 mm measuring

cell. The reason for the systematic deviation between the measuring cells for the lower attenuation liquids is not clear.

In order to clarify the attenuation measurement range, we note that the N100 oil does not contain an overlap in its attenuation value, as found using the 2.4 mm and the 5.7 mm measurement cells, as the A_3^* signal experiences an attenuation of about 10 dB in the 2.4 mm cell at 6 MHz, and about 12 dB at 4 MHz using the 5.7 mm cell. Further experiments are needed before the upper attenuation limit can be established. The upper range of attenuation may be increased as difficulties were experienced for the high viscosity oils (N100 and castor oil) in avoiding air bubbles during the filling process. No attempts of evacuating the air by vacuuming the liquids were performed.

6.5. Amplitude quality indicator and sensitivity factors

The aspects of the amplitude quality indicator were discussed in Chapter 5.2.6. The different sensitivity factors in receive mode are discussed in Paper I and in Chapter 5.2.6, where also the relevant equations are given.

6.5.1. Obtained results using the 5.7 mm measuring cell

The amplitude quality indicator values and the sensitivity factors obtained by using the 5.7 mm measuring cell are presented in Tables 6.25–6.27, using both time- and frequency domain signal processing.

The results for the amplitude quality indicator are given in Table 6.25. The deviation of the amplitude quality indicator from the ideal value is well within 1 % for the lower attenuation liquids. For the higher attenuation liquids (N100 and castor oil) the value of the amplitude quality indicator was found to increase with frequency using the frequency domain signal processing, with a value in the range of 1.4 to 5.8 % for the N100 oil, and in the range of 3.6 to 23.1 % for the castor oil. No such increase in value versus frequency was found using a time domain processing. The increased deviation of the amplitude quality indicator from the ideal value of one for highly viscous liquids using a frequency domain processing coincides with the obtained results for liquid density and attenuation using the same processing, as can be seen in the former sections in this Chapter.

Table 6.25. Values of the amplitude quality indicator versus frequency using the receive transducer, using both a time domain- and a frequency domain signal processing.

Liquid	4 MHz		5 MHz		6 MHz	
	Time	Frequency	Time	Frequency	Time	Frequency
Distilled water	0.998	1.000	0.999	0.999	1.000	0.999
N4	1.001	1.000	1.000	1.000	1.000	0.999
N7.5	1.002	1.000	0.999	0.999	0.999	0.998
N35	1.000	1.002	1.000	1.001	0.997	1.000
N100	0.993	1.014	1.006	1.023	1.000	1.058
Castor oil	1.000	1.036	1.004	1.067	0.983	1.231

Table 6.26. Value of the receive sensitivity ratio R_T/R_R of the electronic channels versus frequency, using both a time domain- and a frequency domain signal processing.

Liquid	4 MHz		5 MHz		6 MHz	
	Time	Frequency	Time	Frequency	Time	Frequency
Distilled water	0.875	0.871	0.850	0.852	0.868	0.876
N4	0.872	0.869	0.860	0.861	0.870	0.877
N7.5	0.876	0.873	0.855	0.856	0.863	0.869
N35	0.878	0.874	0.855	0.856	0.861	0.862
N100	0.877	0.873	0.847	0.847	0.850	0.851
Castor oil	0.880	0.874	0.850	0.849	0.851	0.844

Table 6.27. Value of the receive sensitivity ratio R_A/R_B of the transducers versus frequency, using both a time domain- and a frequency domain signal processing.

Liquid	4 MHz		5 MHz		6 MHz	
	Time	Frequency	Time	Frequency	Time	Frequency
Distilled water	1.006	1.004	0.968	0.965	0.964	0.969
N4	1.011	1.010	0.974	0.970	0.984	0.980
N7.5	1.006	1.006	0.977	0.973	1.007	1.000
N35	0.995	0.995	0.978	0.977	0.990	0.993
N100	1.006	1.005	0.967	0.963	0.983	0.975
Castor oil	0.999	0.998	0.973	0.970	0.976	0.977

The measured value of the receive sensitivity ratio of the electronic channels was found to be significantly less than one, reflecting the loading effect of the transmit electronics on the transmit transducer, as shown in Table 6.26. No clear dependency upon the attenuation characteristics was found, although a systematic behavior versus frequency can be seen. This is believed to be due to systematic effects such as signal processing and diffraction.

For the receive sensitivity ratio of the transducers, a value of one is expected, assuming identical transducers, and "good" acoustic coupling between the transducers and the buffers. No dependency versus the attenuation characteristics was found, although a systematic behavior versus frequency can be seen in Table 6.27. This is believed to be due to systematic effects such as signal processing and diffraction. A deviation of less than 1 % was found between the time- and the frequency domain processing, for a given liquid and at a given frequency.

6.5.2. Obtained results using the 2.4 mm measuring cell

The liquid's amplitude quality indicator and sensitivity factors as measured by the 2.4 mm measuring cell are presented in Tables 6.28–6.30 using both time- and frequency domain signal processing.

Table 6.28. Values of the amplitude quality indicator versus frequency using the receive transducer, using both a time domain- and a frequency domain signal processing.

Liquid	4 MHz		5 MHz		6 MHz	
	Time	Frequency	Time	Frequency	Time	Frequency
Distilled water	0.996	0.999	0.998	0.998	1.002	0.998
N4	0.998	0.998	0.998	0.999	1.000	1.001
N7.5	0.996	0.999	1.000	1.000	1.001	0.999
N35	0.995	1.001	1.002	0.999	1.000	0.998
N100	1.005	1.001	1.000	1.000	0.997	1.003

Table 6.29. Value of the receive sensitivity ratio R_T/R_R of the electronic channels versus frequency, using both a time domain- and a frequency domain signal processing.

Liquid	4 MHz		5 MHz		6 MHz	
	Time	Frequency	Time	Frequency	Time	Frequency
Distilled water	0.873	0.872	0.849	0.850	0.876	0.879
N4	0.876	0.873	0.849	0.849	0.865	0.868
N7.5	0.876	0.874	0.853	0.854	0.866	0.869
N35	0.872	0.870	0.849	0.852	0.865	0.876
N100	0.878	0.876	0.855	0.856	0.870	0.875

The main difference found using the 2.4 mm measuring cell compared with using the 5.7 mm measuring cell, was that the deviation of the amplitude quality indicator from the ideal value is well within 1 % for all the liquids used, as seen in Table 6.28. This is attributed to be due to the reduced attenuation experienced in this measurements cell compared to the larger 5.7 mm measuring cell, with its corresponding reduced waveform distortion.

For the sensitivity factors, only minor differences were found compared to the 5.7 mm measuring cell.

Table 6.30. Value of the receive sensitivity ratio R_A/R_B of the transducers versus frequency, using both a time domain- and a frequency domain signal processing.

Liquid	4 MHz		5 MHz		6 MHz	
	Time	Frequency	Time	Frequency	Time	Frequency
Distilled water	0.998	0.996	1.002	1.003	1.011	1.026
N4	0.998	0.996	0.975	0.974	0.983	0.986
N7.5	0.995	0.994	0.991	0.991	1.001	1.011
N35	0.989	0.986	0.996	0.999	0.972	0.998
N100	0.999	0.997	1.001	1.002	0.994	1.016

6.6. Influential factors

6.6.1. Introduction

In order to examine some influential factors on the operation of the measurement system, the frequency dependence of the mode converted signal is discussed in Chapter 6.6.2. An example of driving the transducer outside its passband is given in Chapter 6.6.3, and an example of the effect on the density of not using the switch in the path of the Tx-transducer is given in Chapter 6.6.4. Measured dispersion, and the effect of Kramers Kronig relations are discussed in Chapter 6.6.5.

6.6.2. Frequency dependence of the mode converted signal

In order to evaluate the frequency dependence of the mode converted echo signal from the buffer–liquid interface, a measurement series using castor oil was performed using the 5.7 mm measuring cell. The measurements were performed using both 2.25 MHz and 5.0 MHz centre frequency transducers using a burst length of 1 period. The pulse-echo waveforms using the 5 MHz transducer, are given in Fig. 6.7, for the 1–6 MHz frequency range. There, the amplitudes of the A_1 echo signals arising from reflection at the buffer–liquid interface (not propagating through the oil) were normalized to account for the transducer's frequency dependent sensitivity. As can be seen in Fig. 6.7, the amplitude of the mode converted signal decays rapidly when increasing the frequency, and is significantly less troublesome at the higher frequencies. Therefore, a relatively high frequency of 5 MHz would be advantageously with respect to the interference from the mode converted echo signal from the buffer–liquid interface. The A_3 echo signal is also seen to be significantly attenuated at the higher frequencies, when using castor oil. The A_3 echo signal may still experience considerable interference from the mode converted signal, depending upon the frequency and the signal duration. The ABC-method is considerable more prone to interference from mode converted signals than the echo12_12 method.

The same behavior was also found using the 2.25 MHz transducer in the 1–6 MHz frequency range. If the effect of the mode converted echo signal could be neglected, a much wider operating range with respect to the maximum allowed echo signal duration and the maximum liquid path length would be possible, as mentioned in Chapter 5.2. In this work, a reasonably high frequency, and a limited number of periods in the burst have been used in order to avoid interference of the mode converted signal with the A_2 and the A_3 echo signals.

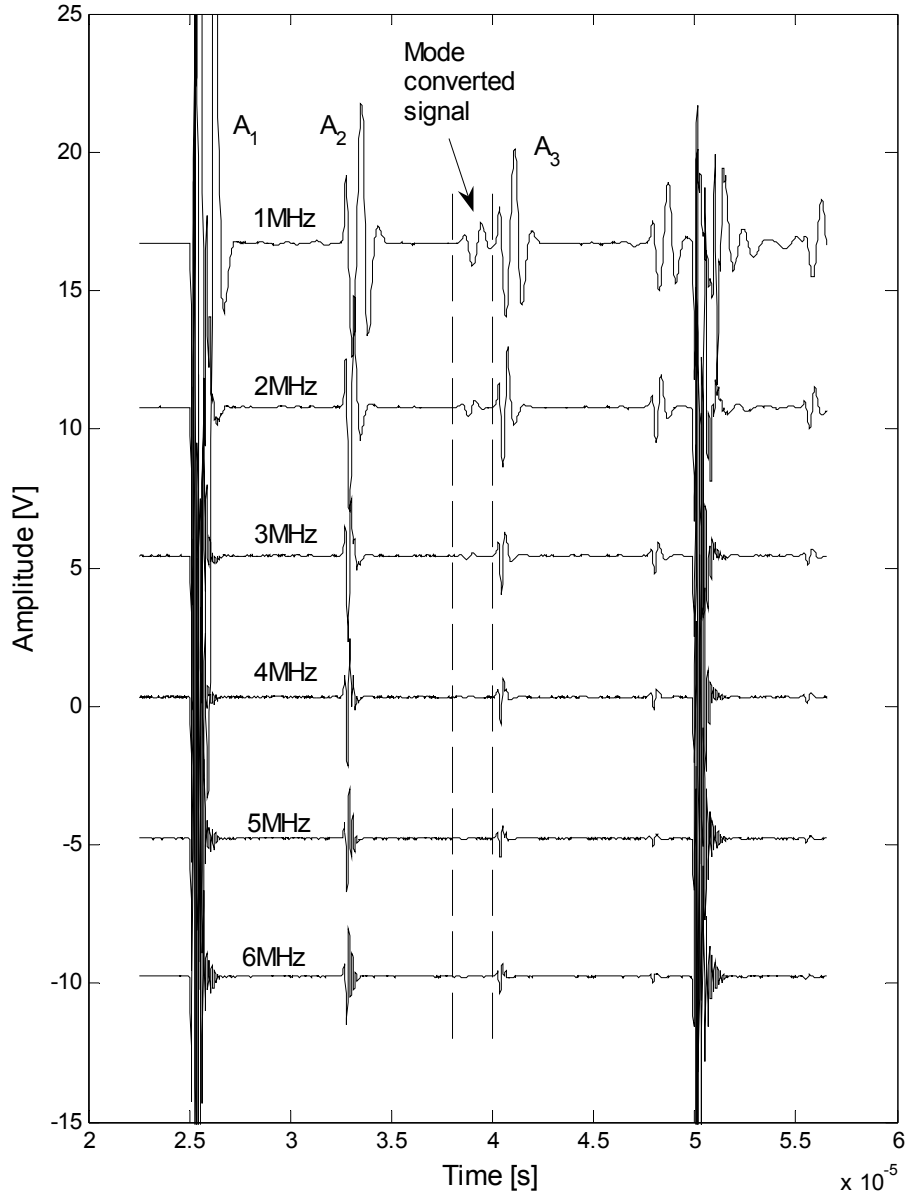

Figure 6.7. Frequency dependence of the mode converted echo signal as measured by the 5 MHz Tx-transducer using a 1 period burst. The mode converted signal appears in the time frame within the dashed lines. Castor oil was used in the 5.7 mm measuring cell. The amplitudes of the A_1 echo signals were normalized, and the measured responses were offset for clarity.

6.6.3. Driving the transducer outside of the passband

According to Papadakis [65], one of the advantages of the ABC-method is its possibility to operate the transducer away from its resonant frequency. Operating the 2.25 MHz transducer in a burst mode using 6 periods at a frequency of 6 MHz is considered outside the usual operating frequency range of this transducer. The echo

signals from the castor oil filled 5.7 mm measurement cell are given in Fig. 6.8. There, several aspects can be noted; 1) The distortion of the waveform as each pulse seems to be split into three parts, an initial high amplitude transient part, a low amplitude stationary part, and finally a high amplitude transient part, and 2) the low pass characteristic of the castor oil attenuates the echo signals that have propagated through the oil due to a more severe damping of the higher frequency components. A significant waveform distortion is observed, reducing the suitability of such high attenuation liquids to be used for accurate characterization. In this particular case, a successful analysis could not be made with the present signal processing due to the severe waveform distortion.

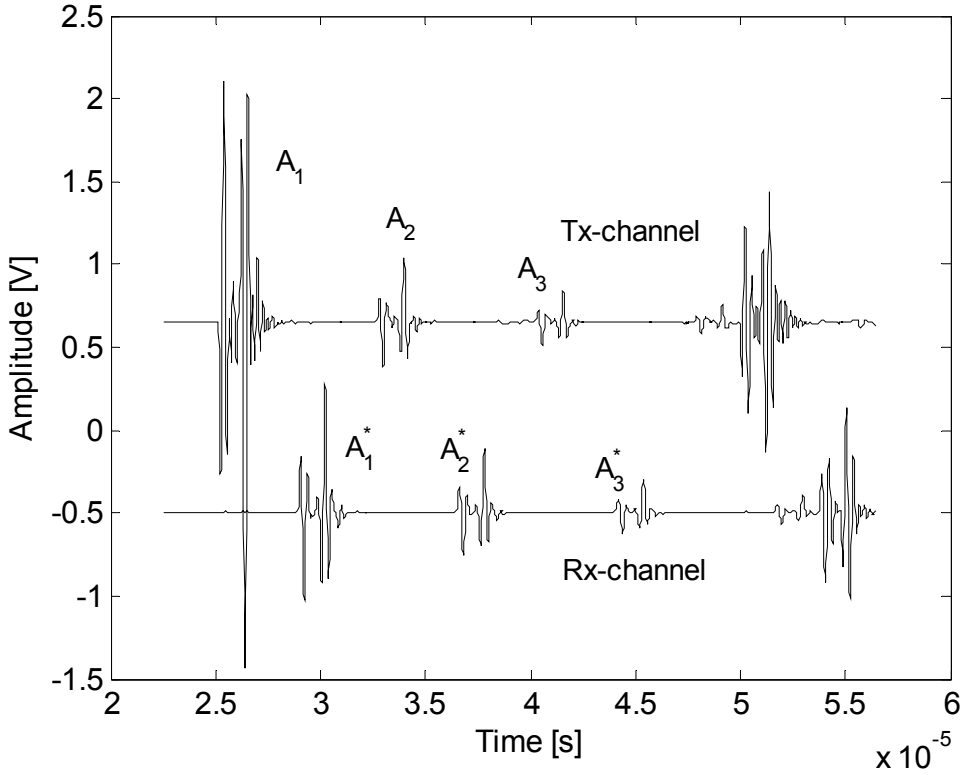

Figure 6.8. Observed waveforms when driving the 2.25 MHz transducer in a burst mode using 6 periods at a frequency of 6 MHz. The liquid used was castor oil in the the 5.7 mm measuring cell. The waveforms were offset for clarity.

6.6.4. Effect of the electronic system on measured density

As discussed in Chapter 5.4, the dominant part of the experimental work was performed using the Supertex HV20720 switch in the path of the Tx-transducer. Some of the results using that arrangement are also given in Paper II. Only a limited number of measurements were performed without using the switch network. A limited comparison will however be given using the switch network and a direct connection between the function generator and the Tx-transducer.

Results are given in Table 6.31 using the switch arrangement and in Table 6.32 using the direct connection. In these tables, each frequency has two columns, the first gives the mean (or systematic) deviation in per cent from the density reference values, whereas the other column gives half the span in per cent between the maximum and the minimum deviation from the reference values. This way, the second column can easier be compared with predicted uncertainties. Measurement results are given for the Cannon N4, N7.5, and the N35 oil, using a frequency range of 4–6 MHz for the 5 MHz transducers. The measurements were performed using the 5.7 mm measuring cell. The N100 oil was not included due to significant waveform distortion, as can be seen in Fig. 6.1.

Table 6.31. Measured densities using the Supertex HV20720 switch arrangement for the Cannon N4, N7.5, and the N35 oil, using the 5.7 mm measuring cell.

Method	4 MHz		5 MHz		6 MHz	
	Mean dev [%]	0.5 · Span [%]	Mean dev [%]	0.5 · Span [%]	Mean dev [%]	0.5 · Span [%]
echo12_12 time domain	-0.35	0.06	-0.17	0.16	-0.18	0.19
echo12_12 frequency domain	-0.48	0.06	-0.32	0.09	-0.42	0.25
ABC time domain	-0.15	0.15	0.05	0.19	0.07	0.41
ABC frequency domain	-0.32	0.17	-0.18	0.08	-0.23	0.49

From the Tables 6.31–6.32, it is found that the systematic deviation is higher when not using the switch arrangement, but the most striking feature is the reduced span obtained for the echo12_12 method at 5 MHz (centre frequency) when not using the switch arrangement. The reason of this difference is not clear. The low values of ± 0.03 % to ± 0.04 % provide that the oils used would approach the maximum allowed uncertainty by the NPD [8]. Further experiments should be performed using both measurement cells and with a broader range of liquids in order to see if such a level of measurement span can be routinely obtained.

Table 6.32. Measured densities obtained using a direct connection between the function generator and the Tx-transducer for the Cannon N4, N7.5, and the N35 oil, using the 5.7 mm measuring cell.

Method	4 MHz		5 MHz		6 MHz	
	Mean dev. [%]	0.5 · Span [%]	Mean dev. [%]	0.5 · Span [%]	Mean dev. [%]	0.5 · Span [%]
echo12_12 time domain	-0.89	0.05	-0.42	0.04	-0.48	0.21
echo12_12 frequency domain	-0.84	0.12	-0.50	0.03	-0.55	0.31
ABC time domain	-0.76	0.37	-0.26	0.06	-0.07	0.21
ABC frequency domain	-0.72	0.22	-0.42	0.12	-0.32	0.47

6.6.5. Dispersion

Dispersion is the change of sound speed with frequency. Through the Kramers Kronig relations [143], dispersion is known to cause attenuation, and vice versa. Dispersion may then be responsible for waveform distortion, both in the temporal- and the frequency domain. A broadband pulse with significant dispersion would introduce a significant uncertainty in the measured density due to the uncertainty of which sound speed to use in the density calculation, in addition to the effect of the distortion on the amplitude measurement.

Szabo [144] proposed in 1995 a time causal theory, which can be used to determine the dispersion from the measured attenuation according to

$$\frac{1}{V_{p(\omega_0)}} - \frac{1}{V_{p(\omega)}} = \frac{2\alpha_0}{\pi} \ln \frac{\omega}{\omega_0} \quad \text{for } y = 1, \tag{6.12}$$

$$\frac{1}{V_{p(\omega_0)}} - \frac{1}{V_{p(\omega)}} = -\alpha_0 \tan\left(y \frac{\pi}{2} \right) \left(\omega^{y-1} - \omega_0^{y-1} \right) \quad \text{for } y > 1, \tag{6.13}$$

in which the attenuation follows a power law of the form

$$\alpha = \alpha_0 \omega^y , \tag{6.14}$$

where α_0 and y ($1 \le y \le 2$) are two material-dependent parameters. In these equations, ω_0 serves as the reference (angular) frequency. Eq. (6.13) can be approximated as [141]

$$V_{p(\omega)} \approx V_{p(\omega_0)} - \alpha_0 V_{p(\omega_0)}^2 \tan\left(y\frac{\pi}{2}\right)\left(\omega^{y-1} - \omega_0^{y-1}\right). \quad (6.15)$$

Distilled water is known not to possess dispersion in a frequency range exceeding 500 MHz [53]. The Cannon oils N4, N7.5, and N35 did not give any measurable dispersion in the 4–6 MHz frequency range, as can be seen from Table 6.33. The other oils gave an averaged measured value of 0.205 m/s/MHz and 0.565 m/s/MHz, for the N100 oil, and for castor oil, respectively, in this frequency range. Therefore, dispersion is not expected to increase the measurement errors to a significant degree.

As an example of using this time causal theory, the attenuation and the dispersion of the N100 oil is given in Fig. 6.9 using the echo12_12 method and time domain signal processing. In Fig. 6.9, α_0 and y were adjusted so that a reasonable correspondence between the measured and the modeled attenuation were obtained. In order for this procedure to be used to obtain dispersion, measurements at more frequencies would be necessary, or the use of spectroscopy, in which the parameter dependence upon frequency may be obtained using short pulses [145].

Although dispersion in this way may be obtained from measured attenuation, the way the individual pulses gets distorted upon traveling through the liquid, is not easily obtainable. Szabo [146] recently proposed a procedure for performing such a simulation in the time domain by using a material impulse response function which represents a closed form causal function describing absorption, dispersion and delay as a function of frequency and increasing distance. By using this material impulse response function, knowledge about how distortion of the individual echo signals influence the operation of the measurement cell would be obtained. However, this approach has not been performed in this work.

Table 6.33. Measured sound speeds in the 4–6 MHz frequency range at a temperature of 27.44 ± 0.04 °C, for both measuring cells, with the given uncertainties reflecting the results of the different measuring cells.

Liquid	Sound speed [m/s]		
	4 MHz	5 MHz	6 MHz
N4	1333.80 ± 0.32	1333.65 ± 0.43	1333.56 ± 0.48
N7.5	1359.96 ± 0.13	1359.88 ± 0.12	1359.80 ± 0.05
N35	1426.75 ± 0.78	1426.71 ± 0.71	1426.68 ± 0.64
N100	1452.43 ± 0.29	1452.61 ± 0.11	1452.84 ± 0.07
Castor oil *	1497.73	1498.36	1498.86
Distilled water **	1503.06 ± 0.21	1502.86 ± 0.10	1502.83 ± 0.08

* Based on using the 5.7 mm measuring cell.

** Based on a 5th order polynomial [46].

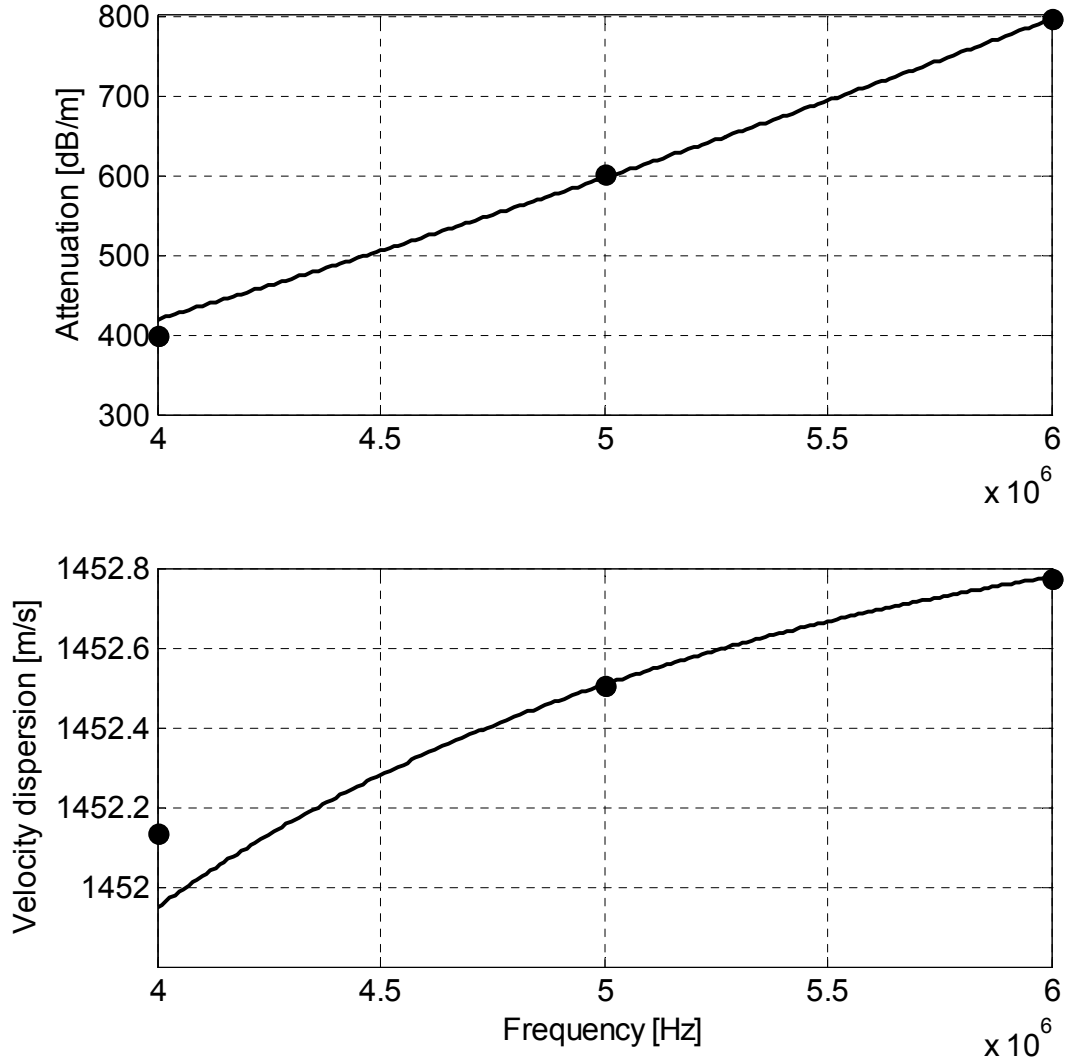

Figure 6.9. Measured (filled circles) and modeled (line) attenuation and dispersion of the Cannon N100 oil. Upper figure: Measured attenuation and fitted curve. Lower figure: Measured dispersion, and the model-predicted dispersion, using the attenuation parameters y=1.58 and α_0=5.4 (dB cm^{-1} MHz$^{-1.58}$). The reference frequency f_0=5 MHz.

6.7. Summary

In this Chapter, measurement results beyond what was covered in Paper II were given. These included use of the relative amplitude approach for measurement of liquid parameters such as density and attenuation using a wide range of shear viscosities. The value of the amplitude quality indicator and the ratio of the different sensitivity factors were also measured. The first demonstration of the mixed amplitude approach for measuring liquid density was also given.

Additionally, it was shown how some of the non-ideal factors may influence the proposed measurement cell's operation if not corrected for, or if possible avoided. These factors included the frequency dependent behavior of the mode converted echo signal from the buffer–liquid interface, the effect of driving the transducer outside its passband, the effect on the measured density by using / not using a switch arrangement between the signal source and the transmit transducer, and the effect of dispersion.

The results from these examinations can be briefly summarized as:

- Liquid density can be measured accurately for liquids having a wide range in shear viscosity (or attenuation). A measurement span of ± 0.15 % in density was obtained for widely different liquids using both a time- and a frequency domain processing operating the transducers at the centre frequency.
- The benefits of using the mixed amplitude approach were shown for the first time when measuring on a liquid possessing significant waveform distortion. It was found that the liquid density could be maintained at approximately the reference value even though the pulses used were significantly exposed to waveform distortion. The echo12_1 method was found to give the best result, as was expected, as the echo signals involved using this method, suffers the least attenuation.
- The attenuation of different liquids was measured successfully covering a wide measurement range.
- Measured values for the amplitude quality indicator and for the different sensitivity ratios were obtained. The obtained values indicate that new methods to ensure proper operation of the measurement system and of the signal processing were successfully devised.
- There are clear indications that the frequency domain signal processing performs worse than the time domain processing in the case of highly viscous liquids. This may, however, be used as an indicator of waveform distortion, if the results from both processing methods are compared, and found to deviate significantly.
- The amplitude of the mode converted echo signal from the buffer–liquid interface was shown to be largest at the lower frequencies.
- Preliminary measurements when the switch arrangement was not used, indicates that the span in measured density deviations from reference values may be reduced from ± 0.15 %, as obtained when using the switch arrangement, to less than ± 0.05 %. More work is necessary in order to clarify this matter. It is also not clear what this means for the measurement uncertainty.
- Reasonably accurate results were obtained when using a time causal theory to predict the dispersion from measured attenuation. It is believed that by

using a recently introduced theory that the effect of attenuation, dispersion, and delay could be properly evaluated for the proposed measurement cell.

- For the different liquids used in this work, a reflection coefficient at the buffer–liquid interface in the range of 0.84 to 0.89 was obtained. Papadakis [65] claimed for the ABC-method that the acoustic impedance of the buffer rod must match that of the sample fairly closely, but not perfectly, and found that reflection coefficients between 0.3 and 0.7 yielded the best attenuation data. Brown [147] later claimed for the ABC-method that nearly equally acoustic impedances of the buffer and the sample were required. However, it was shown in this work that the ABC-method could be successfully applied for widely different acoustic impedances of the buffer and of the sample, and may therefore lead to increased use of acoustics in the field of liquid density measurements.

Chapter 7. Conclusions, perspectives, and recommendations to further work

7.1. Conclusions and perspectives

Work has been performed on the measurement of liquid density using acoustic means, and a new measurement approach was proposed. This new measurement approach consists of using two buffer-rods enclosing the liquid in a symmetrical arrangement, with a transducer fixed to each buffer. Such an approach has also applications within fluid characterization. The parameters that can be measured using this approach are: Sound speed of the liquid and of the buffer material, reflection- and transmission coefficients at the buffer–liquid interface, characteristic acoustic impedance, density, adiabatic compressibility, and attenuation of the liquid.

Two generic approaches were identified for the measurement of the reflection coefficient using two transducers in a mixed pulse-echo mode and a through-transmission mode. These are the relative amplitude approach and the mixed amplitude approach. The relative amplitude approach uses amplitude ratios obtained from the same transducer. Therefore, the transducer- and acquisition channels sensitivity factors in receive mode are cancelled. The mixed amplitude approach uses a mixture of amplitude ratios from the same transducer and from the different transducers, and thereby the sensitivity factors cannot be neglected. The uncertainty characteristics of both these approaches were evaluated, and new measuring methods for the reflection coefficient having close to the lowest possible uncertainty characteristics were identified.

By including the sensitivities of the transducers and of the acquisition channels in the receive mode in the theoretical formulation, several new features were obtained. These are the ratio of the transducers sensitivity in receive mode and the ratio of the acquisition channels sensitivity in receive mode. The ratio of the transducers sensitivity in receive mode may give information about the acoustical coupling quality, and if changes versus time occur. The ratio of the receive channels sensitivity may be obtained by the amplitudes of the acoustic echo signals, or from measurements on the electronic system directly, dependent upon the design of the acquisition system.

An amplitude quality indicator monitoring possible waveform distortion effects was also devised, with its non-distorted reference value equal to one. This quality indicator use in its simplest form amplitude measurements on the echo signals on the

receive transducer in the proposed measuring cell. The amplitude quality indicator's deviation from its reference value was found to exceed a few per cent when waveform distortion was easily visible. This was however only obtained using the frequency domain signal processing. The benefits of using the mixed amplitude approach were shown for the first time when measuring on a liquid possessing significant waveform distortion. It was found that the liquid density could be maintained at approximately the reference value even though the pulses used were significantly exposed to waveform distortion.

Some of the identified measuring methods for the reflection coefficient (such as those utilizing not more than the two first echo signals from each transducer) make possible an increased signal duration compared to the previously known ABC-method, which is beneficial with respect to obtaining the stationary part of the pulses. It was also shown that an increased liquid layer thickness could be obtained using these proposed methods, giving increased freedom with respect to the liquids characteristics.

Using liquids spanning a wide range of viscosities, measured densities were obtained which deviated within ± 0.15 % from reference values, when the systematic deviation was corrected for. It is believed that further improvements in the acquisition system would give improved results. Based on the above points, it is therefore felt that this study on the measurement of liquid density by acoustic means has advanced on the measuring methods known to date.

7.2. Further work

During this work several aspects have appeared that deserves more attention than was possible during this limited investigation. The most important are believed to be:

- For the diffraction correction, two aspects are particularly relevant:
    - A spectral formulation should be used instead of the single-frequency correction used in this work. This would contribute advantageously, particularly in the more transient part of the pulses.
    - Acoustic characterization of the transducers sound field should be performed. Then, a more suitable diffraction correction could be applied to the individual transducers, giving a reduced systematic deviation of the measured liquid densities using the proposed measurement approach. Then, the echo12_12 method would probably experience a systematic deviation of measured densities approaching that of the ABC-method, which uses only one transducer.

- Noise characteristics: In order to reduce the noise characteristics when not using a switch arrangement, an impedance matching transformer should be inserted between the signal generator and the transmit transducer. It is believed that this would give reduced spread in the measurements.
- Bit resolution: When large amplitude differences exists between the echo signals on an acquisition channel, a reduced effective number of bits results for the low amplitude signal compared to the higher amplitude signal. This can be solved in at least three different ways:
    - By using more acquisition channels in which each echo signal gets acquired using a full vertical span by an individual channel.
    - Use of a higher resolution digitizer. Analogue to digital converters exists with 16 bits of resolution with a sampling rate exceeding 100 MSa/s, and complete acquisition systems with such performance are commercially available.
    - By using a down-conversion (heterodyning) of the signal frequency, so that a higher resolution digitizer may be used, sampling at a reduced rate.
- In order to obtain an acoustic liquid densitometer for use in the process industry, the choice of materials must be carefully evaluated, and equally important, the size should be reduced as much as possible. It is believed that the dimensions can be significantly reduced without any major disturbing effect.
- The proposed buffer-rod approach has advantages in the measurement of parameters of liquids compared to the measurement on solids, due to the lack of joint at the buffer–sample interface. The effect of deposits at this interface when measuring on liquids is known to cause problems [4], [72]. However, no work concerning this aspect has been performed in this work.
- The operation of the proposed measuring cell on flowing liquids has not yet been performed.

References

[1] T. Cousins, “Liquid and gas density measurement: Part 1 (Fluid density measurement)”, Measurement + Control, 25, pp. 292–296, December/January 1992/93.

[2] J. Delsing, “On ultrasonic flow meters. Investigations and improvements of the sing-around flow meter”, Ph.D. thesis, Lutedx/(TEEM-1036) / pp. 1–48, Lund Institute of Technology, Lund, 1988.

[3] J. C. Adamowski, “Ultrasonic measurement of density of liquids”, Ph.D. thesis, Escola Politécnica da Universidade de São Paulo, 1993 (in Portuguese).

[4] A. Püttmer, “Ultrasonic Density Sensor for Liquids”, Ph.D. thesis. Shaker Verlag, Aachen, 1998, ISBN 3-8265-4614-8.

[5] M. Hirnschrodt, “Dichtemessverfahren für Flüssigkeiten nach dem akustischen Entspiegelungprinzip”, Ph.D. thesis, Erlangen-Nürnberg Universität, 2000, ISBN 3-18-386508-4.

[6] J. van Deventer, “Material Investigations and Simulation Tools Towards a Design Strategy for An Ultrasonic Densitometer”, Ph.D. thesis, Luleå University of Technology, 2001.

[7] N. Hoppe, “Ultraschall-Dichtesensor – Entwurf, Charakterisierung und Signalverarbeitung”, Ph.D. thesis, Otto-von-Guericke- Universität Magdeburg, 2003.

[8] The Norwegian Petroleum Directorate (NPD), “Regulations relating to measurement of petroleum for fiscal purposes and for calculation of CO_2-tax (The measurement regulations)”, November 2001. Available: http://www.npd.no/regelverk/r2002/frame_e.htm

[9] E. Bjørndal and K-E. Frøysa, “Ultralyd tetthetsmåler for væske”, Norwegian patent No. 322349 (in Norwegian), granted 2006. Available: http://www.patentstyret.no/upload/filarkiv/patenter/seksjong/2006/uke38/322349.pdf

[10] L. E. Kinsler, A. R. Frey, A. B. Coppens, and J. V. Sanders, *Fundamentals of Acoustics*, 3rd edition, John Wiley & Sons, Chapter 6, 1982.

[11] J. P. Weight, “A model for the propagation of short pulses of ultrasound in a solid”, J. Acoust. Soc. Am., 81(4), pp. 815–826, April 1987.

[12] M. R. Riazi, “Characterization and Properties of Petroleum Fractions”, ASTM manual series: MNL50, Chapter 2, 2005. ISBN 0-8031-3361-8.

[13] M. R. Riazi, “Characterization and Properties of Petroleum Fractions”, ASTM manual series: MNL50, Chapter 1, 2005. ISBN 0-8031-3361-8.

[14] F. Spieweck and H. Bettin, “Review: Solid and liquid density determination”, Technisches Messen, 59(6), pp. 237–244, 1992.

[15] F. Spieweck and H. Bettin, “Review: Solid and liquid density determination”, Technisches Messen, 59(7/8), pp. 285–292, 1992.

[16] S. V. Gupta, *Practical density measurement and hydrometry*, Series in Measurement Science and Technology, Institute of Physics Publishing, ISBN 0-7503-0847-8, 2002.

[17] L. C. Lynnworth, Ultrasonic Measurements for Process Control. Theory, Techniques, Applications. Academic Press, Inc., 1989, ISBN 0-12-460585-0.

[18] F. Spieweck, “Sensors for measuring density and viscosity”, Chapter 10 in “Sensors – A Comprehensive Survey”. Edited by W. Göpel, J. Hesse, J. N. Zemel. Volume 7 Mechanical Sensors, Edited by H. H. Bau, N. F. deRooij, B. Kloeck. VCH Publishers Inc., New York, 1994, ISBN 0-89573-679-9.

[19] P. Mason, “Liquid and gas density measurement: Part 2 (Fluid density)”, Measurement + Control, 25, pp. 297–302, December/January 1992/93.

[20] Available at: http://www.mobrey.com

[21] L. C. Lynnworth and V. Mágori, “Industrial Process Control Sensors and Systems”, in Physical Acoustics Volume XXIII – Ultrasonic Instruments and Devices I, References for Modern Instrumentation, Techniques, and Technology, edited by R. N. Thurston, A. D. Pierce, and E. P. Papadakis, p. 343, 1999. ISBN 0-12-477923-9.

[22] P. Vigo, and F. Cascetta, “Sensors for measuring flow”, Chapter 11 in “Sensors – A Comprehensive Survey”. Edited by W. Göpel, J. Hesse, J. N. Zemel. Volume 7 Mechanical Sensors, Edited by H. H. Bau, N. F. deRooij, B. Kloeck. VCH Publishers Inc., New York, 1994, ISBN 0-89573-679-9.

[23] J. Carlson, “Ultrasonic characterization of materials and multiphase flows”, Ph.D. thesis, EISLAB, Luleå University of Technology, Luleå, 2002.

[24] P. Lunde, K-E. Frøysa, and M. Vestrheim, “Multipath ultrasonic transit time gas flow meters”, GERG Project on Ultrasonic gas Flow Meters, Phase II, VDI Verlag, pp. 6–23, 2000. ISBN 3-18-385408-2.

[25] J. Matson, C. H. Mariano, O. Khrakovsky, and L. C. Lynnworth, “Ultrasonic mass flowmeters using clamp-on or wetted transducers”, Panametrics report UR-240, 2002. Excerpts from this report also presented at the *5th International Symposium on Fluid Flow Measurements*, Arlington, Virginia, April 7–10, 2002, and included in the Proceedings of that Symposium.

[26] M. N. Rychagov, S. Tereshcenko, Y. Masloboev, M. Simon, and L. C. Lynnworth, “Mass flowmeter for fluids with density gradients”, *Proc. IEEE Ultrason. Symp*., pp. 465–470, 2002.

[27] C. A. Swoboda, D. R. Fredickson, S. D. Gabelnick, P. H. Cannon, F. Hornstra, N. P. Yao, K. A. Phan, and M. K. Singleterry, “Development of an ultrasonic technique to measure specific gravity in lead-acid battery electrolyte”, IEEE Transactions on Sonics and Ultrasonics, 30(2), pp. 69–77, March 1983.

[28] D. Vray, D. Berchoux, P. Delachartre, and G. Gimenez, “Speed of sound in sulfuric acid solution: Application to density measurement”, *Proc. IEEE Ultrason. Symp*., pp. 969–972, 1992.

[29] Z. Wang, and A. Nur, “Ultrasonic velocities in pure hydrocarbons and mixtures”, J. Acoust. Soc. Am. 89(6), pp. 2725–2730, June 1991.

[30] Z. Wang, and A. Nur, “Wave velocities in hydrocarbon-saturated rocks: Experimental results”, Geophysics, 55(6), pp. 723–733, June 1990.

[31] Z. Wang, A. Nur, and M. L. Batzle, “Acoustic velocities in petroleum oils”, J. Petroleum Technology, 42, pp. 192–200, February 1990.

[32] H-L. Kuo, “Variation of ultrasonic velocity and absorption with temperature and frequency in high viscosity vegetable oils”, Japanese Journal of Applied Physics, 10(2), pp. 167–170, February 1971.

[33] G. W. Marks, “Acoustic velocity with relation to chemical constitution in alcohols”, J. Acoust. Soc. Am. 41(1), pp. 103–117, 1967.

[34] T. Takagi, (in Japanese, with abstract, figures, and tables in English, this article was a review of experimental techniques for measuring ultrasonic speed, its behavior in liquids at high pressures, and the estimation of the liquid density from the speed data), Rev. High Press. Sci. Technol., 3, p. 311, 1994.

[35] B. A. Oakley, G. Barber, T. Worden, and D. Hanna, "Ultrasonic parameters as a function of absolute hydrostatic pressure. I. A review of the data for organic liquids", J. Phys. Chem. Ref. Data, 32(4), pp. 1501–1533, 2003.

[36] L. A. Davis, and R. B. Gordon, "Compression of mercury at high pressure", J. Chem. Phys., 46(7), pp. 2650–2660, April 1967.

[37] J. L. Daridon, A. Lagrabette, and B. Lagourette, "Speed of sound, density, and compressibilities of heavy synthetic cuts from ultrasonic measurements under pressure", J. Chem. Thermodynamics, 30, pp. 607–623, 1998.

[38] B. Lagourette, and J. L. Daridon, "Speed of sound, density, and compressibility of petroleum fractions from ultrasonic measurements under pressure", J. Chem. Thermodynamics, 31, pp. 987–1000, 1999.

[39] S. Dutour, B. Lagourette, and J. L. Daridon, "High-pressure speed of sound, density, and compressibility of heavy normal paraffins: $C_{28}H_{58}$ and $C_{36}H_{74}$", J. Chem. Thermodynamics, 34, pp. 475–484, 2002.

[40] S. Dutour, H. Carrier, and J. L. Daridon, "Compressibilities of liquid pentadecylcyclohexane and nonadecylcyclohexane from high pressure speed of sound and density measurements", J. Chem. Thermodynamics, 35, pp. 1613–1622, 2003.

[41] J. M. Hale, "Ultrasonic density measurement for process control", Ultrasonics, 26, pp. 356–357, November 1988.

[42] K. W. McGregor, "methods of ultrasonic density measurement", Australian Instrumentation and Measurement Conference, Adelaide, pp. 296–298, 1989.

[43] B. Henning, P-C. Daur, S. Prange, K. Dierks, and P. Hauptmann, "In-line concentration measurement in complex liquids using ultrasonic sensors", Ultrasonics, 38, pp. 799–803, 2000.

[44] V. A. Sukatskas, V. K. Armoska, and E. V. Stankyavichyus, "Ultrasonic densimeter for liquids", Meas. Tech., pp. 311–313, 1993. ISSN: 0543-1972.

[45] D. K. Mak, "Comparison of various methods for the measurement of reflection coefficient and ultrasonic attenuation", British Journal of NDT, 33(9), pp. 441–449, September 1991.

[46] W. Marczak, "Water as a standard in the measurements of speed of sound in liquids", J. Acoust. Soc. Am., 102(5), Pt. 1, pp. 2776–2779, November 1997.

[47] S. V. Gupta, *Practical density measurement and hydrometry*, Series in Measurement Science and Technology, Institute of Physics Publishing, Chapter 4.7, 2002, ISBN 0-7503-0847-8.

[48] S. Leeman, L. Ferrari, J. P. Jones, and M. Fink, "Perspectives on attenuation estimation from pulse-echo signals", IEEE Transactions on Sonics and Ultrasonics, 31(4), pp. 352–361, July 1984.

[49] W. P. Mason, W. O. Baker, H. J. McSkimin, and J. H. Heiss, "Measurement of shear elasticity and viscosity of liquids at ultrasonic frequencies", Physical Review, 75(6), pp. 936–946, March 1949.

[50] R. S. Moore and H. J. McSkimin, in Physical Acoustics, Volume VI, (Academic Press, New York), pp. 167–242, 1970.

[51] D. J. McClements, and P. Fairly, "Ultrasonic pulse echo reflectometer", Ultrasonics 29, pp. 58–62, 1991.

[52] D. J. McClements, and P. Fairly, “Frequency scanning ultrasonic pulse echo reflectometer”, Ultrasonics 30, pp. 403–405, 1992.
[53] J. Kushibiki, N. Akashi, T. Sannomiya, N. Chubachi, and F. Dunn, “VHF/UHF range bioultrasonic spectroscopy system and method”, IEEE Trans. Ultrason., Ferroelec. Freq. Contr., 42(6), pp. 1028–1039, November 1995.
[54] P. D. Fox, P. P. Smith, and S. S. Sahi, “Buffer rod design for measurement of specific gravity in the processing of industrial food batters”, *Proc. IEEE Ultrason. Symp*., pp. 679–682, 2002.
[55] M. S. Greenwood, “Ultrasonic fluid densitometry and densitometer”, US Patent 5,708,191, 1998.
[56] M. S. Greenwood, “Pitch-catch only ultrasonic fluid densitometer”, US Patent 5,886,250, 1999.
[57] M. S. Greenwood, J. R. Skorpik, J. A. Bamberger, and R. V. Harris, “On-line ultrasonic density sensor for process control of liquids and slurries”, Ultrasonics, 37, pp. 159–171, 1999.
[58] M. S. Greenwood, “Ultrasonic fluid densitometer for process control”, US Patent 6,082,180, 2000.
[59] M. S. Greenwood, “Ultrasonic fluid densitometer having liquid/wedge and gas/wedge interfaces”, US Patent 6,082,181, 2000.
[60] M. S. Greenwood, and J. A. Bamberger, “Ultrasonic sensor to measure the density of a liquid or slurry during pipeline transport”, Ultrasonics, 40, pp. 413–417, 2002.
[61] N. H. Wang, B. Ho, and R. Zapp, “Velocity–density product and attenuation–density ratio measurements using broadband signals”, IEEE Trans. Instr. Meas., 40(6), pp. 1027–1030, December 1991.
[62] L. C. Lynnworth, and N. E. Pedersen, “Ultrasonic mass flowmeter”, *Proc. IEEE Ultrason. Symp*., pp. 87–90, 1972.
[63] B. R. Jensen, “Measuring equipment for acoustic determination of the specific gravity of liquids”, US Patent 4,297,608, 1981.
[64] J. van Deventer, “One dimensional modeling of a step-down ultrasonic densitometer for liquids”, Ultrasonics 42, pp. 309–314, 2004.
[65] E. P. Papadakis, “Buffer-rod system for ultrasonic attenuation measurements”, J. Acoust. Soc. Am., 44(5), pp. 1437–1441, 1968.
[66] W. Sachse, “Density determination of a fluid inclusion in an elastic solid from ultrasonic spectroscopy measurements”, *Proc. IEEE Ultrason. Symp*., Cat. #74 CHO 896-ISU, pp. 716–719, 1974.
[67] B. R. Kline, “System and method for ultrasonic determination of density”, US Patent 4,991,124, 1990.
[68] J. C. Adamowski, F. Buiochi, C. Simon, E. C. N. Silva, and R. A. Sigelmann, “Ultrasonic measurement of density of liquids”, J. Acoust. Soc. Am., 97(1), pp. 354–361, January 1995.
[69] J. C. Adamowski, F. Buiochi, and R. A. Sigelmann, “Ultrasonic measurement of density of liquids flowing in tubes”, IEEE Trans. Ultrason., Ferroelec. Freq. Contr., 45(1), pp. 48–56, January 1998.
[70] R. T. Higuti, F. R. Montero de Espinosa, and J. C. Adamowski, “Energy method to calculate the density of liquids using ultrasonic reflection techniques”, *Proc. IEEE Ultrason. Symp*., pp. 319–322, 2001.

[71] R. T. Higuti, and J. C. Adamowski, “Ultrasonic densitometer using a multiple reflection technique”, IEEE Trans. Ultrason., Ferroelect., Freq. Contr., 49(9), pp. 1260–1268, September 2002.
[72] R. T. Higuti, F. Buiochi, J. C. Adamowski, and F. Montero de Espinosa, “Ultrasonic density measurement cell design and simulation of non-ideal effects”, Ultrasonics 44, pp. 302–309, 2006.
[73] A. R. Guilbert, M. L. Sanderson, “A high accuracy ultrasonic mass flowmeter for liquids”, In FLOMEKO 96 Proc., pp. 244–249, 1996.
[74] A. Püttmer, R. Lucklum, B. Henning, and P. Hauptmann, “Improved ultrasonic density sensor with reduced diffraction influence”, Sensors and Actuators A 67, pp. 8–12, 1998.
[75] A. Püttmer, and P. Hauptmann, “Ultrasonic density sensor for liquids”, *Proc. IEEE Ultrason. Symp*., pp. 497–500, 1998.
[76] A. Püttmer, N. Hoppe, B. Henning, and P. Hauptmann, “Ultrasonic density sensor–analysis of errors due to thin layers of deposits on the sensor surface”, Sensors and Actuators 76, pp. 122–126, 1999.
[77] A. Püttmer, P. Hauptmann, and B. Henning, “Ultrasonic density sensor for liquids”, IEEE Trans. Ultrason., Ferroelec. Freq. Contr., 47(1), pp. 85–92, 2000.
[78] N. Hoppe, G. Schönfelder, A. Püttmer, and P. Hauptmann, “Ultrasonic density sensor – Higher accuracy by minimizing error influences”, *Proc. IEEE Ultrason. Symp*., pp. 361–364, 2001.
[79] J. Salazar, A. Turó, J. A. Chávez, and M. J. García, “Ultrasonic inspection of batters for on-line process monitoring”, Ultrasonics, 42, pp. 155–159, 2004.
[80] M. Hirnschrodt, and R. Lerch, “Resonance anti-reflection for ultrasonic density measurement”, *Proc. IEEE Ultrason. Symp*., pp. 517–520, 1999.
[81] M. Hirnschrodt, A. Jena, T. Vontz, B. Fischer, and R. Lerch, “Ultrasonic characterization of liquids using resonance antireflection”, Ultrasonics, 38, pp. 200–205, 2000.
[82] M. Hirnschrodt, A. Jena, T. Vontz, B. Fischer, R. Lerch, and H. Meixner, “Time domain evaluation of resonance antireflection (RAR) signals for ultrasonic density measurement”, IEEE Trans. Ultrason., Ferroelec., Freq. Contr., 47(6), pp. 1530–1538, November 2000.
[83] J. Delsing, “Method and apparatus for measuring mass flow”, US Patent 5,214,966, 1993.
[84] J. van Deventer, and J. Delsing, “An ultrasonic density probe”, *Proc. IEEE Ultrason. Symp*., pp. 871–875, 1997.
[85] J. van Deventer, and J. Delsing, “Thermostatic and dynamic performance of an ultrasonic density probe”, IEEE Trans. Ultrason., Ferroelec., Freq. Contr., 48(3), pp. 675–682, May 2001.
[86] B. Fisher, V. Magori, A. von Jena, “Ultrasonic device for measuring specific density of a fluid”, European patent EP0483491, 1995.
[87] L. C. Lynnworth, “Slow torsional wave sensors”, *Proc. IEEE Ultrason. Symp*., 1977.
[88] L. C. Lynnworth, “Slow torsional wave densitometer”, US Patent 4,193,291, 1980.
[89] A. E. Arave, “Ultrasonic densitometer development”, *Proc. IEEE Ultrason. Symp*., pp. 370–375, 1979.
[90] W. B. Dress, “A high resolution ultrasonic densitometer”, *Proc. IEEE Ultrason. Symp*., pp. 287–290, 1983.
[91] S. A. Jacobson, J. M. Korba, L. C. Lynnworth, T. N. Nguyen, G. F. Orton, and A. J. Orazietti, “Low-gravity sensing of liquid/vapour interface and transient liquid flow”, IEEE Trans. Ultrason., Ferroelec., Freq. Contr., 34(2), pp. 212–224, March 1987.

[92] J. O. Kim, and H. H. Bau, "On line real-time densimeter – Theory and optimization", J. Acoust. Soc. Am., 85(1), pp. 432–439, January 1989.
[93] J. O. Kim, and H. H. Bau, "Instrument for simultaneous measurement of density and viscosity", Rev. Sci. Instrum. 60(6), pp. 1111–1115, June 1989.
[94] L. C. Lynnworth, "Torsional wave fluid sensor and system", US Patent 4,893,496, 1990.
[95] J. O. Kim, Y. Wang, and H. H. Bau, "The effect of an adjacent viscous fluid on the transmission of torsional stress waves in a submerged waveguide", J. Acoust. Soc. Am., 89(3), pp. 1414–1422, March 1991.
[96] J. O. Kim, H. H. Bau, Y. Liu, L. C. Lynnworth, S. A. Lynnworth, K. A. Hall, S. A. Jacobson, J. A. Korba, R. J. Murphy, M. A. Strauch, and K. G. King, "Torsional sensor applications in two-phase fluids", IEEE Trans. Ultrason., Ferroelec., Freq. Contr., 40(5), pp. 563–576, September 1993.
[97] V. I. Melnikov and V. N. Khokhlov, "Waveguide ultrasonic liquid level transducer for nuclear power plant steam generator", Nuclear Engineering and Design, 176, pp. 225–232, 1997.
[98] C. C. Smit and E. D. Smith, "The analysis and results of a continuous wave ultrasonic densitometer", J. Acoust. Soc. Am., 104(3), pp. 1413–1417, September 1998.
[99] C. L. Shepard, B. J. Burghard, M. A. Friesel, B. Percy Hildebrand, X. Moua, A. A. Diaz, and C. W. Enderlin, "Measurements of density and viscosity of one- and two-phase fluids with torsional waveguids", IEEE Trans. Ultrason., Ferroelec., Freq. Contr., 46(3), pp. 536–548, May 1999.
[100] L. C. Lynnworth, R. Cohen, and T. H. Nguyen, "Clamp-on shear transducers simplify torsional and extensional investigations", *Proc. IEEE Ultrason. Symp*., pp. 1603–1607, 2004.
[101] L. C. Lynnworth, "Ultrasonic nonresonant sensors" in: Sensors – A Comprehensive Survey. Edited by W. Göpel, J. Hesse, J. N. Zemel. Volume 7 Mechanical Sensors, Edited by H. H. Bau, N. F. deRooij, B. Kloeck. VCH Publishers Inc., New York, pp. 311–312, 1994, ISBN 0-89573-679-9.
[102] N. G. Pope, D. K. Veirs, T. N. Claytor, and M. B. Histand, "Fluid density and concentration measurement using noninvasive in situ ultrasonic resonance interferometry", Proc. IEEE Ultrason. Symp., vol. 2, McAvoy, B. R., ed., p. 855, 1992.
[103] N. G. Pope, D. K. Veirs, and T. N. Claytor, "Fluid density and concentration measurement using noninvasive in situ ultrasonic resonance interferometry", US Patent 5,359,541, 1994.
[104] D. N. Sinha, "Noninvasive identification of fluids by swept-frequency acoustic interferometry", US Patent 5,767,407, 1998.
[105] D. N. Sinha, and G. Kaduchak, "Noninvasive determination of sound speed and attenuation in liquids", In Experimental Methods in the Physical Sciences, Volume 39 (Modern Acoustical Techniques for the Measurement of Mechanical Properties). Chapter 8, 307-333, Academic Press, September 2001. ISBN 0-12-475986-6.
[106] D. N. Sinha, personal communication, 2003.
[107] Available http://www.safety-scan.com
[108] M. S. Greenwood, and J. A. Bamberger, "Self-calibrating sensor for measuring density through stainless steel pipeline wall", J. Fluids Engineering, 126(2), pp. 189–192, March 2004.
[109] J. A. Bamberger, and M. S. Greenwood, "Non-invasive characterization of fluid foodstuffs based on ultrasonic measurements", Food Research International, 37(6), pp. 621–625, 2004.
[110] J. A. Bamberger, and M. S. Greenwood, "Measuring fluid and slurry density and solids concentration non-invasively", Ultrasonics, 42, pp. 563–567, April 2004.

[111] E. H. Trinh, and C. J. Hsu, “Acoustic levitation methods for density measurements”, J. Acoust. Soc. Am., 80(6), pp. 1757–1761, December 1986.
[112] D. J. Shirley, “Method for measuring in situ acoustic impedance of marine sediments”, J. Acoust. Soc. Am., 62(4), pp. 1028–1032, October 1977.
[113] L. C. Lynnworth, “Industrial applications of ultrasound – A review. II. Measurements, tests, and process control using low-intensity ultrasound”, IEEE Transactions on Sonics and Ultrasonics, 22(2), pp. 71–101, March 1975.
[114] B. Devcic-Kuhar, D. Harrer, R. Thalhammer, M. Gröschl, E. Benes, H. Nowotny, and F. Trampler, “Three layer thickness extensional mode piezoelectric resonator for determining density and sound velocity of liquids”, *Proc. IEEE Int. Freq. Contr. Symp.*, pp. 81–89, 1997.
[115] M. A. Hakulinen, J. Töyräs, S. Saarakkala, J. Hirvonen, H. Kröger, and J. S. Jurvelin, “Ability of ultrasound backscattering to predict mechanical properties of bovine trabecular bone”, Ultrasound in Med. & Biol., 30(7), pp. 919–927, 2004.
[116] K. A. Wear, A. P. Stuber, and J. C. Reynolds, “Relationships of ultrasonic backscatter with ultrasonic attenuation, sound speed and bone mineral density in human calcaneus”, Ultrasound in Med. & Biol., 26(8), pp. 1311–1316, 2000.
[117] J. Töyräs, H. Kröger, and J. S. Jurvelin, “Bone properties as estimated by mineral density, ultrasound attenuation, and velocity”, Bone, 25(6), pp. 725–731, 1999.
[118] J. Mathieu, and P. Scheitzer, “Measurement of liquid density by ultrasound backscattering analysis”, Meas. Sci. Technol., 15, pp. 869–876, 2004.
[119] J. Mathieu, and P. Scheitzer, “Numerical study of the wire form function versus the liquid density of the surrounding medium”, *Proc. IEEE Ultrason. Symp.*, pp. 293–296, 2005.
[120] A. Püttmer, P. Hauptmann, R. Lucklum, O. Krause, and B. Henning, “SPICE model for lossy piezoceramic transducers”, IEEE Trans. Ultrason., Ferroelec. Freq. Contr., 44(1), pp. 60–66, January 1997.
[121] J. van Deventer, T. Löfqvist, and J. Delsing, “PSpice simulation of ultrasonic systems”, IEEE Trans. Ultrason., Ferroelec. Freq. Contr., 47(4), pp. 1014–1024, July 2000.
[122] L. Wu, and Y-C. Chen, “PSPICE approach for designing the ultrasonic piezoelectric transducer for medical diagnostic applications”, Sensors and Actuators 75, pp. 186–198, 1999.
[123] L. E. Kinsler, A. R. Frey, A. B. Coppens, and J. V. Sanders, *Fundamentals of Acoustics*, 3rd edition, John Wiley & Sons, p. 461, 1982.
[124] N. Hoppe, A. Püttmer, and P. Hauptmann, “Optimization of buffer rod geometry for ultrasonic sensors with reference path”, IEEE Trans. Ultrason., Ferroelec. Freq. Contr., 50(2), pp. 170–178, February 2003.
[125] J. Berrebi, “Self-Diagnosis Techniques and Their Applications to Error Reduction for Ultrasonic Flow Measurement”, Ph.D. thesis, Luleå University of Technology, 2004.
[126] Panametrics-NDT, “Ultrasonic transducers for nondestructive testing”, catalogue available at http://www.olympusndt.com/data/File/panametrics-UT.pdf
[127] A. O. Williams, Jr., “The piston source at high frequencies”, J. Acoust. Soc. Am., 23(1), pp. 1–6, January 1951.
[128] J. Kushibiki, and M. Arakawa, “Diffraction effects on bulk-wave ultrasonic velocity and attenuation measurements”, J. Acoust. Soc. Am., 108(2), pp. 564–573, August 2000.
[129] E. P. Papadakis, “Ultrasonic attenuation in thin specimens driven through buffer rods”, J. Acoust. Soc. Am., 44(3), pp. 724–734, 1968.

[130] E. P. Papadakis, K. A. Fowler, and L. C. Lynnworth "Ultrasonic attenuation by spectrum analysis of pulses in buffer rods: Method and diffraction corrections", J. Acoust. Soc. Am., 53(5), pp. 1336–1343, 1973.

[131] T. P. Lerch, R. Cepel, and S. P. Neal, "Attenuation coefficient estimation using experimental diffraction corrections with multiple interface reflections", Ultrasonics 44, pp. 83–92, 2006.

[132] W. Kester, "ADC Input Noise: The Good, The Bad, and The Ugly. Is No Noise Good Noise?", Analog Dialogue 40-02, February 2006. Available at: http://www.analog.com/analogdialogue

[133] D. Jarman, "A Brief Introduction to Sigma delta Conversion", Intersil Application Note AN9504, May 1995. Available at: http://www.intersil.com

[134] J. C. Candy and G. C. Temes, "Oversampling Methods for A/D D/A Conversion, Oversampling delta-Sigma Converters", IEEE Press, pp. 2–3, 1992.

[135] W. Kester, "Which ADC architecture is right for your application?", Analog Dialogue 39-06, June 2005. Available at: http://www.analog.com/analogdialogue

[136] Available at: http://www.density.co.uk

[137] Available at: http://www.cannoninstrument.com

[138] CRC Handbook of Chemistry and Physics, 62nd edition, 1981–1982, CRC Press, Inc., Boca Raton, Florida, editor R. C. Weast, p. F-42.

[139] D. E. Schuele, F. A. Gutowski, and E. F. Carome, "Interferometric determination of ultrasonic absorption in castor oil", J. Acoust. Soc. Am., 29(10), pp. 1081–1085, October 1957.

[140] B. J. Wuensch, T. F. Hueter, and M. S. Cohen, "Ultrasonic absorption in castor oil: Deviations from classical behavior", J. Acoust. Soc. Am., 28(2), pp. 311–312, March 1956.

[141] J. Tong and M. J. W. Povey, "Pulse echo comparison method with FSUPER to measure velocity dispersion in n-tetradecane in water emulsions", Ultrasonics 40, pp. 37–41, 2002.

[142] L. E. Kinsler, A. R. Frey, A. B. Coppens, and J. V. Sanders, *Fundamentals of Acoustics*, 3rd edition, John Wiley & Sons, Chapter 7, 1982.

[143] K. R. Waters, J. Mobley, and J. G. Miller, "Causality-imposed (Kramers-Kronig) relationships between attenuation and dispersion", IEEE Trans. Ultrason., Ferroelec. Freq. Contr., 52(5), pp. 822–833, May 2005.

[144] T. L. Szabo, "Causal theories and data for acoustic attenuation obeying a frequency power law", J. Acoust. Soc. Am., 97(1), pp. 14–24, January 1995.

[145] R. A. Kline, "Measurement of attenuation and dispersion using an ultrasonic spectroscopy technique", J. Acoust. Soc. Am., 76(2), pp. 498–504, August 1984.

[146] T. L. Szabo, "The material impulse response for broadband pulses in lossy media", *Proc. IEEE Ultrason. Symp*., pp. 748–751, 2003.

[147] A. E. Brown, "Rationale and summary of methods for determining ultrasonic properties of materials at Lawrence Livermore National Laboratory", Acoustic Properties of Materials Group, Nondestructive Evaluation Section, Manufacturing & Materials Engineering Division. Report UCRL-ID-119958, 45 pages, 1997. Available at: http://www.llnl.gov/tid/lof/documents/pdf/225771.pdf

Appendix A: PSPICE code based on OrCAD 15.7

```
****    CIRCUIT DESCRIPTION

** Creating circuit file "TRAN.cir"
* Local Libraries:
lib "nom.lib"

*Analysis directives:
.TRAN         10n 60u 20u 5n

* source PULSE-ECHO-T_LINE
V_Vsin        N00201 0 DC 0 AC 1 +SIN 0 60 {FREQ} 0 0 0
V_Vpulse      N00199 0 DC 0 AC 1 +PULSE 0 1 0 1n 1n {PERIODS * 1 / FREQ}
E_MULT1       PULSE 0 VALUE {V(N00199)*V(N00201)}

R_Rgen1       PULSE N66228  {Rg}
R_Rgen2       N59525 0  {Rg}

T_Tx-buffer   N66228 0 N59728 0 Z0={Z_buffer} TD={t_ buffer}
T_Rx-buffer   N59529 0 N59525 0 Z0={Z_ buffer} TD={t_ buffer}
T_Liquid      N59728 0 N59529 0 Z0={Z_liq} TD={t_liq}
```

```
PARAM
PERIODS=5
FREQ=5meg
RG=2meg
Z_ buffer=17meg
Z_LIQ=1.5meg
V_ buffer=6450
DIST_ buffer=80m
T_ buffer={dist_ buffer/v_ buffer}
V_LIQ=1500
DIST_LIQ=5.7m
T_LIQ={dist_liq/v_liq}

.PRINT          TRAN V([N59525])
.END
```

Appendix B: Transducer compliance sheets

Below are the complience sheets given for the used 5.0 MHz centre frequency transducers.

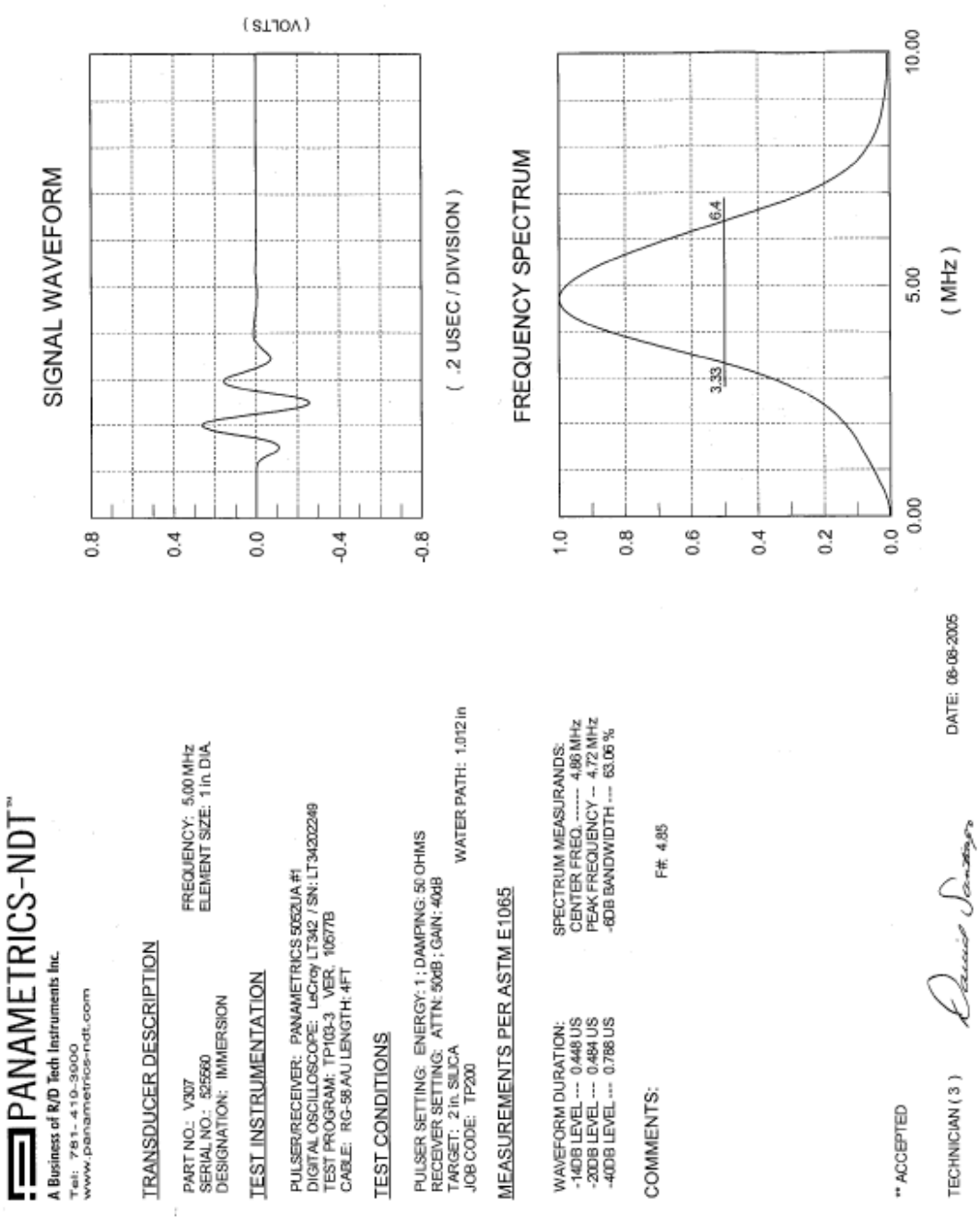

PANAMETRICS-NDT™

A Business of R/D Tech Instruments Inc.

Tel: 781-419-3900

www.panametrics-ndt.com

TRANSDUCER DESCRIPTION

PART NO.: V307
SERIAL NO.: 519103
DESIGNATION: IMMERSION

FREQUENCY: 5.00 MHz
ELEMENT SIZE: 1 in. DIA.

TEST INSTRUMENTATION

PULSER/RECEIVER: PANAMETRICS 5052UA #1
DIGITAL OSCILLOSCOPE: LeCroy LT342 / SN: LT34202249
TEST PROGRAM: TP103-3 VER. 1055G4
CABLE: RG-58 A/U LENGTH: 4FT

TEST CONDITIONS

PULSER SETTING: ENERGY: 1 ; DAMPING: 50 OHMS
RECEIVER SETTING: ATTN: 50dB ; GAIN: 40dB
TARGET: 2 in. SILICA
JOB CODE: TP200

WATER PATH: 1.022 in

MEASUREMENTS PER ASTM E1065

WAVEFORM DURATION:
-14DB LEVEL --- 0.448 US
-20DB LEVEL --- 0.540 US
-40DB LEVEL --- 0.956 US

SPECTRUM MEASURANDS:
CENTER FREQ. ------- 4.98 MHz
PEAK FREQUENCY -- 4.74 MHz
-6DB BANDWIDTH --- 58.73 %

COMMENTS:

F#: 4.98

** ACCEPTED

TECHNICIAN (3)

DATE: 03-30-2005

SIGNAL WAVEFORM

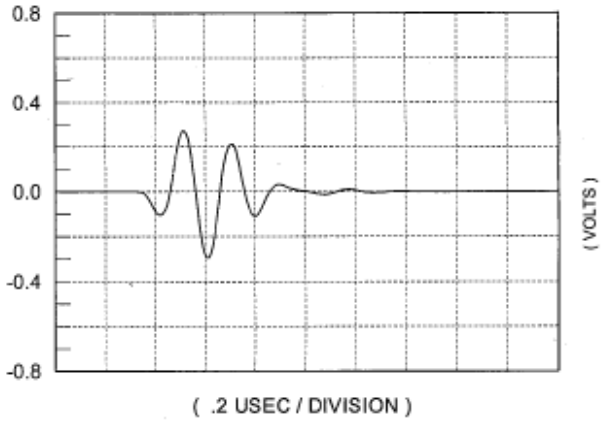

(.2 USEC / DIVISION)

FREQUENCY SPECTRUM

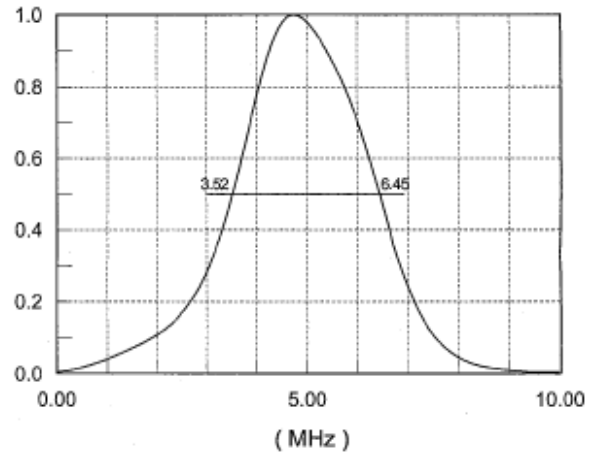

Appendix C: Electronics diagram

The detailed electronics diagram is given in Fig. C.1, and the corresponding components used are given in Table C.1.

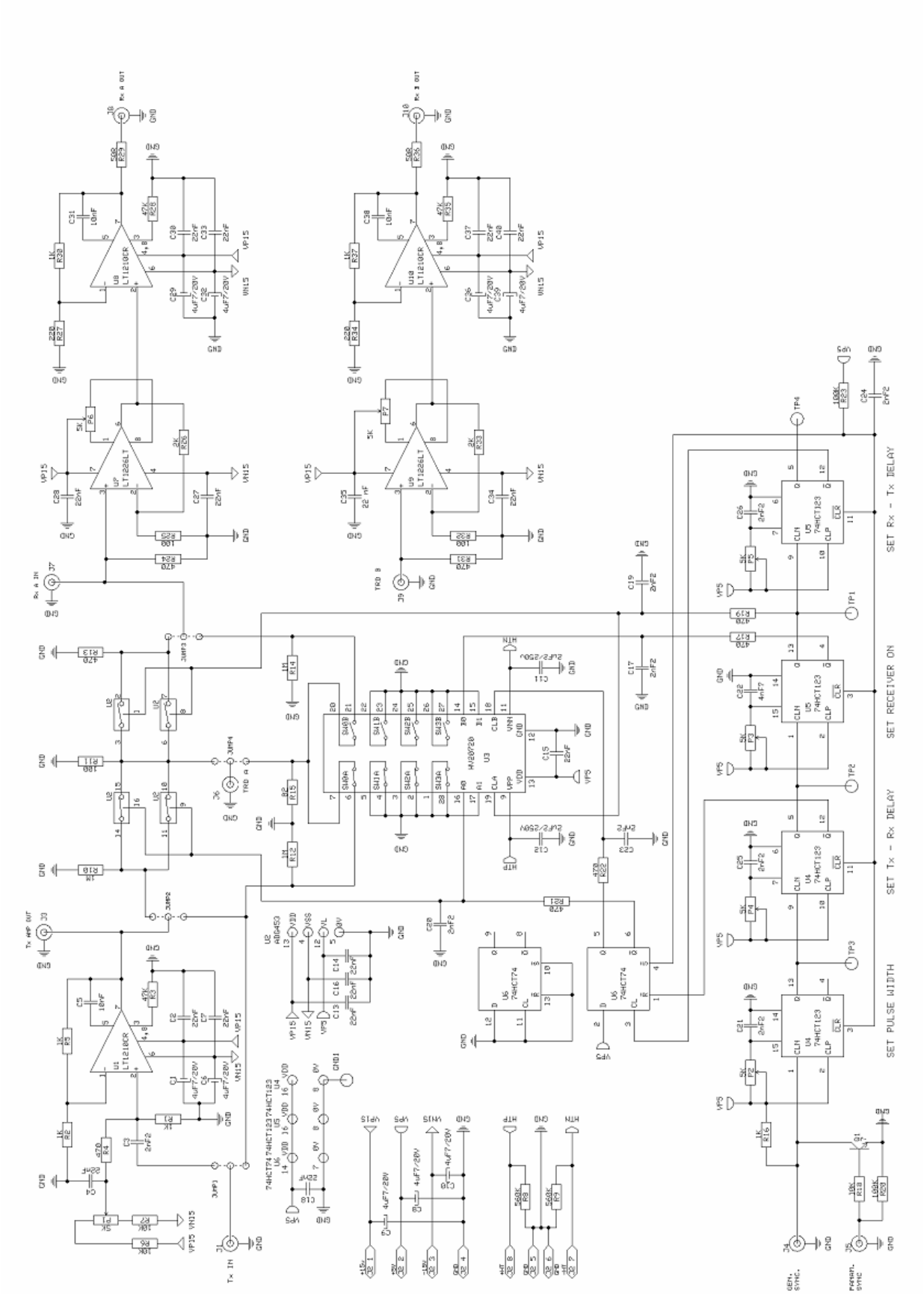

Figure C.1. Detailed diagram of the electronics used (switch and preamplifiers).

Table C.1. Component values for the electronics used.

R1 = 1K	R21 = 470Ω	C1 = 4µF7/20V	C21 = 1nF	P1 = 5K	JUMPX = 3 PIN STIFT
R2 = 1K	R22 = 470Ω	C2 = 22nF	C22 = 4nF7	P2 = 50K	
R3 = 47K	R23 = 100K	C3 = 2nF2	C23 = 100pF	P3 = 50K	TPX = TP
R4 = 1K	R24 = 470Ω	C4 = 22nF	C24 = 22nF	P4 = 50K	
R5 = 1K	R25 = 100Ω	C5 = 10nF	C25 = 1nF	P5 = 50K	GND1 = TP
R6 = 10K	R26 = 2K	C6 = 4µF7/20V	C26 =1nF	P6 = 5K	
R7 = 10K	R27 = 220Ω	C7 = 22nF	C27 = 22nF	P7 = 5K	J1 = BNC
R8 = 560K	R28 = 47K	C8 = 4µF7/20V	C28 = 22nF		J2 = MOLEX
R9 = 560K	R29 = 47Ω	C9 = 4µF7/20V	C29 = 4µF7/20V		J3-J10 = BNC
R10 = 1M	R30 = 1K	C10 = 4µF7/20V	C30 = 22nF		
R11 = 100Ω	R31 = 470Ω	C11 = 2µF2/250V	C31 = 10nF	U1 = LT1210CR	
R12 = 1M	R32 = 100Ω	C12 = 2µF2/250V	C32 = 4µF7/20V	U2 = ADG453	
R13 = 470Ω	R33 = 2K	C13 = 22nF	C33 = 22nF	U3 = HV20720	
R14 = 1M	R34 = 220Ω	C14 = 22nF	C34 = 22nF	U4 = 74HCT123D	
R15 = 82Ω	R35 = 47K	C15 = 22nF	C35 = 22nF	U5 = 74HCT123D	
R16 = 1K	R36 = 47Ω	C16 = 22nF	C36 = 4µF7/20V	U6 = 74HCT74D	
R17 = 470Ω	R37 = 1K	C17 = 100pF	C37 = 22nF	U7 = LT1226LT	
R18 = 100Ω		C18 = 22nF	C38 = 10nF	U8 = LT1210CR	
R19 = 470Ω		C19 = 100pF	C39 = 4µF7/20V	U9 = LT1226LT	
R20 = 10K		C20 = 100pF	C40 = 22nF	U10 = LT1210CR	

Appendix D: Reference data for the distilled water

The reference values of the sound speed c and of the density ρ of distilled water versus temperature as used in this work, as given by [46] and [47], respectively, are given below. From [46], it follows that the sound speed can be given according to

$$c = \sum_{i=0}^{5} a_i T^i,$$

where T is the temperature in [°C]. The coefficients a_i are given in Table D.1.

Table D.1. Sound speed of distilled water versus temperature [46].

i	a_i
0	$1.402385 \cdot 10^{3}$
1	$5.038813 \cdot 10^{0}$
2	$-5.799136 \cdot 10^{-2}$
3	$3.287156 \cdot 10^{-4}$
4	$-1.398845 \cdot 10^{-6}$
5	$2.787860 \cdot 10^{-9}$

The reference density of distilled water can be given according to [47]

$$\left(1 - \rho / \rho_{\max}\right) \cdot 10^{6} = A_1 \cdot T_A + A_2 \cdot T_A^2 + A_1 \cdot T_A^3 + A_1 \cdot T_A^4 + A_1 \cdot T_A^5,$$

where $T_A = T - T_0$, where $T_0 = 3.983035$ °C, and $\rho_{\max} = 999.974950$ kg/m^3, and with the A-coefficients given in Table D.2.

Table D.2. Density reference data for the distilled water used versus temperature [47].

$A_1 = -2.381848 \cdot 10^{-2}$ °C^{-1}
$A_2 = 7.969992983 \cdot 10^{0}$ °C^{-2}
$A_3 = -7.999081 \cdot 10^{-2}$ °C^{-3}
$A_4 = 8.842680 \cdot 10^{-4}$ °C^{-4}
$A_5 = -5.446145 \cdot 10^{-6}$ °C^{-5}

Appendix E: Reference data for the Cannon oils used

According to the reference data printed on the bottles labels, the shear viscosity and the density are given for the temperatures given in Table E.1 and in Table E.2, respectively.

Table E.1. Shear viscosity reference data for the Cannon oils used versus temperature.

Temperature [°C]	N4 [mPa·s]	N7.5 [mPa·s]	N35 [mPa·s]	N100 [mPa·s]
20	5.242	11.37	74.93	282.8
25	4.531	9.495	56.62	202.3
37.78	3.253	6.314	30.21	94.87
40	3.084	5.917	27.38	84.15
50	2.478	4.526	18.26	51.41
80	1.445	2.373	7.087	16.17
98.89	1.102	1.726	4.539	9.433
100	1.085	1.697	4.430	9.163

Table E.2. Density reference data for the Cannon oils used versus temperature.

Temperature [°C]	N4 [kg/m^3]	N7.5 [kg/m^3]	N35 [kg/m^3]	N100 [kg/m^3]
20	786.2	800.9	867.5	881.9
25	782.8	797.6	864.3	878.9
37.78	774.2	789.2	856.2	870.9
40	772.7	787.8	854.8	869.6
50	765.9	781.2	848.4	863.4
80	745.5	761.5	829.5	844.9
98.89	732.6	749.0	817.6	833.3
100	731.9	748.3	816.9	832.7

The polynomial representations of the given shear viscosities and of the given densities were found using the Matlab POLYFIT function. The shear viscosities (η) were found using a 6th -order polynomial of the form

$$\eta = \mathrm{A}\cdot T^5 + \mathrm{B}\cdot T^4 + \mathrm{C}\cdot T^3 + \mathrm{D}\cdot T^2 + \mathrm{E}\cdot T + \mathrm{F},$$

where T is the temperature. The polynomial coefficients for the shear viscosities are given in Table E.3.

Table E.3. Polynomial coefficients for the shear viscosities in descending order.

N4	8.027800996632078e-012 - 4.251961523834876e-009 + 9.318749582089515e-007 - 1.116553733884319e-004 + 8.134991935095743e-003 - 3.756290304073943e-001 + 1.025773996784350e+001
N7.5	5.498941879307834e-011 - 2.434566185052924e-008 + 4.551398815240738e-006 - 4.712199102686059e-004 + 2.977636621138541e-002 - 1.176182434043158e+000 + 2.609890599151584e+001
N35	1.229029488457648e-009 - 5.291705684157601e-007 + 9.444851181189126e-005 - 9.064703600535342e-003 + 5.060825165382785e-001 - 1.631728295948373e+001 +2.578624008531363e+002
N100	7.176784894248693e-009 - 3.055172327380530e-006 + 5.367475271918628e-004 - 5.032552891662730e-002 + 2.709057654932220e+000 - 8.226135081011114e+001 +1.170440460981944e+003

The densities (ρ) were found using a 2nd -order polynomial of the form

$$\rho = \mathrm{G}\cdot T^2 + \mathrm{H}\cdot T + \mathrm{I}.$$

The polynomial coefficients for the densities are given in Table E.4.

Table E.4. Polynomial coefficients for the densities in descending order.

N4	-5.571091756185493e-005 - 6.724415542437948e-001 + 7.996681477592475e+002
N7.5	-3.316222035647934e-005 - 6.534523095367939e-001 + 8.139662819837994e+002
N35	5.803127107980051e-005 - 6.393504592532027e-001 + 8.802594959838316e+002
N100	4.606130931110368e-005 - 6.216415611702170e-001 + 8.943586481751656e+002